CZECH UNIVERSITY OF LIFE SCIENCES IN PRAGUE

DEPARTMENT OF WATER RESOURCES AND

ENVIRONMENTAL MODELING

FACULTY OF ENVIRONMENTAL SCIENCES

CALIBRATION OF RAINFALL SIMULATOR WITH DIFFERENT JETS AND PRESSURE CONDITIONS

DIPLOMA THESIS

SUPERVISOR: Ing. Jiří Pavlásek, Ph.D.

AUTHOR: James Kobina Mensah Biney

2017

CZECH UNIVERSITY OF LIFE

SCIENCES PRAGUE

Faculty of Environmental Sciences

DIPLOMA THESIS PROPOSAL

James Kobina Mensah Biney, BSc

Environmental Modelling

Thesis title

Calibration of rainfall simulator with different jets and pressure conditions

---

Objectives of thesis

Main aim of the thesis is estimation of simulated rain intensities and its variability and spatial distribution produced by transportable rain simulator.

Methodology

Based on laboratory experiments, evaluation of rain intensities produced by rain simulator will be estimated. Different type of nozzles and pressure in hydraulic system will be used.

Also, the variability and space distribution will be evaluated. Coefficient of uniformity will be computed for individual experiments.

Relation between pressure in the system and rain intensities will be estimated with help of linear regression.

The proposed extent of the thesis

50 pages

Keywords

artificial rain, rain

Recommended information sources

Dunkerley, D., 2008: Rain event properties in nature and in rainfall simulation experiments: A comparative review with recommendations for increasingly systematic study and reporting. Hydrol. Process. 22: 4415–4435.

Juras, R., Pavlásek, J., Děd, P., Tomášek, V., Máca, P. A portable simulator for investigating rain-on-snow events. Zeitschrift für Geomorphologie, 2013, 57(s. 1), pp. 73-89.

Van Dijk, A. J. M., Bruijnzeel, L.A. and C.J. Rosewell. 2002. Rainfall intensity – kinetic energy relationships: A critical literature appraisal. J. Hydrology 261:1-23.

Expected date of thesis defence

2016/17 SS – FES

The Diploma Thesis Supervisor

Ing. Jiří Pavlásek, Ph.D.

Supervising department

Department of Water Resources and Environmental Modeling

Electronic approval:13.4.2017

doc. Ing. Martin Hanel, Ph.D.

Head of department

Electronic approval: 13. 4. 2017

prof. RNDr. Vladimír Bejček, CSc.

Dean

DECLARATION

I hereby declare that calibration of rainfall simulator with different jets and pressure conditions is my own work, it does not include any material published or written by another person, or has been submitted for the award of any other university degree and that all the sources I have used and quoted have been indicated and acknowledged by complete references.

SIGNATURE ……. DATE……

(JAMES KOBINA MENSAH BINEY)

SUPERVISOR'S DECLARATION

I hereby declare that preparation and presentation of this thesis was supervised in accordance with the guidance binding the supervision of Diploma Thesis laid down by the Czech University of Life Sciences.

SIGNATURE …… DATE ……...

(JIŘÍ PAVLÁSEK)

ACKNOWLEDGEMENT

First and foremost, I will like to say a big thank you to the almighty God for his constant love and protection over my life and that of my family.

Many thanks also go to the department of Water Resource and Environmental modeling for granting me an unlimited access to the Laboratory for my work. I am totally indebted to my supervisor Ing. Jiří Pavlásek Ph.D. for his passionate and unreserved support, guidance, encouragement, and patience which has contributed to the success of this work.

I cannot also forget my love and personal wife Mrs. Dorcas Biney and my angel Alexandra Biney for their total patience and understanding during such a period, to them, I say God richly bless you .To my mum Emelia Quaye, I say thank you and may God bless you so much for your guidance and love toward me, to my late dad Justice Kobina Mensah Biney, even though you no more with us, but your support both alive and not alive has brought me this far, and to my brothers I say thank you and may God bless you all.

ABSTRACT

It is a fact that without rainfall simulators it would have taken a longer period obtaining data for assessing the impact of different types of rainfall on the environment. Rainfall simulators have been and continue to face a lot of issues since it was developed in the 1930s.One of this issue has to do with their inability to mimic the characteristics of natural rain. Due to the lack of standard design and measurements, most researchers end up developing devices suiting their particular needs, but the issues still persist. Rainfall features which include rainfall intensity and its spatial uniformity, drop size distribution, frequency, seasonal pattern, kinetic energy, and duration confirm that natural rainfall conditions are simulated with sufficient accuracy. This work seeks to calibrate an existence rainfall simulator in the laboratory to determined its usefulness for other field purposes in the future.

The simulator used was a single nozzle type which was developed by the department of Water Resources and Environmental Modelling (Czech University of Life Sciences). Three different Lechler nozzles were each used for the calibration (fixed depth of 160cm) with pressures of 1.6, 1.8, 2.0, and 2.2 bars. Constant flow throughout the experiment was provided by an electrical pump. The rainfall spatial distribution was measured with 82 (three different categories of size) vessels serving as rain gauge equally distributed on the experimental plot (100 by 100 cm).

An assessment for the coefficient of determination, spatial drop size distribution (creating of distribution maps), spatial variability (use of boxplot) and the calculation of Christiansen coefficient of uniformity (CU) were all based on the collected data. Though the CU values range from 65% to 88%, the expectation was to achieve a CU value of 80% and more, but it was only the nozzles with the highest discharge that show that range of 80% and above signifying a uniform spatial rainfall distribution. The result also shows that the generated rainfall characteristics of spatial variability and that of the spatial rainfall distribution in rainfall simulator, just like in natural rainfall event, are not homogeneous. So, for continuous simulation of natural rainfall, it will be very difficult to achieve the same characteristics. The rainfall intensity generated for this work range from 16.03mm/h to 55.19mm/h.

Keywords: Nozzle-type rainfall simulator, rainfall intensity, drop size distribution, spatial variability, calibration of rainfall characteristics.

ABSTRAKT

Dešťové simulátory jsou velice důležitým nástrojem pro získání informací o vlivu srážek s různými charakteristikami na životní prostředí. I přes kontinuální vývoj dešťových simulátorů od doby jejich vzniku v třicátých letech minulého století není stále možné věrně reprodukovat přírodní deště. I přesto, že většina simulátorů byla přesně vyvinuta pro konkrétní podmínky a potřeby výzkumu, nebylo dosaženo univerzálního řešení. Zjištěné charakteristiky deště zahrnující intenzitu deště, prostorové rozložení deště, zastoupení různé velikosti dešťových kapek, dobu opakování, sezónní změny, kinetickou energii deště a dobu trvání umožňují simulovat srážky s určitou podobností s přírodní srážkou. Tato práce se zabývá kalibrací dešťového simulátoru v laboratoři a stanovení charakteristik simulovaného deště.

Použitý simulátor používá k simulaci deště jednu trysku a byl sestrojen na Katedře vodního hospodářství a environmentálního modelování České zemědělské univerzity v Praze. Pro kalibraci byly použity tři různé trysky umístěné 160 cm nad povrchem a měření probíhalo za různých tlakových podmínek 1,6; 1,8; 2,0 a 2,2 baru. Konstantní průtok během simulace byl udržován pomocí elektrického čerpadla. Prostorové rozložení simulovaného deště bylo stanoveno pomocí 82 misek (byly použity tři různé tvary misek) rovnoměrně rozmístěných na ploše 100 x 100 cm, které sloužily jako srážkoměrné nádoby. Na základě měřených hodnot byl vyhodnocen koeficient determinace, plošné rozložení simulované srážky (byla sestavena mapa rozložení intenzit deště), prostorová variabilita (vyhodnocená pomocí krabicových grafů) a Christiansenův koeficient uniformity (CU). Hodnoty CU byly stanoveny v rozmezí 65 % až 88 %, kdy vyšších hodnot (nad 80 %) bylo dosaženo při použití trysky simulující déšť s vyšší intenzitou. Výsledky ukazují, že simulovaná srážka není homogenní, je prostorově variabilní. Při simulacích je velice obtížné dosáhnout podobných charakteristik, jako jsou charakteristiky přírodního deště. Testovaný přístroj je schopen simulovat srážky o intenzitách do 16,03 mm/h do 55,19 mm/h.

Klíčová slova: tryskový dešťový simulátor, intenzita deště, distribuce srážek, prostorová variabilita, kalibrace charakteristik simulovaných srážek

TABLE OF CONTENT

CHAPTER 1

INTRODUCTION

There had been an increasing usage of rainfall simulators over recent years as research tools extensively for laboratory and field characterization of hydrologic and geomorphologic studies to determine runoff, infiltration and erosion characteristics as well as studies of sediment transfer(Mayer,1994).

Rainfall simulators, being limited in elevation normally use nozzles to produce water under pressure in order to generate rain with kinetic energy and drop size characteristics similar to that of natural rain. Accuracy estimation of results from rainfall simulator is very critical for any research or experiment purposes. Usually, rain gauges varying in sizes and height are used on the field or in the laboratory to measure total rain for each calibration purposes.

Model calibration is the technique of ascertaining that the model can produce field measured quantities (Kibet LC, et al., J. Environ. Qual., 2011**).** Once model results match observed values from rainfall measurement, there is greater confidence in the consistency of the model. But in many instances when simulated rain is used, relating it with natural rain can be a challenge. Uncertainty about the validity of data due to the absence of correspondence amid natural and simulated rain can be occasionally introduced because the characteristics of natural rain are not adequately represented in rainfall simulation research (Dunkerley D., 2008). Several times, the rainfall simulations have high rain rates and they do not bear similarity to natural rain events and these measures are not similar.

The nozzle is a critical part of any rainfall simulator. Nozzles perform three functions:

1. Regulate flow

2. Atomize the water into droplets

3. Disperse the spray in a desirable pattern.

Normally, the nozzle can be most appropriate for certain purposes and not as much of desirable for others and are also, designed to be operated within a certain pressure range. Higher than proposed pressures increase the distribution rate, decrease the droplet size, and could alter the spray pattern. This can result in excess spray drift and uneven coverage. The spray delivery rate decreases when the pressure is low and the spray material may not form a full-width spray pattern unless the nozzles are designed to operate at lower pressure.

As realized by Grismer (2011), nozzle-type simulators which run under high pressure will generate a wide range of drop sizes with a likelihood to impart significant initial velocity to smaller drops. Higher pressure applied usually develop good drop size distributions with probability to access the rainfall intensity desired whereas lesser pressures give poor drop size distribution and spatial uniformity of rainfall. The pressure is also operative in the application area, i.e. low pressure decreases the application area, while high pressure increases it.

Calibration process should not only focus on the nozzles but rather, the whole compartment forming the rainfall simulator. Example, the pump must have adequate capacity to operate a hydraulic agitation system, as well as supply the required volume to the nozzles. The pump capacity should be at least 25 percent larger than the largest volume required by the nozzles. This will permit for agitation and loss of capacity due to pump wear. A pressure gauge should have a total range twice the maximum expected reading and should also specify spray pressure correctly.

The rainfall simulator has been a very important tool over the years, since, rainfall simulation offers a year-round, attractive and active way of experiencing artificial rain for water erosion studies, while not being dependent on (outdoors) weather conditions. Without rainfall simulators, however, the time required to gather sufficient infiltrability, runoff, and soil loss data would be prohibitive (Meyer, 1988), especially in non-humid climates, where much of the work is being done.

Despite the many positives, it is clear that universal rainfall applicable to all situations does not exist which is a fact. Rather, rainfall simulators are faced with some challenges outlined by Renard (1985) which are:

1. the areas treated are usually small, ranging from a fraction of a square meter, up to several hundred square meters, depending on the design. This small area may not be representative of the general area of concern.

2. Most simulators do not produce drop-size distributions that are representative of natural rainfall.

3. Most simulators do not produce rainfall intensities with the temporal variations of natural rainfall.

4. Some simulators do not produce raindrops with terminal velocities of natural rainfall. The Lower velocities in combination with the smaller drop size result in lower Kinetic energy than that produced by natural rainfall.

Rainfall simulator at the laboratory has less disruption of wind, humidity, and temperature. One option to help solve some of these challenges is the calibration of rainfall simulator in the laboratory since some studies have shown that many application errors are due to improper calibration.

CHAPTER TWO
AIM AND OBJECTIVES

The main aim of this study is the calibration of a nozzle type rainfall simulator in the laboratory using different jets nozzle and pressure conditions so as to select the appropriate nozzles and best pressure conditions for a future field work. Also, the estimation of simulated rain intensities and its variability and spatial distribution will be carry out as a selecting guide for this experiment.

This work is not about the comparison with other researchers work on rainfall simulator but rather focusing on the calibration of an existing rainfall simulator by selecting a nozzle with pressure conditions which can mimic the characteristics of natural rain to be useful for other purposes in the future.

CHAPTER THREE

LITERATURE REVIEW

3.1 Rainfall Simulator-background

The general knowledge behind rainfall simulation is to permit controlled releases of water to fall onto a confined plot of soil and to measure the runoff and soil loss that occurs as a result. It has been an appropriate technique in numerous fields, from hydrology to agriculture and soil science to geomorphology. In the 1930s, the Soil Conservation Service (USA) developed the rainfall simulator as a way to measure credibility and infiltration capacity of soil. Since then, rainfall simulation has evolved from a simple procedure, in some cases involving nothing more than a common sprinkling can, to a complex process involving electronic and hydraulic machines (Meyer, 1988).

Also, Esteves et al., (2000); Seeger (2007) Ries et al., (2009); Aksoy et al., (2012) stated that the key purpose of the rainfall simulator is not only to produce and replicate rain but to additionally, regulate the intensity and duration of rainfall correctly and precisely. According to Meyer (1988); Wollmer, (1994); Foster et al., (2000), the failure of simulators to correctly mimic all features of natural rainfall mean that most data collected by rainfall simulators(RSs) should be used only for the comparison of conditions while the studies of natural rainfall should be used to establish baseline averages.

3.2. Characteristics of Natural Rainfall

The unpredictability, intermittent and random nature of natural rainfall makes difficult the study of its effects on soils while rainfall is occurring. This makes the understanding fundamental mechanism of natural rainfall characteristics which include, rainfall intensity and its spatial uniformity, drop size distribution, frequency, seasonal pattern, kinetic energy and duration virtually impossible especially during simulation for research purposes. Also, no two natural rainfall event is identical in terms of variation considering these characteristics. These parameters are not only altering within one single rain event but also, varying in space and time (Serrano-Mucla et al., 2013).

One of the key climatic essentials and its distribution which can be highly variable in space and time, particularly over complex terrain is precipitation. Long-term variations of precipitation affect the structure of vegetation directly (Lexer et al., 2002). Hence, recording of previous variations and simulation of future variations and changes of homogeneous precipitation regions are major tasks of climate research. The alteration in climatic change worldwide is not only based on rainfall magnitude but also on the seasonal distribution and interannual variability. The arid and semiarid region are the keenest area to experience such changes in rainfall regimes.

Worldwide, a clear warming pattern is present in terms of temporal evolution temperature but, precipitation trend varies from region to region because its changes are more spatially and seasonal variable than that of temperature. Precipitation can be classified into liquid (rain and drizzle), solid (diverse form) and mixed. Figure 1 depicts the main types of precipitation. Annual precipitation variations depend both on the general atmospheric circulation and local (topographic) conditions. Overall atmospheric moisture is projected at 12 to 14 km^3, a volume that would form a water layer 25 mm thick on the Earth's surface. Up to 90% of water vapor is concentrated in the layer up to 5 km, which quickly decreases with altitude. Atmospheric moisture turnover is 9 to 10 days. About 580 000 km^3 of water fall from the atmosphere in dissimilar forms of precipitation during a year (Borzenkova,2002).

Precipitation may be continuous(temperate-intense) and produced mainly from stratocumulus clouds, heavy rain, from cumulonimbus, or drizzle (light rain), often from stratus clouds depending on the mechanism of cloud development structure. Generally, raindrops diameter is between 5 to 6 mm, while that of light rain drops are smaller (between 0.2 and 0.5 mm). This diameter hardly reaches 6 mm, or more because bigger raindrops are destroyed during falling. Small raindrops are of nearly spherical shape, but bigger ones are flattened when falling, particularly in the lower. The raindrop terminal velocities range from two meters per second for the smallest to about 10 meters per second for the largest. These largest drops, which appear only in heavy rain, especially at the start of a rain storm, can be more than six millimetres in diameter(Borzenkova,2002).

Examples of recent studies reported regarding the European seasonal warming trend shows a high upsurge in temperature in central-northern Europe during winter, an overall fast increase in spring and particularly summer and a significantly lower increase in autumn (Bartolini et al., 2012). Annual precipitation was also found to have increased in northern Europe (Schonwise

and Rapp, 1997) and decrease in southern Europe (Bartoline et al., 2012). According to (Tosic et al., 2014), some studies have already shown an overall rainfall decrease over the Balkan peninsula throughout the second half of the twentieth century.

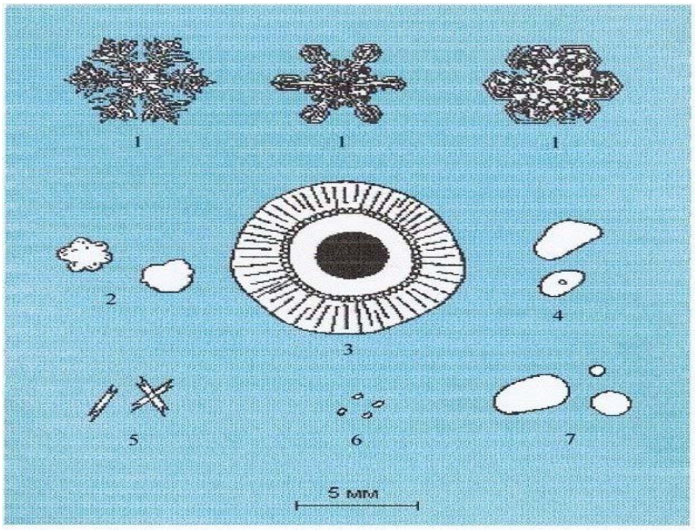

Figure 1. The main types of the precipitation. 1 - snow; 2 - small hail; 3 - large hail; 4 – ice pellets (graupel); 5 - snow pellets (ice needles, ice crystals); 6 - droplets of drizzle; 7 – rain. (www.eolss.net/sample-chapters/c07/e2-02-05-02.pdf).

Simulated rain is widely used as a way of controlling and standardizing experimental conditions, but according to Agassi and Bradford (1999), there are some doubts about the validity of data and conclusions arising from some rainfall simulation studies due to the lack of correspondence between natural and simulated rain. Reproducing natural rain event characteristics in rainfall simulation studies necessitate that we have appropriate knowledge of the corresponding natural rainfall characteristic which includes rainfall intensity, drop size distribution, and kinetic energy of the raindrop (terminal velocity).

3.2.1 Rainfall Intensity

According to Li. and Liu (2004), rainfall intensity is the thickness of falling water within 60 mins which can show how heavy or low a rain is, and normally uses millimetre/hour as its unit (mm/h). It is also described as the most important parameter to describe rain. Classifying rain

as light, moderate, heavy, or violent is based on rainfall intensities of 0-2mm/h, 2-10mm/h, 10-50mm/h, or even greater than 50mm/h, respectively, met office (meteorological office of the UK). Natural rainfall intensities vary widely in both time and space during a natural rainstorm, this can be from zero to several millimetres per minute which make result in the range of storm events very important. For erosion and hydrologic, very low intensities are not of much interest likewise very higher intensities may be so rare which makes their importance limited. Intensities of range 0,2 and 2mm/min are usually of great importance. Rain intensity is not about how often it rains, it is about how heavy it rains even if very heavy downpours only occur once in a hundred years.

3.2.2 Drop size distribution

The size of the distribution of natural rainfall can be very wide, sometimes ranging from near zero to 6 mm in diameter. The median drop diameter of an erosive rainstorm can be between 1 and 3 mm but with an increasing intensity, this value can also increase (Meyer,1994). The distribution of raindrop size depends, among other parameters, the rain rate. Both the average raindrop and the droplet number of concentration increase with rain rate increase. Since the raindrop size directly influences other rainfall parameters, such as terminal velocity and kinetic energy, as well as erosive of rainfall, it plays a considerable role in soil erosion processes. Thus, where the rainfall comprises a wide range of drop sizes, there will also, be a wide range of terminal velocities under normal conditions.

Due to a large number of more or less random processes in the formation of raindrops, predicting the drop size distribution from the first principle can be very difficult. Nevertheless, with the introduction of some modern techniques now, information about raindrop shapes such as canting angles and orientation can be derived significantly (Helseth, 2016). Additionally, raindrop distribution size follows certain regularity grounded on studies from measurement already done. Even if comprehensive and precise evidence on drop size distribution has been collected, the issue of merging such data with the terminal velocity of simulated or natural rainfall into momentum still persist, kinetic energy or some comparable function (Hudson,1981).

3.2.3 Kinetic Energy

The kinetic energy of a given rainfall event represents the total energy that is available for detachment of the soil through rain splash (Renard et al.,1997; Fornis et al.,2002). It is extensively recognized as the potential of rain to disengage soil particles. From the combined

effects of the fall velocity and drop size distribution of raindrops, the rainfall kinetic energy is obtained. Most researchers normally linked more easily available measurement such as rain intensity to kinetic energy, because some of the rainfall characteristics are not common among measured metrological parameters. Such relationships though are important for obtaining the existing kinetic energy from the intensity, but extensive differences exist amid their stated shapes and coefficients.

The rainfall kinetic energy can be articulated in two forms: kinetic energy as a function of time and kinetic energy as a function of volume (Kennel, 1981). For rainfall, the kinetic energy is generally expressed as a function of volume, since manual methods (e.g. filter paper and flour pellets) have been extensively used to derive the kinetic energy from drop size distribution (DSDs) and thus the exposure or sampling time is not exactly known (especially to a precision of microseconds), making it problematic to determine the kinetic energy correctly (Salles et al., 2002). Additionally, rainfall depth data are available at most meteorological stations and so it is comparatively simple to compute the total kinetic energy from the product of the overall rainfall depth and rate of kinetic energy. A relationship between raindrop and rain rate and kinetic energy is shown in figure 2.

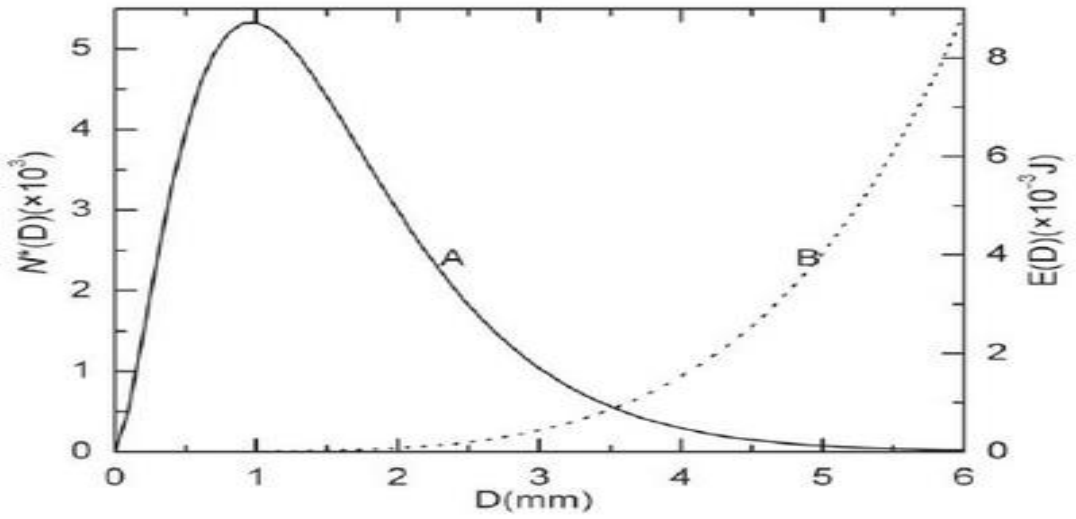

Figure 2: Raindrop size distribution(A) for rainfall rate of 60mm/h and (B) kinetic energy of a single raindrop for different equivalent diameter (Ma et al., 2008)

The size and shape of impacting raindrop and their impact velocity can be influenced by the wind accompanying rain. An observation by Disrud and Krauss (1971) was that, soil detachment from clouds, visible to wind driven rain was more than that caused by rain without the wind. In reality, the wind near the surface will be lower than that at elevation and the drop will suffer differential horizontal deceleration as smaller drops experience a greater drag than the larger drops (Neil, 2004). Tropics rainfalls are high in intensity and high energy load than in temperate regions.

Rainfall varies across the season and it seems that there are also regional differences in the way in which it varies. However, according to van Dijk et al. (2002), there has been a tendency to emphasize on issues such as drop size and kinetic energy at the expense of a corresponding concern with event intensity and duration properties. Another characteristic which has not been properly explored is that of the drop arrival rate on the ground, expressed in impacts per unit area and time, though physical intuition suggests that drop arrival rate could be a parameter of relevance to the understanding of splash, surface seal formation, canopy interception, and other environmental processes.

In conclusion, van Dijk et al. (2002) commented that "in terms of process-based investigation, it seems that our knowledge of the distribution of drop size and terminal velocity in natural rainfall is well in advance of our thoughtfulness of the way in which these relate to detach and carriage soil particles by a splash. If rain falling at high intensities is compared to that falling at low intensities, the former appears to be considerably more effective in detaching soil than is to be expected from the difference in kinetic energy alone. Although results from laboratory studies go some way to explaining this phenomenon, such experiments have been fraught with interpretational difficulties. Moreover, the translation of laboratory results to field simulations is not straightforward because of the fundamental differences between the drop size distributions and fall velocities of artificial and natural rainfall.''

3.3 Rainfall Simulator Design Consideration

Evaluating various infiltration and erosion control or treatment technologies by rainfall simulation methods have been widely used (Sutherland 1998a, 1998b). Sutherland (1998a) noted that the "formative years" prior to 1990 resulted in a mass of information that lacked scientifically credible, standardized methods or data from real applications. His argument ''was for standardized evaluation methods that have field applicability and better prominence

on the study of surface, or near surface processes controlling erosion and having knowledge on infiltration, are a matter that has only been to some extent addressed in succeeding studies.''

According to Grismer(2012), in the past 2-4 decades, comparatively portable rainfall simulators with corresponding plot areas of 1-2 m^2 that are well suited to a wide range of field studies have been more commonly deployed, particularly where access is difficult, or if multiple replications are needed across a larger area. Comparatively portable rainfall simulators have also been used to study runoff and erosion properties in an extensive range of environments; nevertheless, these rainfall simulators have a tendency to compromise natural rainfall characteristics in practice, due to portability, cost design and/or management limitations (Meyer 1988). However, direct field measurements of runoff and erosion rates as well as to some degree modeling methods capable of forecasting these rates from less-disturbed forest and rangeland soils (as related to bare compacted or tilled soils) remain few. 'While runoff and erosion rates per unit area from rangeland and forest soils are generally much less than that from more disturbed soils, substantially larger areas within watersheds often comprise these soils and may contribute substantial loading to streams''. (Griesmer,2012)

According to Grismer (2007), the use of USLE as a determinant factor of net erosion mass per unit area is now limited and information about the runoff particle-size distribution, nutrient content and contaminant concentrations from erosion control treatments or soil restoration efforts for specific storm events are needed to assess their relative performance. ''Concerns about the lack of standardized RS methodologies or designs and precise determination of the process being measured are not new'' Lal (1998) and Agassi and Bradford (1999) suggested there is an inability to compare results between studies, and possibly as a result, generation of undependable erosion rate estimates.

Meyer (1988) contended that the results from simulated rainfall only give reasonable, rather than comprehensive, erosion data; and that to compare the simulation results to that of natural events, data from comparable plots focus on long-term natural rainfall events must be accessible for assessment, later, Hamed et al. (2002) also reported such a comparison. However, as there is a little replacement available for generating process-based erosion information and infiltration rate, RSs in the field will continue to be developed and used.

3.3.1 Basic design-overview

Replication as closely as possible the physical characteristics of natural rainfall, and to do so with a device that matches the process scale of interest and resources accessible are two of the

challenges encompass the design of rainfall simulator. According to Esteves et al. (2000) and Battany and Grismer (2000),'' rainfall simulators can also be classified according to the type of raindrops that are generated. The first group is the non-pressurized simulators (the drop-forming) and that of the second group is the pressurized simulators (nozzle type) (intensities of 10 to 200 mm/hr and drop sizes of 0.1 to 6 mm)''. This classification is so important and a key component of any rainfall simulation project. All other decisions depend on the method of drop formation (Mayer,1988). Accordingly, each type has its own methodological consequences and biases and is appropriate for different circumstances.

RSs have ranged from the modest, very small portable infiltrometer with 15 cm diameter rainfall area (Bhardwaj and Singh, 1992), to the intricate Kentucky rainfall Simulator covering a 4.5 m by 22 m plot (Moore et al., 1983). The design or type of RS has been directed at meeting the often-competing demands of "replicating natural" rainfall, effortlessness of portability across remote areas, problematic or sharp terrain, costs of construction and consistency of simulated rainfall across the test plots in relations to intensity, drop sizes and kinetic energies.'' Replicating both the range of drop sizes and kinetic energy of natural rainfall has proven quite difficult; similarly, is the development of a controllable, unchanging, or even spreading of rainfall across the plot'' (Grismer, 2011).

The drop-former type as shown in figure 2 consists of a constant-head water reservoir placed at the top of the Simulator, which feeds a grid of several hundred capillary tubes (Commandeur and Wass, 1994). Also for drop forming simulators, the common practice has been to form drops at the tip of a material by some suitable device. The weight of the drop has to overcome the surface tension force of the drop former and the droplets start with an initial velocity of zero. (R, Pall et al.1983)

Drop-formers that use yarn strings and plastic tubes operate at very low pressures and generally, produce a narrow range of drop sizes whose drop kinetic energy depends on the drop-forming mechanism height above the soil plot. Agassi and Bradford (1999) contended that drop-former RSs that produce only single drop size are generally used in fundamental erosion studies and that such simulators should not be used to compute interrill erosion mechanisms of wash and splash (Bradford and Huang, 1993). Bradford and Huang (1993) disclosed that erosion rates determined from a nozzle and single-drop-size type RSs at the same intensity can be fairly different. Although they argue that capillary tube type RSs with a

hanging screen provide a good substitute to the nozzle type simulators, but they added that their usefulness is limited to the laboratory.

According to Clarke and Walsh (2007), modified drop-formers operating at larger intensities can develop uni-modal drop-size distributions as found and shown in Figure 3 which was also previously developed. For example, using a mesh screen placed some distance below the needles, breaks the uni-size drops into a range of smaller and larger drops (Roth and Helming, 1992). The Roth and Helming (1992) RS consisted of 2500 capillaries 0.3 m suspended below which was a screen with a 3- mm wide opening resulting in drop sizes ranging from 0.5-5.0 mm and a median drop size of 2.89 mm that fell from 7 m above the test plot. Their RS produced rainfall with drop velocities approaching close to 95% of terminal velocity at intensities of 30 and 60 mm/hr.

Drop-forming simulators are unworkable for field use since they need such an enormous distance (10 meters) to reach terminal velocity and that they do not produce a distribution of drops unless a variety of drop-forming sized tubes are used (Grierson and Oades, 1977). Another undesirable effect of the drop forming simulator was their inadequate application to small plots. Because of this, numerous points of raindrop production must be closely packed to generate an intense sufficient downpour of rain (Bubenzer, 1979b).

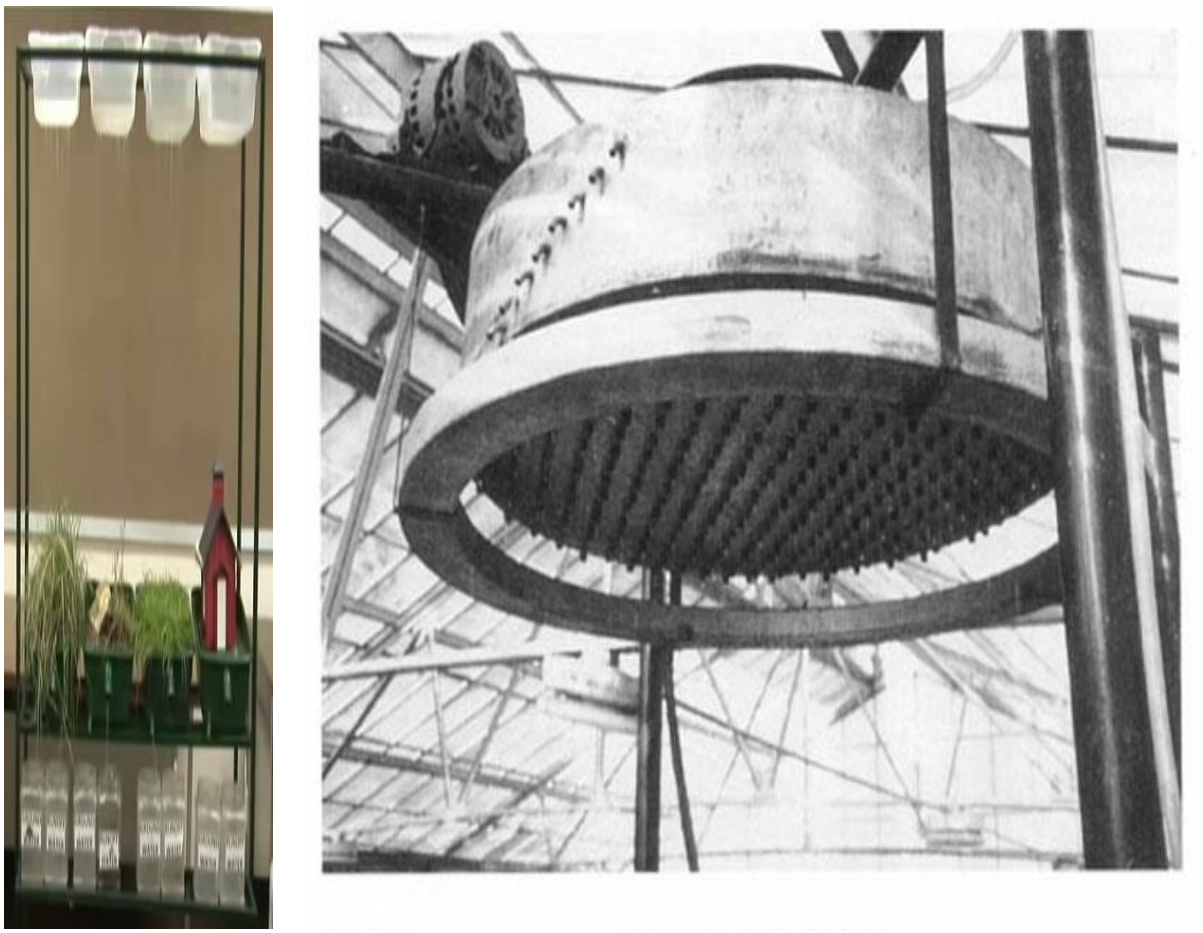

Figure 2: showing a photo of a drop forming rainfall simulator. Source and http://www.fao.org/docrep/T0848E/t0848e-11.htm

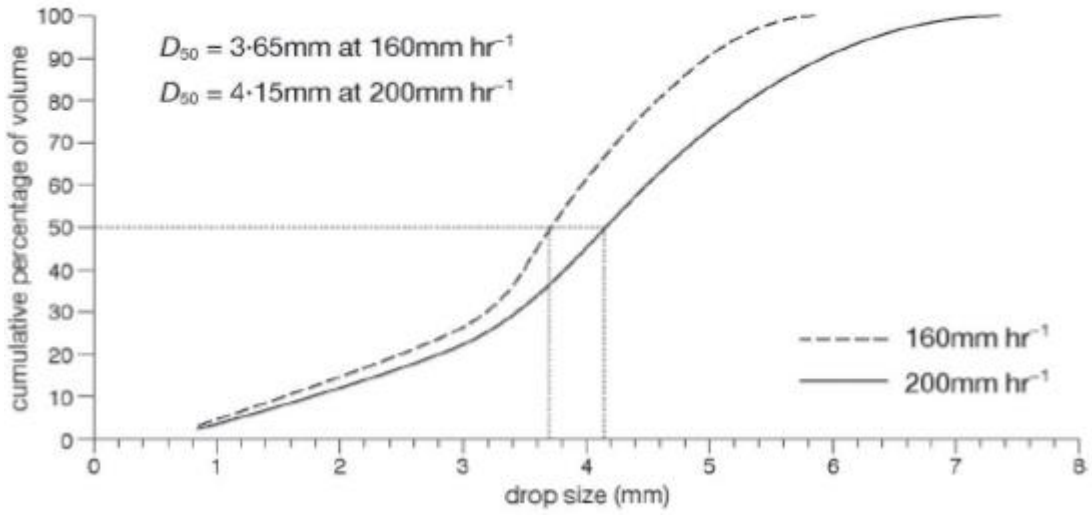

Figure 3: Cumulative drop-size distribution from a modified drop-former rainfall simulator operation at a relatively high rainfall intensities (Clarke & Walsh,2007) D_{50}=mean

For the nozzle simulators type, it can either be gravity fed or pressurized and can be potentially very large, depending on how many nozzles are used (Wilcox et al.,1986; Mayer,1988). Drop-size distribution across the width of a spray of the fan type follows a bell- like distribution with bigger size drops more centrally located while lesser drops encompass the fan edges. Agassi and Bradford (1999) emphasized that drop velocity for a fan-type veejet nozzle preferred by numerous researchers vary from an extreme vertically above the demarcated area and decreasing toward the demarcated area edges. This discrepancy in velocity is reduced by increasing the height of the nozzle directly above the demarcated area and by reducing the travel angle (Meyer and Harmon, 1979). Stationary full jet spray nozzles tend to generate spatially comic drop distributions (Hall, 1970).

Single-nozzle type RSs tend to generate less evenly distributed intensities as compared to multi-nozzle systems as noted by Loch (2001). Multi-nozzle RSs have a tendency to develop restricted zones of higher relative rainfall rates associated with overlapping spray patterns. Nozzle-type RSs that use rotating or oscillating spray nozzles have an inevitable rainfall intensity periodicity (Kinnel, 1990) over the plot surface (i.e. 893 rain surges, followed by a period of repose), such that rain intensities and uniformities not only depend on nozzle water pressure but also on fan sweep oscillation frequency (Paige et al., 2003). Also, Paige et al. (2003) notice that veejet nozzles working from a drop height of 2.44 m and at a nozzle operating pressure of 41 kPa results in a median drop size of 2.985 mm while increasing that pressure to 55 kPa increases the breadth of the drop-size distribution to a range of 0.29 – 7.2 mm while decreasing the median drop size to some extent a value of 2.857 mm. Figure 4 below is an example of the nozzle type.

Figure 4: showing nozzle type rainfall simulator. Source: https://www.ars.usda.gov/northeast-area/beltsville-md/beltsville-agricultural-research-center/emfsl/docs/environment and http://catchmentsolutions.com.au/water-quality/

In general, Simulators needing nozzles can be fastened to a metal frame or framework and assemble in an array or in a grid pattern over the study area. The more nozzles used, the greater the water pressure needed, and the most water-intensive the simulator becomes. The output range of drop size nozzle simulator is closer to, but still not exactly that of natural rain. The operator's ability to manipulate the water pressure and the nozzle design can account for this limitation. This type of nozzle (pressurized) is also noted for their variability of usage (including in the field) and that their intensities can be varied more than the drop forming type (Grierson and Oades, 1977).

In the past decade alone, the use of roughly 40 different RSs in erosion related research has been reported in more than a dozen different types of journals, of which close to 80% are of the nozzle type and the remainder drop-former type. Table 1 below shows some summarized examples of the characteristics of several more recently reported rainfall simulators (Grismer,2011).

Advancement in nozzle-type RS has been of multiple and different spray nozzles and the use of a computer, controlled solenoid switches/valves that rotate, sweep or vibrate the spray nozzles (Norton and Savabi, 2010). likewise, with the drop-former type, RSs is the inclusion of larger areal density, hypodermic needles in vibrating, or rotating chambers, or use of “screens” below the drop-formers to partially manipulate drop-size distributions.

RS Description Lab - Field NZ=Nozzle DF=Drop former	Drop fall height (m)	Intensity range or used (mm/hr)	Median (D_{50}) drop size (mm)	Rainfall KE ($J/m^2.mm$) or Power	Intensity Distribution Uniformity (CU, %)	Plot size (m^2)	Reference
Field-NZ Three screened "F" nozzles	3.0	60-120	3.7	1450-2900 J/m^2-hr		0.6x0.76 m	Designed by Gifford (1968); used by Guerrant et al. (1990)
Field- NZ 1-3 screened "F" nozzles @29 kPa	1.4	2-86		23	87-92	1-3	Miller (1987)
Field-NZ 6.35 mm impact sprinkler nozzle	1.37	12-63	1.8				Designed by Miller & Mahannah (1982); in Guerrant et al. (1990)
Field-NZ 180^0 fan nozzle & 6.35 mm impact sprinkler	2.13	80-100	1.6				Guerrant et al. (1990)
Field-DF	2.5					0.9x1.52 m	Freebairn and Gupta (1990)
Field-NZ Guelph RS with full jet nozzles	1.5	18-200			88-90	1.0	Tossell et al. (1990a & b)
Field-NZ	3.0	48 & 58		13.1		2.56	Navas et al., (1990) & Navas (1993)
Field-DF 500-23 gage needles in $1m^2$ rotating disk	1.4	80-100	2.5	1060-1330 J/m^2-hr		0.6x0.76 m	Designed by Malekuti & Gifford (1978); used by Guerrant et al. (1991) & Naslas et al (1994)
Field-DF 554-0.56 mm Teflon tubes per m^2	2.7	45	3.0	75% of terminal	91	0.76x0.76 m	Commandeur (1992)
Field-DF	2.0					0.5	Wierda and Veen (1992)
Field-NZ 20 full-cone nozzles	2.2	21	95% < 2	13.5		80	Marques et al (2007)
Field-NZ/DF	0.033–0.054	72	5.9	4		0.0625	Designed by Kamphorst (1987); Jordan & Martinez-Zabala (2008)
Field-NZ	3.5	56.5 & 90				0.23	Designed by Navas et al. (1990) & Lasanta et al. (2000). In Martinez-Zavala et al. (2008)
Field-NZ	3.5	56.5				0.13 (circular)	Designed by Navas et al. (1990) & Lasanta et al. (2000); used by Jordan et al. (2008)
Field-NZ Oscillating veejet 80100 nozzle	2.0	~100		29.5		1.5 x 2.0 m	Designed by Loch (2001) Sheridan et al. (2008)
Field-NZ Operated @ 45 kPa	2.5	20, 30 & 40				0.6	Pappas et al. (2008)
Field-NZ Veejet 80100 nozzles above rotating disks, operated @ 36 kPa	2.3	94-573	1.8 & 2.0	>90% of terminal	81-85	0.7	Sobrinho et al. (2008)
Field-NZ		69				40	Tatard et al. (2008)
Field–mod. DF 216 holes of 0.5 mm diameter	1.5	24.5 & 32	3.6			0.95 x 1.2 m	Vahabi & Nikkami (2008) Vahabi & Mahdian (2008)
Field-NZ Oscillating Veejet nozzles @ 41 kPa	2.5	70	1.05			0.3 (lab)	Designed by Foster et al. (1979), in Rimal & Lal (2009)
Field-NZ Micro-sprinklers	2.2	75		28.1		2.5	Singh & Khera (2009)
Field-NZ Oscillating Veejet 80100 nozzles @ 41-42 kPa	3.0	100				1.0	Folz et al. (2009)
Field-NZ Oscillating jet	3.5	60				1.0	Designed by Asseline & Valentin (1978); used by Blavet et al. (2009)

Table 1: Summary of example reported RS characteristics from studies between 2007 and 2010(M.E. Grismer,2011)

Field-NZ Oscillating flat fan Veejet 80150 nozzles	2.13	170-200	3.5	22.6	87	1.0	Designed by Meyer & Harmon (1979) as modified by Kato et al. (2009)
Field-NZ Four Fulljet ½ HH 40WSQ nozzles w/ solenoid valves @ 45 bar		47				1.2x3.9 m	Designed by Strauss et al. (2000); Armstrong & Quinton (2009)
Field-NZ TeeJet® TG SS 14W nozzles	1.8	85 & 170	4.5			2.7	Designed by Schiettecatte et al. (2005); in Jin et al. (2009)
Field-NZ 4 full-cone Unijet nozzles	1.8	119-124			~91	1.0 x 2.5 m	Sangüesa et al. (2010)
Field-NZ Fulljet 24WSQ & 50-WSQ nozzle @ 34.5 kPa	3.0	45 & 85	1.0 & 1.6		85-86	2 x 2 m	Dufault & Isard (2010)
Field-NZ Full-cone nozzle with solenoid valve (90-300 kPa)	2.0	21-83	0.5 - 2.8	15.1			Designed by Miller (1987),
Field-NZ Full-cone nozzle with solenoid valve (90-300 kPa)	1.0-1.4	20-80	0.5-2.8	15.1	80-92		Perez-Latorre et al. (2010)
Field-NZ Oscillating flat fan Veejet 80100 nozzles	2.2	10-130	2.2	27	~90	1 x 6m	Norton & Savabi (2010)
Field-NZ 1-3 180° plane-jet NZs @ 20° angle & 100 kPa	1.0-1.4	20 (1 nz) 59 (3 nz)	0.5 - 2	10.1	80-92		Perez-Latorre et al. (2010)
Lab-NZ	1.96	64.3 & 95.6					Designed by Morin et al. (1967); Sepaskhah & Shahabizad (2010)

Table 1(continuation): Summary of example reported RS characteristics from studies between 2007 and 2010(M.E. Grismer,2011)

3.4 Testing and Evaluation of Simulators

The design, development, testing and operational characteristic of two very different nozzles simulators were described by both Wilcox et al. (1986) and Esteves et al. (2000). This nozzle type was: a hand-portable small-plot single-nozzle simulator for use on slopes up to 70%, and a large portable, multiple-nozzle simulator for use on huge cultivated plots. using stock hardware parts, the two simulators can be easily assembled. A price list was even added by Wilcox et al. (1986).

The drop-size, intensity and the relationship between them were measures by Wilcox et al. (1986) using the floor-pellet method, which had been propagated by Laws & Parsons (1943). In the flour-pellet method, a thick layer of fine, uncompact flour with a smooth surface is visible to rainfall for an ephemeral measured period and then left to dehydrate until the resultant dough-pellets are firm (generally 24 hours or more). The pellets are then recovered from the flour, weighed, sorted through a sequence of sieves, and their size distribution plotted. Esteves et al. (2000) did not clearly state which method of calibration they used for their simulator, even though they briefly mention two different methods, the coloured

absorbing paper method, which was established by Wiesner in 1895, and the disdrometer method.

For the absorbent paper method, it consists of sheets of filter paper which has to be exposed to the rain for a brief interval but before it has to be dusted with water-soluble dye. The resulting spots are rendered permanent by the dye, and from these, the size of the drops can be calculated (Laws and Parsons, 1943). The disdrometer is an expensive machine, but the measurement and calculation of the raindrop size distribution are done automatically and continuously. It was developed in order to cut down on the amount of number-crunching that often is related to calculating these kinds of distributions.

The hand-portable simulator was developed to fill a necessity for a light, adaptable, low-cost simulator that can be used in almost any location with interchangeable nozzles. The focus for such a work was based on the physical dimensions of the component pieces, the intensity generated by dissimilar pressures and nozzle heights, and the drop-size distribution at dissimilar locations over the plot surface for different pressures. It was revealed that the hand-portable simulator generates a lesser drop-size diameter than natural rainfall for any given intensity and that the relationship was undesirable. This result was established by Esteves et al. (2000). This exemplifies one of the key problems with pressurized nozzle simulators.

Way back in the past, Laws, and Parsons (1943) recognized that there exists a positive relationship between natural rainfall intensity and drop-size. But they concluded that with pressurized nozzles, the relationship was reversed. Intuition tells us that this most probably occurs because of the "atomization" of the water drops that occurs when the pressure is out (when the water exits the nozzle). A typical example to this is by putting your thumb over the tip of the nozzle of a garden hose, this can tell you that the greater the water pressure, the greater the atomization (the smaller the drop size). Even though the physics or mechanism of such a phenomenon is not clearly analyzed in the rainfall simulation literature, however, I think it is an area that needs more research.

The large portable multiple-nozzle simulator is made up of a network of standing pipes and 6 upward-jetting nozzles, each of which can spray to a height of 8m and cover a plot size of 7x7m. This reflects the importance of the relationship between fall height and velocity for different size drops established by Laws (1941). In order for a raindrop to attain a "terminal velocity" comparable to that of natural rainfall, it must drop from a height of at least 9 meters. The stand-up pipes are held in place by guy ropes. Even though the important of

spatial uniformity of rainfall was mention, but it was only Esteves et al. (2000) that include a detailed analysis and maps of variation (coefficient of uniformity was dependent on rainfall intensity, and water pressure.

In general, rainfall simulators are not developed to be used in all circumstances under all conditions, but to fill specific roles in research. Large, electronic and hydraulic simulators that cover plots more than 100m² can mimic natural rainfall fairly well and are used to establish quantitatively correct infiltration, runoff, and erosion averages. Small portable simulators are used to establish relative data for specific situations (Meyer, 1988; Foster et al., 2000). Nevertheless, Foster et al. (2000) note that non-existence of standardization of simulator design makes it problematic to relate data from dissimilar simulators and they recommend the establishment of a key European laboratory funded by the EU. In addition to observation by Foster and Grismer (2012), their comment was that, in the frame of research that employed rainfall simulation, there is no sole standardized design or procedure for conducting rainfall simulations. Actually, at the 2011 "International Rainfall Simulator Workshop" at Trier University, Germany, a collaborative community of scientists from 11 contributing countries concluded that a standard procedure for rainfall simulation and simulators is needed in order to ensure the comparability of results and to encourage further technical expansions to overcome physical limitations and restrictions (Ries et al., 2013).

Downsides of many portable simulators are the small plot size (often less than a square meter) that can be covered by each simulation and, therefore, the unsuitability of the data for extrapolation. Many simulations over a large area are required to generate enough data to support individual simulations. Rainfall simulation is an essential, though imperfect technique for relating geomorphic and soil hydrologic response to rainfall characteristics.

The first step in the development of a rainfall simulator should be the establishment of selection criteria depending upon the rainfall characteristics required and objectives of the research program. Any discussion of using rainfall simulators must start by defining precisely what information is essential. Simulators can be a suitable tool for some purposes but quite unsuitable for others and the aims will affect the utmost factors when choosing the accurate type of simulator. For instance, in studies of infiltration and runoff, it is not compulsory for the simulated rainfall to have precisely the same characteristics as natural rain. In other studies, it may be significant that the erosion processes are not distorted by the simulated rain being different from natural rain (Hudson,

CHAPTER FOUR

METHODOLOGY

Controlling the intensity and duration accurately and precisely is one of the key attributes of a rainfall simulator(RS). Measurements have been carried out in the laboratory to ensure constant conditions and to exclude exterior influences to select the right jet and appropriate pressure condition for the field experiment in the future.

4.1 Construction (structure)

The simulator was designed to be lightweight, portable, and emphasizes the use of inexpensive and readily available materials requiring minimal construction and operation expense. The frame of the simulator was constructed from a 32 mm (1.25 inch) diameter aluminum hexagon pipe. The top of the simulator was permanently assembled and covered with a tarpaulin, but the legs and braces were detachable. Adjustable angle fittings are used to attach the legs and side braces.

The height of the frame can also be increased with the aid of the four legs on the bottom corners. The legs are designed to get the simulator into a leveled horizontal position if the rainfall simulation runs on uneven terrain. The height of the nozzle can be adjustable, and it is possible to increase the height by the legs on the corners by various depth to over 160cm. To make the simulator easy to disassemble and reassemble, the swivel pins in the adjustable angle fittings were drilled out and replaced with larger, removable locking pins. With these quick coupling fittings attached to the legs and braces, the simulator can be dismantled/assembled by maneuvering the pin. The fittings are numbered to ensure proper alignment upon re–assembly.

The frame was constructed so that windscreens attached to each side and secured at the top and bottom to not affect rainfall simulation. Because even a gentle wind can affect the trajectory of the rain droplets (Delima et al, 2002) and this makes it complex to determine the amount of rain on the demarcated area (Covert and Jordon, 2009). The frame was designed to be sturdy and can withstand windy conditions using four stakes and tie–down straps positioned at each leg of the simulator. The tee was connected to a 25 mm (1–inch) diameter PVC water supply pipe, which was attached to the aluminum frame via 25 mm (1–inch) conduit hangers.

4.2 Simulated Rainfall Generation

A pressurized simulator, where the raindrop is produced by a single nozzle, was considered in this experiment. The RS was set up as shown in Figure 5 and an area size of 100 cm by 100 cm was demarcated as the area under consideration. The nozzle assembly used in the simulator was a single Spraying Systems Full jet nozzle, described previously by Shelton et al. (1985). The nozzle was centered at the top of the frame 1.6 m high and was threaded directly into a 13 mm (0.5–inch) PVC tee. The horizontal and vertical position of the nozzles can also be adjusted according to the requirement of specific simulation. This demarcated area can be enlarged by employing more nozzles. Each nozzle can be switch on and off by a ball valve. A metal plate of the same size as the demarcated area was placed in the selected area directly at the center under the RS. The metal plate was covered with vessels to replicate a soil field which received drained water (rain drop). Eighty-two 100 mm (3.9-inch) diameter vessels were used instead of a rain gauge and were placed on the metal plate underneath the RS on a 1.5 -2.0 grid at a spacing of 0.125 cm (inch). The plate was horizontally and vertically marked permanently for each of the eighty-two vessels (containers) which was used as shown in Fig 6. The containers were also labeled from one to eighty-two to correspond with the same mark on the metal plate throughout the experiment for consistency.

The water supply section consisted of a 200-litre used tank (mounted in the Lab) as a water reservoir, an electric pump with pressure chamber to ensure a constant water supply from the tank. This also keeps the pressure and flow rate constant. Also, the water supply was an independent section from the main RS structure but was linked to the system through a manually operated ball valve. The main ball valve behind the motor pump can switch the whole simulation process on/off, and this ball valve can also be used to adjust the water pressure in the system. The water pressure is not measured directly on the nozzle, but in front of the nozzle on the income piping. The flow rate was controlled for each nozzle by the manually operated valve. When the valve was in closed position and the pump was switched on (with water in the reservoir), a mini circulation system was created which helped to remove any trapped air within the supply tube to the RS.

The sequence was started by first ensuring that the selected nozzle for a particular test run is still or position in the middle. then the pump turned on and the pressure gauge set to the correct pressure. The rainfall intensity was determined by the amount of water collected in the

containers during the experiment. After each repetition, the runoff water (raindrop that falls outside the demarcated area) was not considered for this experiment. Also, the kinetic energy of rainfall was also not calculated for this work. Water pressure was observed since a decline of water level in the supply tank caused a loss of pressure at the nozzle. The lower and high flow rates caused insufficient rainfall conditions, regarding the rainfall intensity and drop size.

A low-pressure regulator was also used in combination with a liquid-filled pressure gauge to ensure that a particular chosen bar nozzle was maintained. An in-line filter was placed in the flow stream to prevent foreign particles from clogging the regulator and the nozzle. The flow was monitored manually from the starting time to the ending time because the experiment was repeated when there is any interruption in water flow or massive droplets of water accrued or detection of overfilled containers.

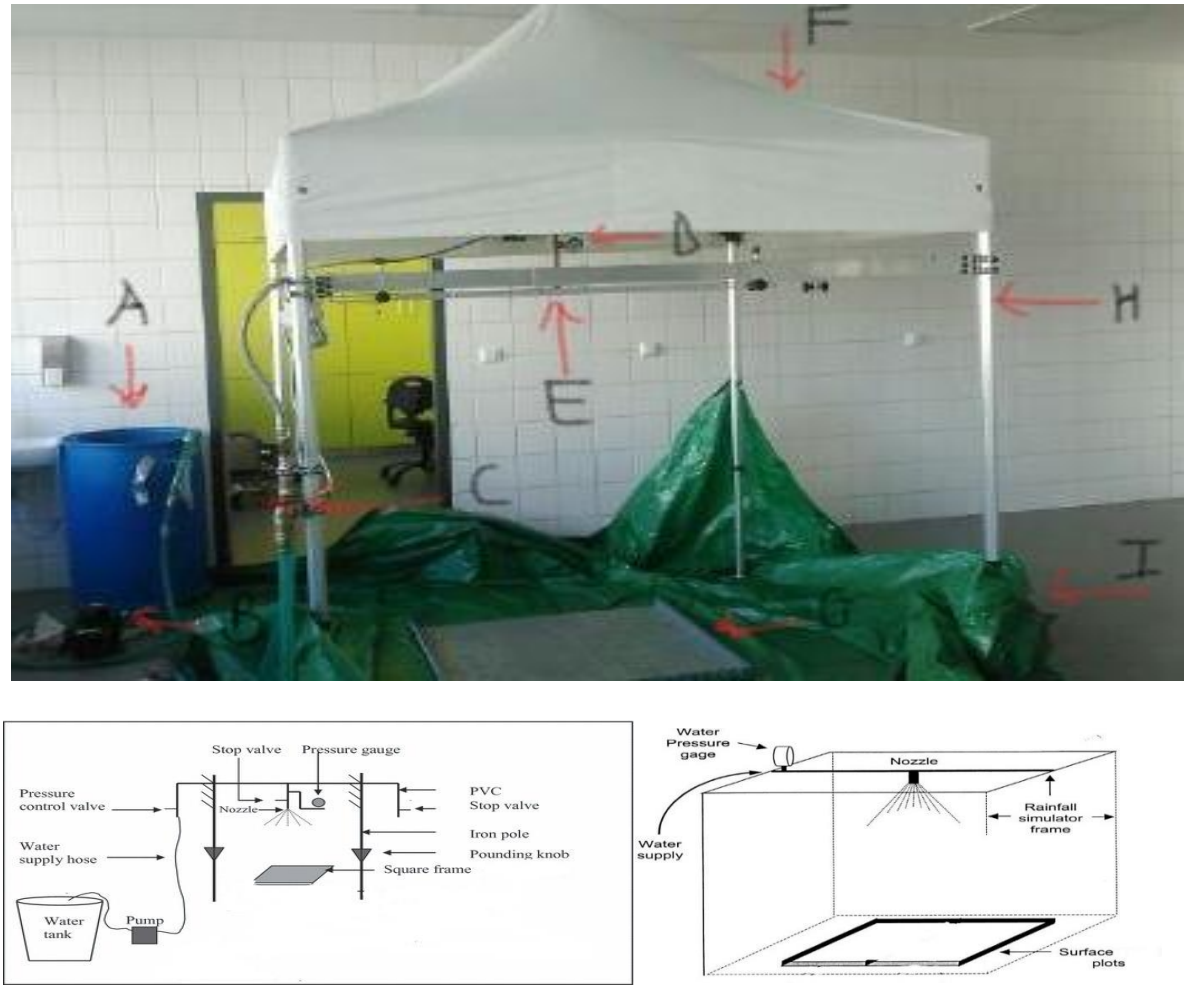

Figure 5: Set up of the Rainfall Simulator with a sketch showing its operation. A—Water Tank B—Electric Pump C—Main ball Valve D—Pressure gauge meter E—Nozzle position F—Top Cover G--- 100 by 100 cm metal plate H—simulator stand I—Windscreen.

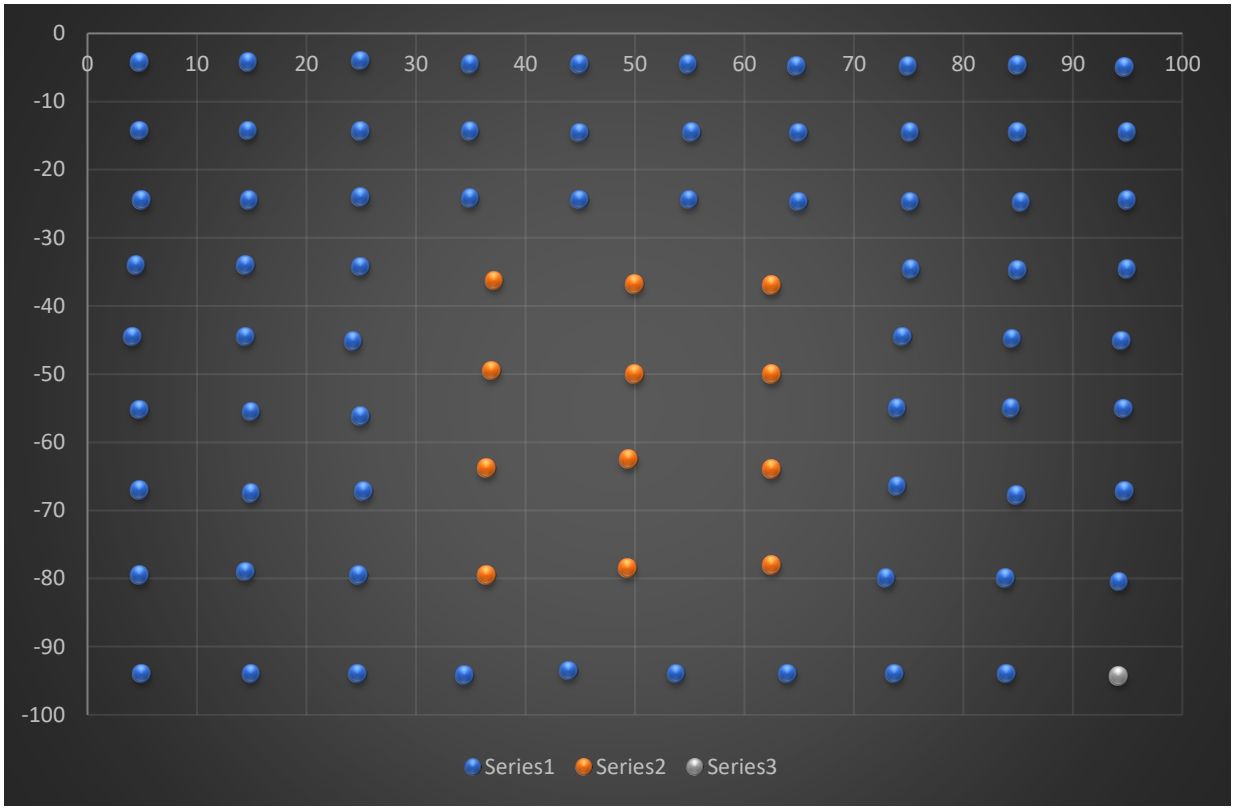

Figure 6: Showing the position of the vessels on the metal plate (it was not evenly showing well on the chart but was done properly on the plate as shown in fig 4) the vessels were not all of the same sides and there were 82 in numbers for 100 boxes on the chart. Series 1 was the medium size, series 2 the biggest size and series 3 the smallest size vessel.

4.3 Selecting of nozzle size to use

One of the aims of this work was to selected an appropriate nozzle with the appropriate pressure condition for a future field work. Three standard sizes nozzle used for rainfall simulation as shown in Figure 7.1-7.3, was selected to represent high and low rainfall because each nozzle has an optimal performance pressure and flow to achieve proper size and intensity. Also, selecting of the nozzle for a particular study is mostly determined in relation to the intensity of the natural rainfall event to be represented. The nozzle selected for the high rainfall is Lechler 460.608.30.CA. For the low rainfall, two nozzles were selected which were very similar but slightly difference with output size. They also have the same number and for this work, these two low rainfall nozzles will be classified as follow; low A and B (Lechler 460.368.30.CA).

Low nozzle (low A rainfall) ---------- Lechler 460.368.30.CA

Low nozzle (low B rainfall) ----------Lechler 460.368.30.CA

Highest nozzle (high rainfall) ----------Lechler 460.608.30.CA

Figure 7.1: Photo of the highest nozzle

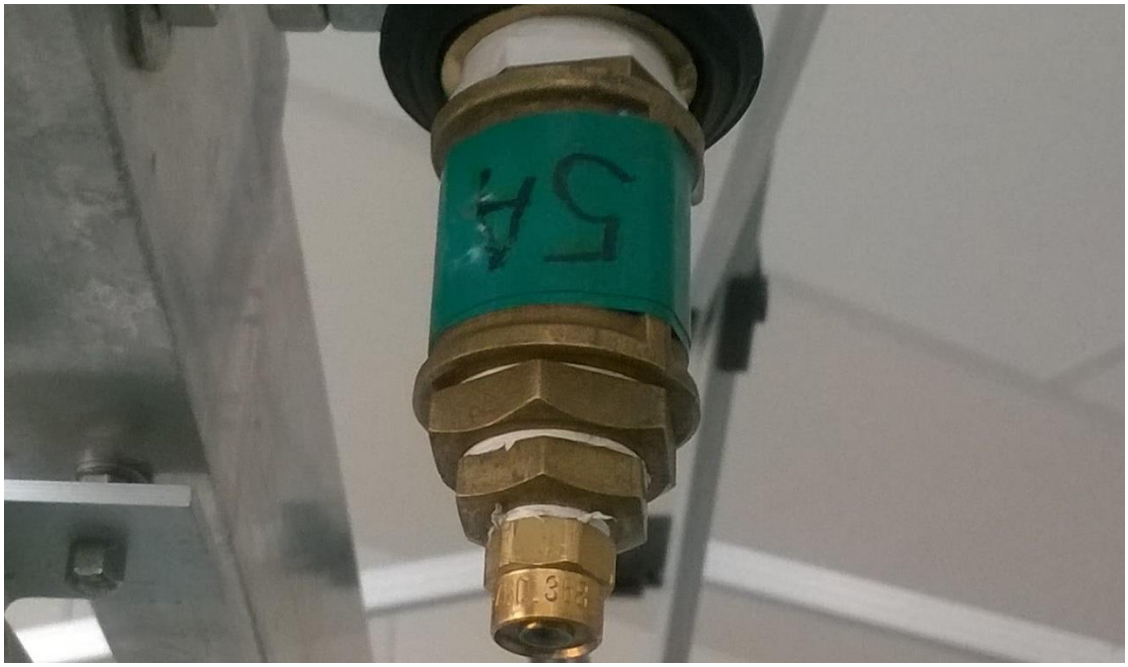

Figure 7.2: Photo of Low(A) nozzle

Figure 7.3: Photo of Low(B) nozzle

4.4 Calibration of Rainfall Simulator

The calibration of the rainfall simulator was carried out in the hydrological/hydraulic laboratory of the department of Water Resource and Environmental Modelling, Czech University of Life Sciences. The calibration was a focus on the selected nozzles.

4.4.1 Nozzle calibration

The rainfall intensities by the nozzles were calibrated under various water pressure condition first at varied depth and then fixed height condition. The varied depth of 100.1,150 and 160cm was done with a random selected water pressures condition for only one of the least nozzle used (Lechler 460.368.30.CA). Even though such a result was desirable and was even analyzed, it was not the main focus of this experiment. This also helped me to fine tune the position of the nozzle at the height of 160cm. The main focal point was using all the three nozzles at a fixed elevation of 160cm with varied water pressures of 1.6,1.8.2.0 and 2.2 bars. These pressures were also simulated during the calibration process. The rainfall intensity was determined by the volume of outflow from the demarcated area of 100 by 100cm.

4.5 Methods for Evaluating the Rainfall Characteristics

The evaluations for this experiment was done based on spatial variability, the coefficient of determination, the spatial variation of intensity uniformity and result on the spatial rainfall distribution.

4.5.1 Spatial rainfall distribution

The measurement of the spatial rainfall distribution pattern on the demarcated section was carried out in order to get information about the homogeneity or heterogeneity of the rainfall as produced by the rainfall simulator and its reproducibility. The eighty-two vessels (containers) used for the collection of raindrop was of three different sizes. They included: containers numbering one to sixty-nine (medium size), seventy to eighty-one (largest size), which were placed within the center most part (container with number 74 was directly in the center with each of the nozzles) and vessel eighty-two (smallest size). All the containers were distributed to cover the whole area of the 100 cm by 100 cm metal plate as shown in Figure 8 and were read manually.

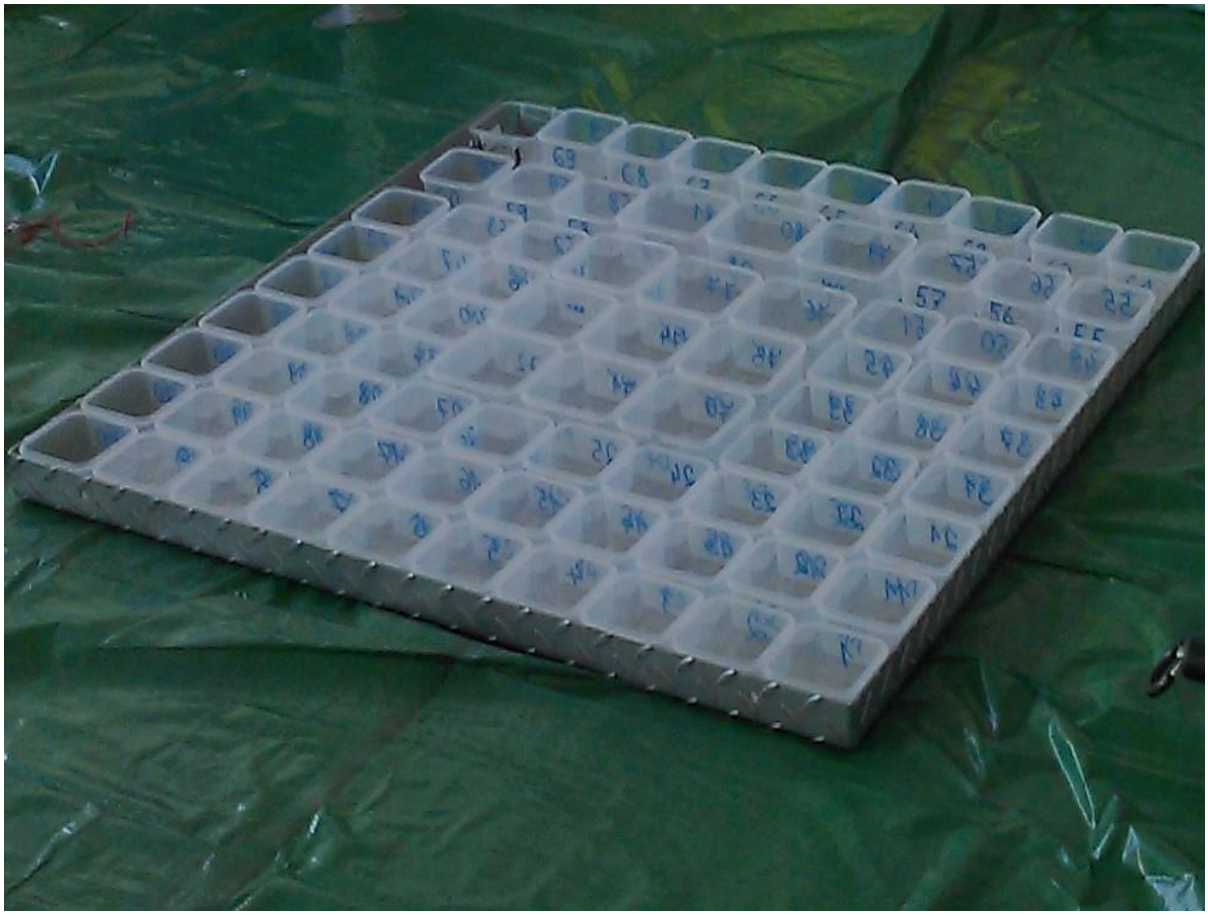

Figure 8: Distribution of the 82 containers on the demarcated metal plate (100cm by 100cm)

For each of the three nozzles selected, four different readings were taken at fixed elevation of 160cm but the varied pressure of 1.6 bar, 1.8 bar, 2.0 bar and 2.2 bars. Each of the eighty-two

containers was weighed empty before the start of the sequence (taking the initial time) then distributed on the metal plate. All the individual containers were weighed again after the end of each sequence (final time) this time containing raindrops to determine the actual weight of the raindrop at each location across the demarcated area. The result was calculated into rainfall intensity values (mm/hr) and spatial display. The exposure time for each sequence was between 30 to 76 mm. For the nozzle with the highest rainfall, the time sequence was immediately stopped when at least one container was almost filled to the brim. The whole result (data analysis) was also computed for.

4.5.2 Coefficient of Determination (R^2)

The mean intensity rainfalls were analysis against the given pressures for each nozzle to determine if there exist a good or bad linear relationship.

4.5.3 Spatial Variability

The individual rainfall intensities for each pressure conditions were analyzed against the given pressure for each nozzle using boxplots for information on spatial rainfall variability. Within each type of grouping variable, a single boxplot is a graph that contains one box for that data. According to points that are the same distance apart from each other, a grouped box plot is a graph where the data is grouped. The boxplot has the capability to take spatial data and envisage the lowest value, first quartile, median, third quartile and the maximum value (Burt and Barber, 1996)

4.5.4 Rainfall spatial variation of intensity

For falling drops, its spatial uniformity, which is directly influenced by the spatial variability of rain intensity, will have a direct influence on the effective energy per unit area. Because of this, the absolute value of raindrop kinetic energy over the demarcated area at a given intensity and that of the spatial uniformity of natural should be precisely reproduced by the functional rainfall simulator being used. Henceforth, ensuring the distribution of raindrops produced by a rainfall simulator to be comparatively uniform over the demarcated area cannot be ruled out. This result is very important so Christiansen uniformity coefficient which is a standard equation for uniformity was used on the collected data. According to (Egodawatta, 2007, Moazed et al., 2010), a Christiansen uniformity coefficient (CUC) of 80% or more is satisfactory to ensure simulated rainfall patterns are representative.

$$CU = 100\% \left[1 - \frac{\sum_{i=1}^{n} |x_i - \bar{x}|}{\bar{x} * n}\right]$$

Where:

CU is the Christiansen uniformity coefficient

$$\sum_{=1}^{n} |x_i - \bar{x}|$$

x_i = individual amount per rain gauge(vessel)[ml]

$\bar{x}$ = arithmetic mean of applied water per rain gauge[ml]

n = total number of rain gauges(vessels).

(Christiansen,1942)

CHAPTER FIVE

RESULTS

5.1 Coefficient of Determination (R^2)

Figures 9 & 9.1 and table 2 shows the result for the calibration of the low and high rainfall using Low (A&B) and that of the highest nozzles under various pressure conditions. The figures also show the rainfall intensity estimation regressions on the basis of water pressure in the system which was based on a fixed elevation of 160cm. Figure 9.2 and table 3 also shown the result for the calibration and rainfall intensity estimation regression for only Low (A) nozzle which was based on selected pressures and varied depths of 100.1,150 and 160cm.The result was to give some idea about the relationships between fixed and varied elevations (depths) in terms of different pressure conditions

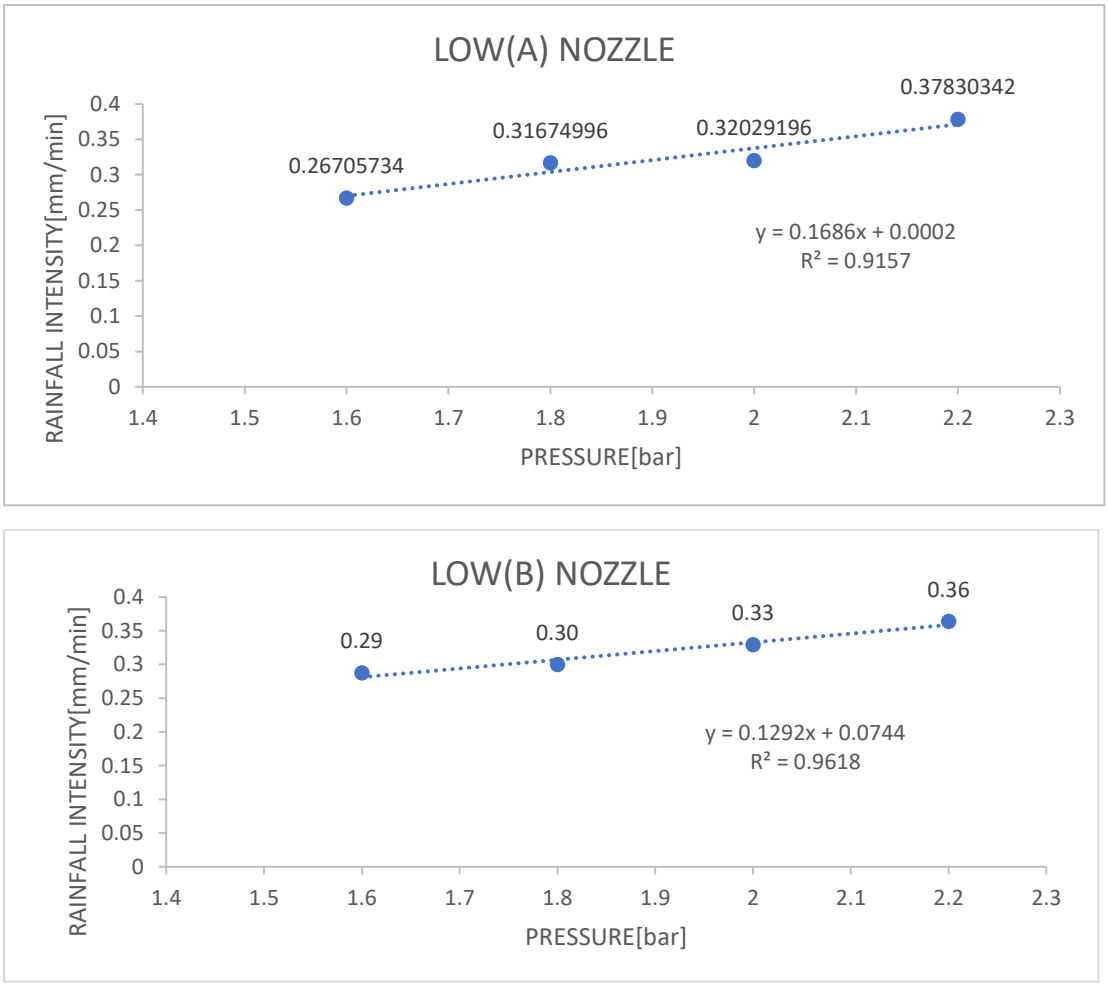

Figure 9: Regression for the dependence of rainfall intensity on water pressure in the system for both nozzle Low(A) &Low(B) at a fixed depth of 160cm above the demarcated area.

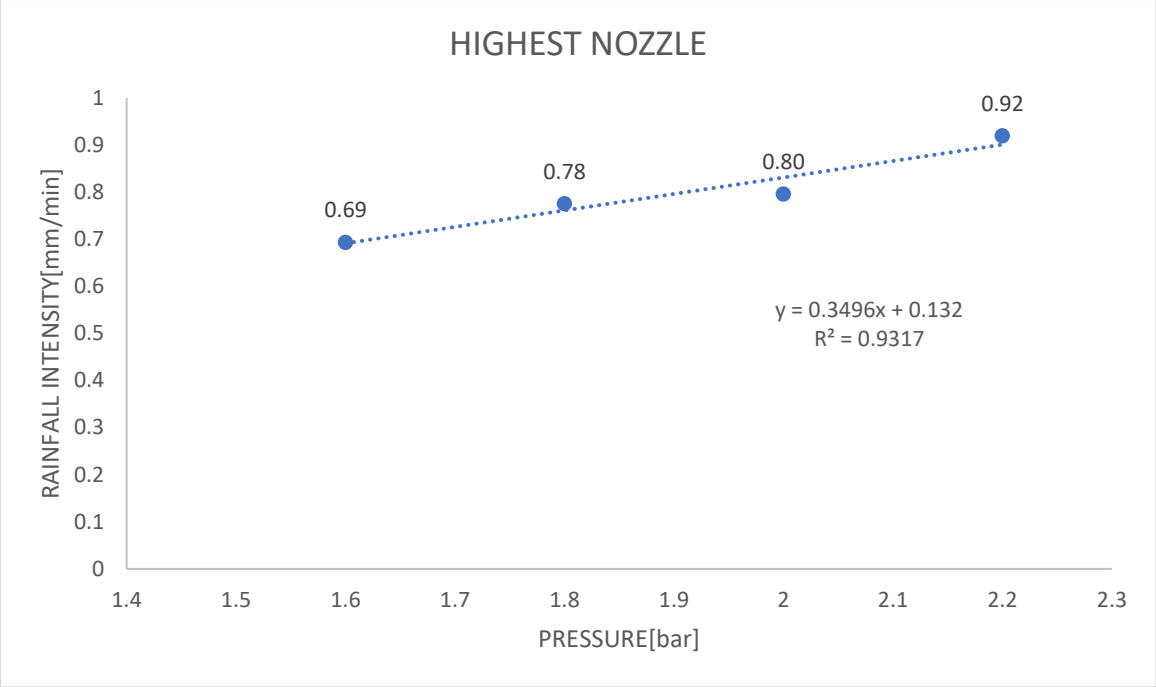

Figure 9.1: Regression as a dependence of rainfall intensity on water pressure in the system for the highest nozzle at a fixed depth of 160cm above the demarcated area

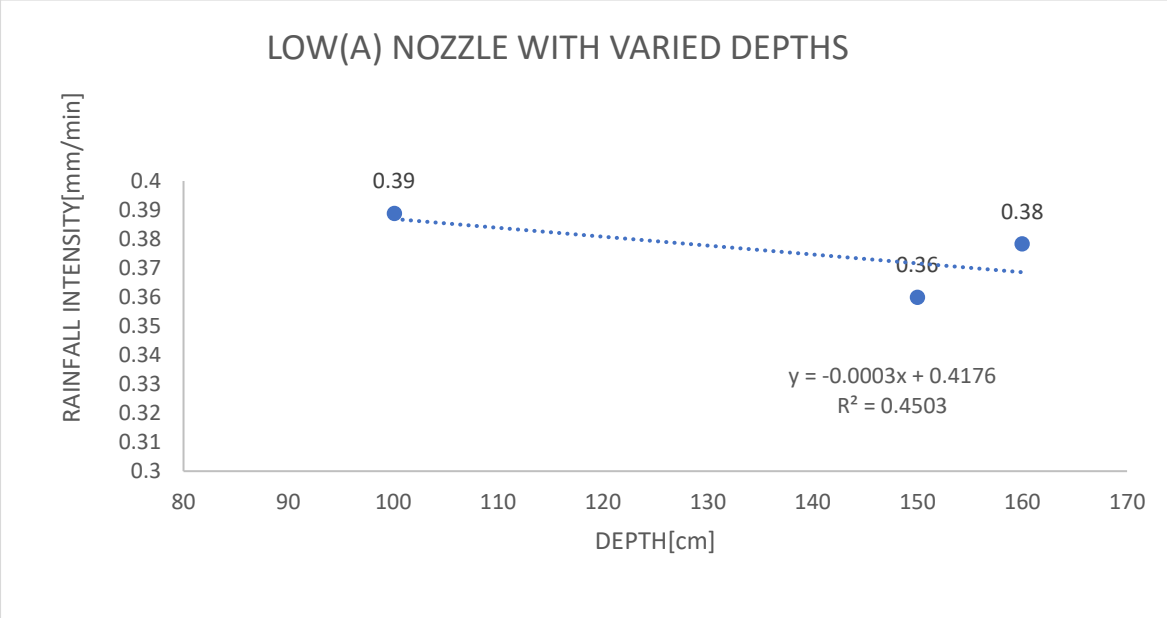

Figure 9.2: Regression of the dependence of rainfall intensity on depth in the system for nozzle (Low A) position 100.1cm,150cm and 160cm above the demarcated area.

	Average Rainfall Intensity(mm/h)		
Pressure(bar)	Highest Nozzle	Low(B) Nozzle	Low(A) Nozzle
1.6	16.02	41.61	17.23
1.8	19.00	46.53	17.97
2.0	19.23	47.76	19.74
2.2	22.70	55.19	21.81

Table 2: Result of measured rainfall intensities for a fixed depth of 160cm of the three nozzles at selected pressure conditions.

Height above the demarcated area(cm)	Average rainfall Intensity(mm/h)
100.1	23.33
150	21.6
160	22.7

Table 3: Result of measured rainfall intensities for three different vertical positions of the Low(A) nozzle at selected pressure conditions

5.2 Spatial Variability (using boxplot)

Figure 10.1,10.2 and 10.3 shown the boxplot for the rainfall variability for the three selected nozzles Low(A&B) and that of the Highest. The solid line signifies the median and that of the lower and upper error bar shows the whisker.

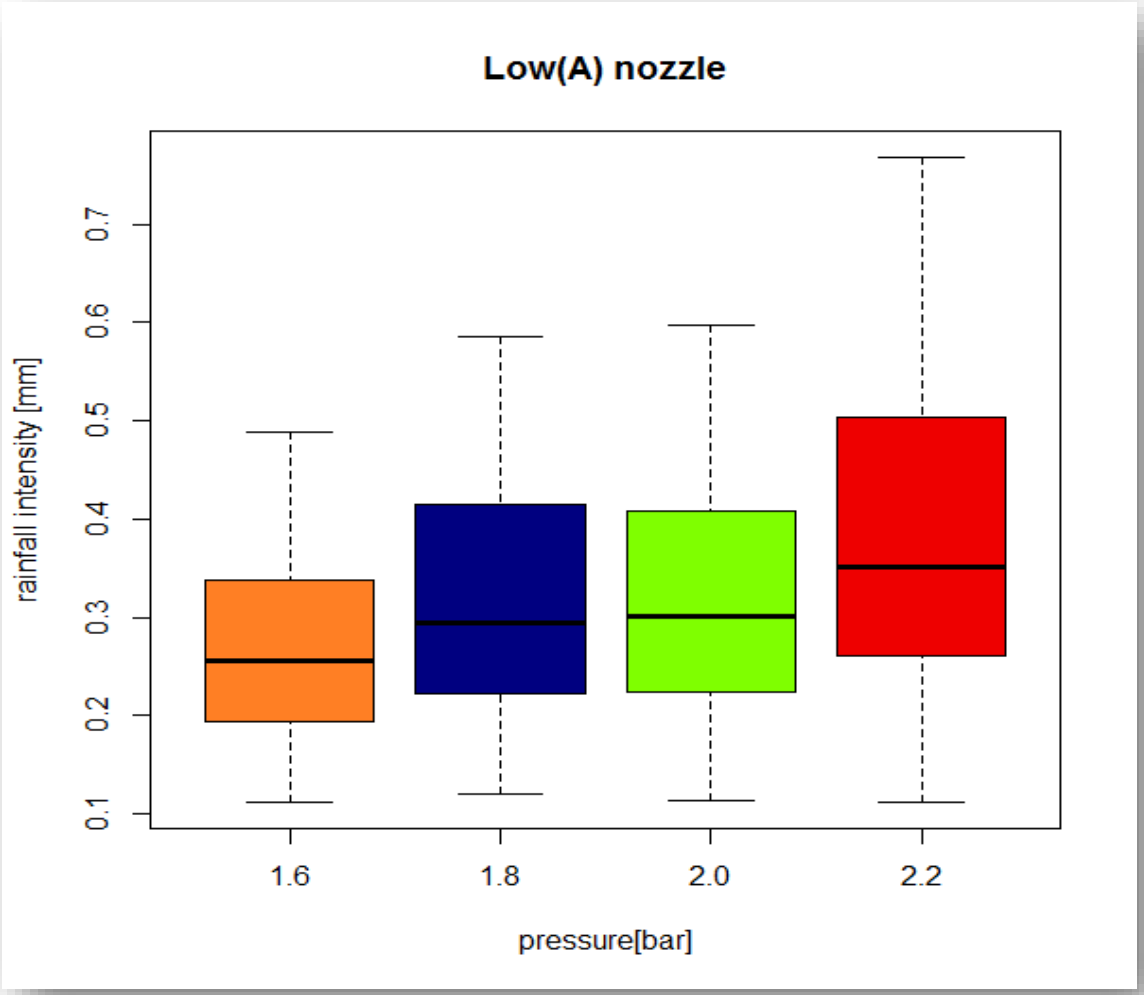

Figure 10.1: Comparison of the raindrops variation using the rainfall intensities to that of the various pressure conditions expressed as a box plot for the total demarcated area for Low(A) nozzle. The lower and upper boundaries of each box represent the 25th and 75th percentile respectively and the whisker bars are the 10th and 90th percentile respectively.

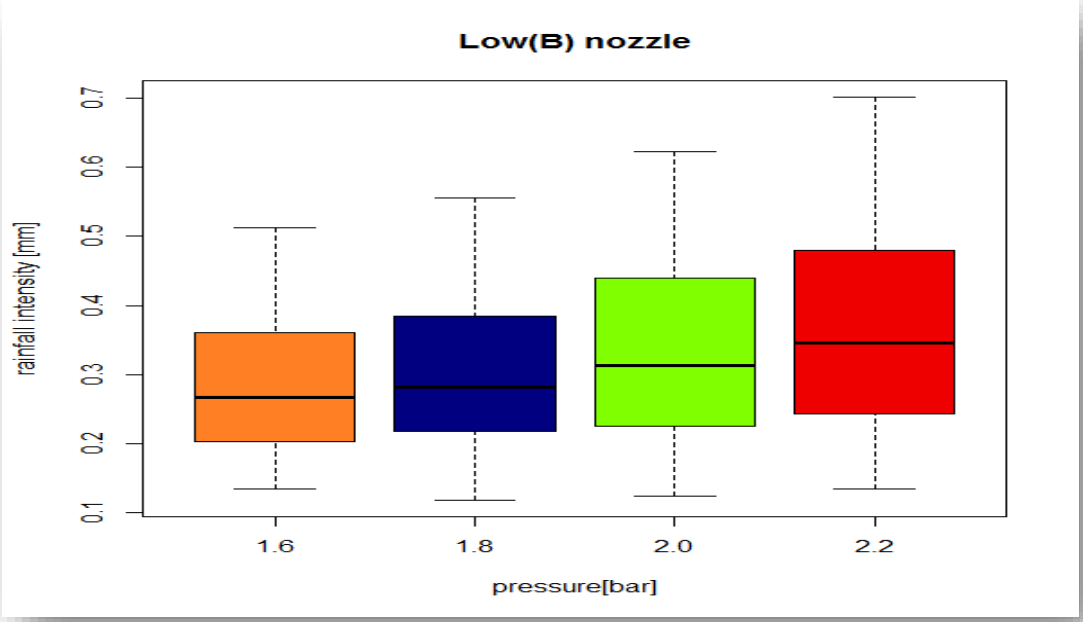

Figure 10.1: Comparison of the raindrops variation using the rainfall intensities to that of the various pressure conditions expressed as a box plot for the total demarcated area for Low(B) nozzle. The lower and upper boundaries of each box represent the 25th and 75th percentile and the whisker bar are the 10th and 90th percentile respectively

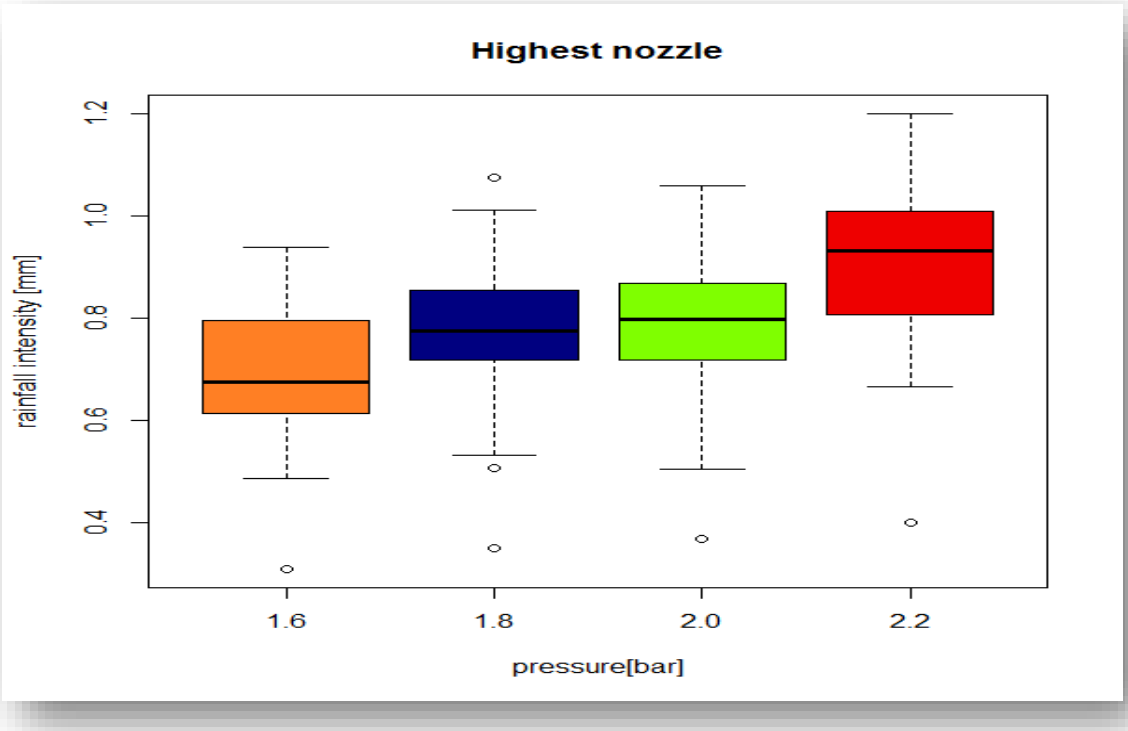

Figure 10.3: Comparison of the raindrops variation using the rainfall intensities to that of the various pressure conditions expressed as a box plot for the total demarcated area for Highest nozzle. The lower and upper boundaries of each box represent the 25th and 75th percentile and the whisker bars are the 10th and 90th percentile respectively.

5.3 Spatial rainfall distribution maps

Fig 11.1-11.3 show results for the spatial rainfall distribution map created for some selected pressures condition for all the three nozzles that were used. Other pressures condition results can be found in the appendix(B) section of this work.

Highest nozzle (at 2.2 bar)

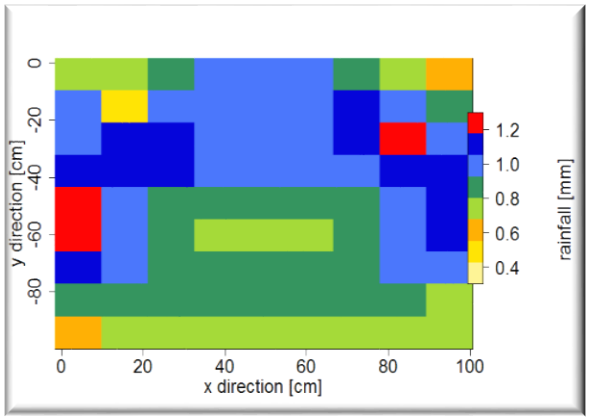

Highest nozzle(at 1.8 bar)

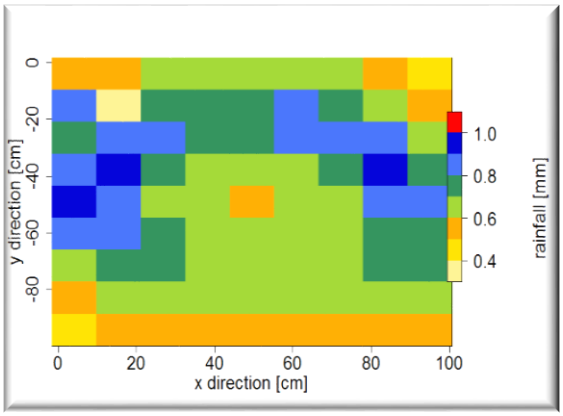

Figure 11.1: Spatial rainfall intensity distribution in rainfall simulator (measure with containers) with two flow rates for the highest nozzle.

Low(A) nozzle (at 1.6 bar)

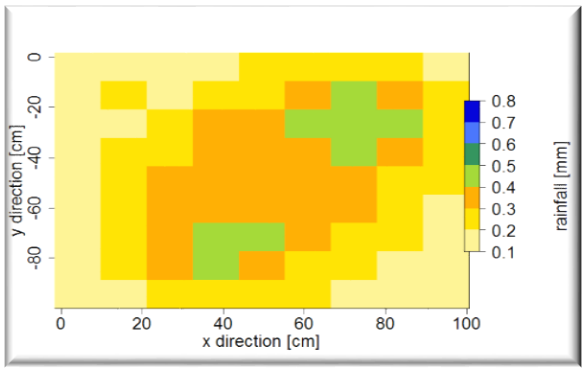

Low(A) nozzle(at 2.0 bar)

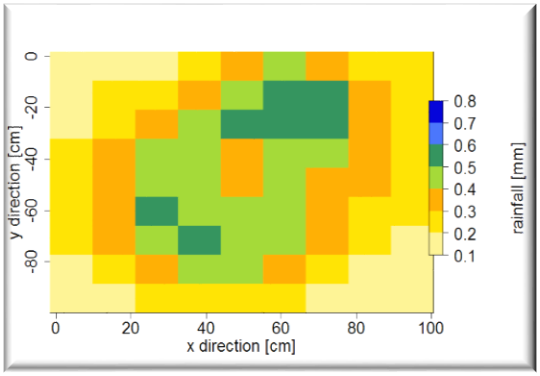

Figure 11.2: Spatial rainfall intensity distribution in rainfall simulator (measure with containers) with two flow rates for Low(A) nozzle.

Low(B) nozzle (at 1.6 bar)

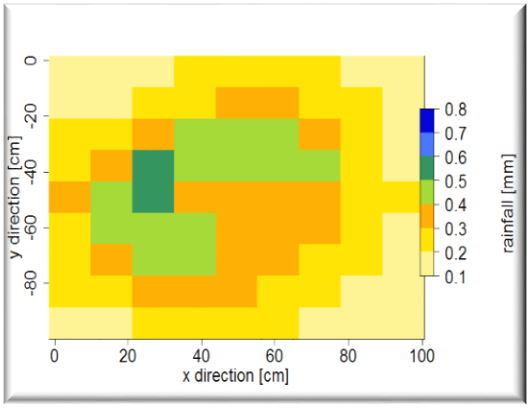

Low(B) nozzle (at 1.8 bar)

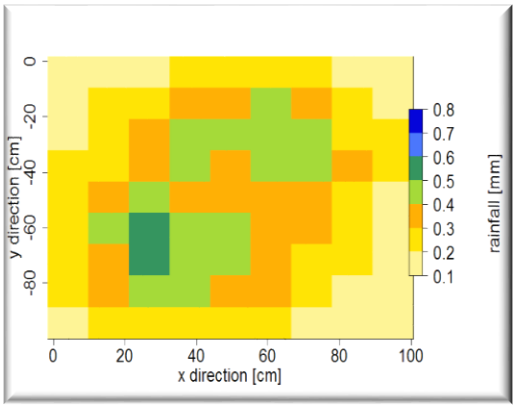

Figure 11.3: Spatial rainfall intensity distribution in rainfall simulator (measure with containers) with two flow rates for the least nozzle.

5.4 Rainfall spatial variability of intensity(CU)

Table 4 below show the rainfall spatial variation using the Christiansen uniformity coefficient to analyzed the uniformity for the three selected nozzles.

Nozzle	Pressure(bar)	CU value of uniformity (%)
Low(B)	1.6	69.87
	1.8	70.43
	2	68.85
	2.2	66.21
Low(A)	1.6	72.01
	1.8	68.81
	2	67.75
	2.2	65.27
Highest	1.6	85.98
	1.8	87.69
	2	87.32
	2.2	87.05

Table 4: Result showing the rainfall spatial variability of uniformity by using Christiansen uniformity coefficient(CU)

CHAPTER SIX

DISCUSSION

Selecting the most appropriate nozzle (using simulated rainfall) with similar characteristics as natural rainfall, which will be used for a future field work was the major aim of this research. The three selected nozzles were examined based on correlation coefficient values, spatial variability, rainfall spatial variation of intensity and that of their spatial rainfall distribution. From the result; the rainfall intensity was observed to be dependent upon nozzle size, water pressure at the nozzle, and the elevation of the nozzle above the demarcated area. Each of the three nozzles were tested using on operation pressure of 1.6, 1.8, 2.0 and 2.2 bars. The elevation was fixed at 160cm because that was one of the focus for this experiment.

Nevertheless, to also have a fair idea about the relationship between fixed elevation and varied elevation, the simulated rainfall was also tested against the varied elevation of 100.1, 150 and 160cm for Low(A) nozzle only as shown in figure 9.2. Even though the result shows a decreasing trend as the depth increases but at 160cm there was a bit of increase which is very difficult to explain. Maybe there might be a mistake on my part because I also used this position (160cm) to fine tune my nozzle position for the actual work, which was based on a fixed elevation of 160cm. The generated mean rainfall intensity ranged from 16.2mm/h as the least to 55.19mm/h as the highest. The largest nozzle as expected produced this highest intensity and the small nozzle produces the least intensity. The result of the data analysis performed on each nozzle and pressure condition can be located in the appendix(A) section of this work.

6.1 Correlation coefficient of determinant values(R^2)

It should be noted that the correlation coefficient values for the three nozzles were rather high (ranged from 0.916 to 0.96) and almost the same, but for the varied depth that is Low(A) was very low value in comparison to the fixed elevation. This high value for the fixed elevation indicates an almost perfect linear relationship between the rainfall intensity and that of the available pressures used, meaning the higher the pressure the greater is the rainfall intensity. Since the dependence of rainfall intensity on the pressure in the system is well described by the formulas with high correlation coefficient values this can be a good criterion when selecting the appropriate pressure conditions. The low value for the varied depths shows a rather poor relationship between the intensity and depth.

6.2 Spatial Variability

The trends of plotted boxplots for the three nozzles at different pressure conditions are similar, but almost the same for the Low(A) and Low(B) nozzles (figures 10.1 & 10.2). The three plot show how the percentile increase in difference as the pressure increases. The median values also show similar trends across each of the pressures used. As the pressure increases, the median also gradually increases except for the Low(A) nozzle where at a pressure of 1.8 and 2.0 bar the median values are almost the same. This gradual increase in the median can be an indicative of a more variable spatial pattern.

During the examination of the boxplot for the larger nozzle (figure 10.3), it can be noted that the variable amount of simulated rainfall was received across the study area. The occurrence of lower and higher outliers out of the range of the whiskers was also noted since these outliers were not found in the other two nozzles boxplots. The small interquartile range for the higher nozzle indicates it localized variability of simulated rainfall, meaning there was no large range of value for each pressure. This may relate to the heavy influence of outliers affecting the spatial variability of the simulated rainfall.

The boxplots for the Low(A) and Low(B) nozzle at pressures of 2.0 and 2.2 bar show larger interquartile range that is consistent with the classification of such nozzle value as average. This larger interquartile range may also illustrate a weakness in using ratio to create representative spatial indices.

6.3 Spatial rainfall distribution

The rainfall distribution pattern on the demarcated area is not regular for all the three nozzles used, a fact that is quite normal for a simulator with only one nozzle (Ries and Langer, 2002). The observed changes in spatial distribution between the different test runs can be explained by the different nozzles and pressure condition used. For the Low(A) and Low(B) nozzle (Figure 11.2 and 11.3), these changes are almost similar. From the flow rate for the highest nozzle at 1.8 and 2.2 bars (Figure 11.1), the average intensities were around 46.2 and 55.19mm/h respectively, which was achieved with a time of 39 and 34 minutes(mins) respectively. This nozzle resulted in the higher average rainfall intensities. For low(A) nozzle at 1.6 and 2.0 bars (Figure 11.2), the flow rate average intensities were 16.03 and 19.2 mm/h respectively and were achieved with a time of 60 to 70 mins. For the low(B) nozzle (Figure 11.3) flow rate, the average intensities were17.24 and 17.96 mm/h with a time of 76 and 56 mins respectively. Surprisingly, average rainfall intensities for the Low(B) was higher for the

above pressures bar in comparative to the Low(A) output but at a pressure bar of 2.2, the Low(A) nozzle was rather higher which should be the normal trend. This result was not shown here but can be located in the appendix section of this work.

6.4 Rainfall Spatial Variability of Intensity (Using CU)

To be sure on which nozzle and pressure conditions were appropriate for the future work, the Christiansen uniformity coefficient(CU) was also used on the collected data as shown in Table 4. The aim was to get a value of 80% and more as proposed by both Egodawatta (2007) and Moazed et al., (2010) as a good figure for better uniformity. From the result in Table 4, it is clearly shown that all the pressure conditions for the highest nozzle achieved that in a range of 85% to 88%, and the pressure condition at 1.8 bars was the highest with a value of 87.69%. The other two nozzles, Low(A) and Low(B) had a value in the range of 65% to 73% while the lowest value occurs at a pressure of 2.2 bars for nozzle Low(B).

Even though the highest nozzle was more uniform than the others per the result in Table 4, there was not a better conclusion on its pressure trend from 1.6 to 2.2 bars as compared to that of nozzle Low(A), which shown that the lower the pressure the more uniform is the flow rate. Maybe there might be an issue with the reading at 1.6 bars because from 1.8 to 2.2 bar the trend as in nozzle Low(A) was established for the high-test nozzle. Also, based on the Christiansen coefficient values obtained nozzle Low (A & B) can be classified as spatial heterogeneity, this I suspect has to do with the area selected, which I think was too wide for those nozzles to have achieved better uniformity of the flow at the selected pressure conditions.

Therefore, when using the rainfall simulator, the first point to consider is to simulate natural rainfall conditions and, if you would like to simulate natural rain conditions, part of rain intensities are below 0.3mm/sec based on this work. Even after trying to simulate very low intensities, meeting the droplet diameter and kinetic energy of natural rain was not possible. Still, for continuous simulation of rainfall, it is very difficult to keep all of the characteristics of natural rain. Since achieving the kinetic energy required a very high elevation or depth so maybe the drop forming simulator will do, but testing that will be impossible for this work because it is not available. So, it is a problem to simulate the same characteristics of natural rain but for the reaction of the volume of rain, it can be done.

In a comparison of the three nozzles, fig (11.1) for the highest nozzle with Christiansen uniformity above 85% showed a better distribution than that of the other two nozzles. This nozzle can be used for future work especially at a pressure condition of 1.8 bars. The result of the experiment revealed the production of light, moderate and heavy rainfall. The spatial distribution is heterogeneous, while it is concentrically decreasing from the center towards the border of the demarcated area even though it could have been better shown. The benefit of this attribute is that the RS offers possibilities to study a great variety of process intensities at the same simulation. One of the properties of a pressure driven RS is that, increasing the flow rate will increase the pressure resulting in little drops with less kinetic energy as was also observed in this experiment.

6.5 Limitation

When using a valve to regulate the water flow through one of the nozzles (Low B), a spike occurs in the distribution of rainfall, directly under the nozzle. Water trapped between the valve and the nozzle tip forms a huge drop when the valve is closed, resulting in excessive drop sizes directly below the nozzle. I think this large drop may have some influence on the result. Even though it may also not be a severe problem when used in pasture situations, but when used on the plowed ground the large drops would have a significant impact on the kinetic energy while hitting the soil which will result in excessive cratering and erosion.

Miller (1987) noted a similar problem when using a solenoid to regulate water flow through the 30WSQ nozzles and corrected the problem by placing a siphon hose between the valve and the nozzle, which kept the droplet from falling when the nozzle closed. I had little success using that, but I think another possible solution to overcome this problem could be to insert a small piece of a furnace filter or other such material directly below the nozzle that would scatter and absorb the energy of the drop while compromising an irrelevantly small area of the plot.

CHAPTER SEVEN

CONCLUSION

An existing rainfall simulator, which has been used for other purposes, was calibrated in the laboratory with different nozzles and pressure conditions to ensure its usefulness for another field of works in the near future. One of the main conclusions of this work, which was grounded on the results, was that the generated rainfall characteristics of spatial variability and that of the spatial rainfall distribution in rainfall simulator, just like in natural rainfall event, are not homogeneous.

The nozzle with the highest discharge, especially at a pressure of 1.8 bars, proof to be the most appropriate selected for the future field work. The nozzles Low(A&B) can also be useful for other purposes but firstly there should be further check (experiments) on the area size (coverage area), definitely lesser than 100cm by 100cm. A rough try was performed with lesser area size calculation and this points to a higher CU value signifying a better uniformity as compared to using the whole area, even though the result is not shown. Spatial heterogeneity of simulated rainfall and its variability between different experiments is a limitation to the reproducibility of simulation and thus to the quality of data generated. As this is unavoidable due to the construction of the nozzle, it is necessary to observe the demarcated area carefully during each rainfall simulation.

Simulating all the matching characteristics of natural rainfall is impossible, even, trying as much as possible to simulate low intensities within this work, still meeting the droplet diameter and kinetic energy was impossible. Though low rain rate may be a challenge to simulate, their prevalent manifestation warrants greater attention, predominantly in studies like canopy interception, the alteration of soil surface properties, infiltration, and the fate of rain in the ecosystem.

More intense events, when they happen, normally, last for only a small fraction of the total rain time. There is no doubt that extreme rain events when they occur, occasionally yield dramatic consequence on the landscape. However, this does not weaken the argument that we should pursue a balanced understanding of the nature and effects of rain event across an entire range of event magnitudes and frequencies.

Calibration of the rainfall simulator should not focus on only the nozzle but on all other associated components and the laboratory is the perfect place for this to be done because it ensures a windless environment, which is key when performing the calibration. The modification of this simulator to use more than one nozzle at a time so as to compare the result with using a single nozzle will not be a bad idea at all since the use of single nozzle simulators has always proven to be a challenge.

REFERENCES

- **AGASSI, M., and BRADFORD. J. M., 1999**: MeAthodologies for interrill soil erosion studies. Soil & Tillage Res. 49:277-287.
- **AKSOY, H., COKGOR, N. E., GEDIKLI, S., YOON, A., KOCA, J., INCI, S. B., and ERIS, E., 2012**: A rainfall Simulator for Laboratory-Scale assessment of rainfall-runoff-sediment transport processes over a two-dimensional flume. Catena 19, 63-72.
- **AIZHEN, LI., HOUFENG, LIU., 2004**: Foundation of meteorology and climatology, Beijing: China Meteorological Press; 2004. P. 95-100.
- **BATTANY, M. C., GRISMER, M.E., 2000**: Development of a portable field rainfall simulator for use in hillside Vineyard runoff and erosion studies. Hydrol. Process. 14, 1119-1129.
- **BARTOLINI, G., DI STEFANO, V., MARACCHI, G., ORLANDINI, S., 2012**: Mediterranean warming is especially due to summer season evidence from Tuscany (central Italy). Appl. Climatol. 107,279-295, Htt://dx.doi.org/10.1007/s00704-011-0481-1
- **BHARDWAJ, A. AND SINGH, R., 1992**: Development of a portable rainfall simulator infiltrometer for infiltration-runoff and erosion studies. Agricultural Water Management 22(3):235-248.
- **BORZENKOVA, I.I., 2002**: Hydrological Cycle Vol. II – Type and Characteristics of Precipitation. Department of Climatology, State Hydrological Institute, Russia. http://www.eolss.net/sample-chapters/c07/e2-02-05-02.pdf
- **BRADFORD, J.M., HUANG, C., 1993**: Comparison of interrill soil loss for laboratory and field procedures. Soil Tech. 6:145-156.
- **BUBENZER, G.D., 1979**: "Inventory of Rainfall Simulators." Proceedings of the Rainfall Simulator Workshop, Tucson, AZ, March 7-9, 1979. USDA Science and Education Administration. Agricultural Reviews and Manuals. ARM-W-10/ July 1979.
- **BURT, J.E. AND BARBER, G.M., 1996**: Elementary Statistics for Geographers, The Guilford Press, New York.
- **CHRISTIANSEN, J. E., 1942**: Irrigation by sprinkling. Univ. California. Agric. Exp. Stn. Bull. 670.
- **CLARKE, M.A., AND WALSH. R.P.D., 2007**: A portable rainfall simulator for field assessment of splash and slope wash in remote locations. Earth Surf. Processes & Landforms 32:2052-2069.
- **COMMANDEUR, P.R. AND WASS E.F., 1994**: Rainfall simulation, soil infiltration and surface erosion on skid road surfaces. Canada–British Columbia Forest Resource Development Agreement, BC Ministry of Forests, Victoria, BC. FRDA Report No. 228:28.
- **COVERT, A. AND JORDON, P., 2009**: A portable rainfall simulator: Techniques for understanding the effects of rainfall on soil erodibility. -Streamline Watershed Manag.Bull.13: 5-9.
- **DELIMA, J.L., M.P., TORFS, P.J.J.F. & SINGH, V. P., 2002**: A mathematical model for evaluating the effect of the wind on downward-spraying rainfall simulators. - Catena 46: 221-241.
- **DISRUD, L. A., KRAUSS, R.K., (1971)**: Examining the process of soil detachment from clod exposed to the wind-driven simulator. Trans. ASAE. 14:90-92.
- **DUNKERLEY, D., 2008**: Rain event properties in nature and in rainfall simulation experiments: A comparative review with recommendations for increasingly systematic study and reporting. Hydrol. Process. 22: 4415–4435.

- **EGODOWATTA, P. 2007**: Translation of Small-plot Scale Pollutant Build-up and Wash-off Measurements to Urban Catchment Scale. Faculty of Built Environment and Engineering Ph.D. Thesis, Queensland University of Technology, Australia.
- **ESTEVES, M., CADET, P., LAPETITE, J. M., PLANCHON, O., SILVERA, N., 2000**: The 'EMIRE' Large rainfall simulator: design and field testing. Earth Surf. Process. Landf. 25, 681-690.
- **FISTER, W., ISERLOH, T., RIES, J. B., SCHMIDT, R. G., 2012**: A portable wind and rainfall simulator for in situ soil erosion measurement, Catena 91, 72-84.
- **FOSTER, I.D.L., BRANDSMA, R.T., CHAPMAN, A. S., FULLEN, M.A., 2000**: Drip-screen rainfall simulators for hydro-and pedo-geomorphological research: The Coventry experience. Earth Surface Processes and Landforms 25: 691-707.
- **GRISMER, M.E., 2011**: Rainfall simulator studies- A review of designs, performance, and soil erosion measurement variability. Draft report as of march 4, 2011.
- **GRISMER, M.E., 2007**: Soil restoration and erosion control; Quantitative assessment and direction. Transactions of the ASABE. 50(S): 1619-1626 (doi 10.13031/2013. 23956) 2007.
- **GRIERSON, I. T., AND OADES, J.M., 1977:** A rainfall simulator for field studies of runoff and soil erosion, J. Agr. Eng. Res., 22, 37-44.
- **HALL, M.J., 1970**: A critique of methods of simulating rainfall. Water Resources Research 6:1104-1114.
- **HAMED, Y., ALBERGEL, J., ASSELINE, J., BALAH, M., BERNDTSSON, R., EL-NIAZY, M., NASRI, S., and PE´PIN, Y., 2002**: Comparison between rainfall simulator erosion and observed reservoir sedimentation in an erosion sensitive semi-arid catchment. Catena 50:1-16.
- **HELSETH, L. E., 2016**: Electrical energy harvesting from droplet passing a hydrophobic polymer with a metal film on its back side. J Electrstat. 2016; 81: 64-70.
- **HUDSON, N. W., 1981**: `Instrument for studies of the erosive power of rainfall', in
- Erosion and Sediment Transport Measurement, Proceedings of the Florence Symposium, June 1981. IAHS Publ.133, 383±390.Hudson, N. W. 1995.Soil Conservation. Iowa State University Press, Iowa, pp. 55±68.

- **HUDSON, N.W.,1993**: Field measurement of soil erosion and runoff. FAO soils bull.68 Rome.

- **ISERLOH, T., FISTER, W., SEEGER, M., WILLGER, H., RIES, J. B., 2012:** A small portable rainfall simulator for a reproducible experiment on soil erosion. Soil Tillage Res. 124, 131-137.

- **KIBET, L.C., A.L. ALLEN, P.J.A. KLEINMAN, G.W. FEYEREISEN, C. CHURCH, L.S.**
- **SAPORITO, ET AL. 2011**. Phosphorus runoff losses from subsurface-applied poultry litter on Coastal Plain soils. J. Environ. Qual. 40:412–420. doi:10.2134/jeq2010.0161.

- **KINNELL, P.I.A., 1990**: Modelling erosion by the rain-impacted flow. Catena 17:55–66.
- Lal, R., 1988: Erodibility and erosivity. In: R. Lal (ed.) Soil Erosion Research Methods. Soil and Water Conservation Society, Ankeny, IA. pp. 141-160.
- Laws, J.D., 1941: Measurement of the fall velocity of water drops and raindrops. Trans. AGU 22:709-721.
- **Laws, J. O. and Parsons, D. A., 1943**: "The Relation of Raindrop-Size to Intensity." Transactions of the American Geophysical Union 24(2), 452-460.
- Lexer, M.J., Honninger, K., Scheifinger, H., Matulla, C., Groll, N., Kromp-Kolb, H.,

- **SCHADAUER, K., STARLINGER, F., ENGLISCH, M., 2002:** The sensitivity of Austrian
- forests to scenarios of climatic change: a large-scale risk assessment based
- on a modified gap model and forest inventory data. Forest Ecology and Management
- 162, 53–72

- **LOCH, R.J., BRIDGE, B.J., BOURKE, J.J., MASTERMAN, N., ROBOTHAM, B.G., ORANGE, D.N., SHERIDAN, G., and ZELLER, L., 2001**: A multi-purpose rainfall simulator for field infiltration and erosion studies. Australian J. of Soil Research 39(3):599-610.
- **MET OFFICE (METEOROLOGICAL OFFICE OF THE UK), 2007**: National Meteorological Library and Archive: Fact sheet No.3- water in the atmosphere. < htt:// www.Labary.met office.gov.uk/>; 2007: 6.
- **MEYER, L.D., 1988**: Rainfall simulators for soil conservation research. In: R. Lal (ed.) Soil erosion research methods. Soil and Water Conservation Society, Ankeny, IA. pp. 75-96.
- **MEYER, L.D., AND HARMON W.C., 1979**: Multiple-intensity rainfall simulator for erosion research on row side slopes. Transactions of the American Society of Agricultural Engineers 22:100–103.
- **MEYER, L., 1994**: Rainfall simulator for soil erosion research in Lal. (Ed), Soil erosion research methods. St. Lucie press and soil and water conservation society. Delray Beach. pp .83-103.
- **Miller, W P., 1987**: A solenoid-operated, variable intensity rainfall simulator. Soil Sci. Soc. Am. J. 51(3):832-834.
- **Moore, I.D., Barfield, B.J. and Hirschi, M.C., 1983**: Kentucky rainfall simulator. Trans. ASAE 26:1085-1089.
- **Moazed, H., Albaji, M., Bavi, Boroomand-Nasab, S. and Naseri, A, 2010**: Effect climate and hydraulic parameters on water uniformity coefficient in solid set systems. Journal of Applied Science, 10, 1792-1796.
- **NEIL, I.F., 2004**: The representation of rainfall drop-size distribution and kinetic energy; Hydrology and earth system sciences 8(5), 1001-1007.
- **Norton, L.D., and R. Savabi., 2010**: Evolution of a linear variable intensity rainfall simulator for surface hydrology and erosion studies. Applied Engr. in Agricult. 26(2): 239-245.
- **Paige G.B., Kennedy, J.R., Stone, J.J. and Smith, J. R., 2003**: The Walnut Gulch rainfall simulator: A computer-controlled variable intensity rainfall simulator. Applied Engr. in Agric. 20(1):25-31.
- **Renard, K. G., Foster, G.R., Weesies, G.A., Cool, D. K. and D. C. Yoder, D.C., 1997**: In Predicting Soil Erosion by Water: A Guide to Conservation Planning with the Revised Universal Soil Loss Equation (RUSLE). USDA-ARS, Agriculture Handbook Number 703.
- **RENARD, K.G., 1985**: Rainfall Simulators and USDA Erosion Research: History, Perspective, and Future. Rainfall Simulator Workshop, Tucson, Arizona: Society for Range Management 14–15 January 1985, website, http://www.tucson.ars.ag.gov/unit/publications/PDFfiles/724.pdf, visited 23 January 2010.
- **RIES, J.B., FISTER, W., ISERLOH, T., WISTORF, S., SEEGER, M., 2009:** Calibration of simulated rainfall characteristics for the study of soil erosion on agricultural land. Soil & Tillage Research (106): 109–116.
- **RIES, J.B., LANGER, M., 2002:** Runoff generation in abonded fields in the central Ebro basin. The result from rainfall simulation experiment. Garcia-Ruiz, J.M., Jones, J.A.A, Arnaez, J.(Eds), Environmental changes and water sustainability. Institution pirenaico de ecologia, Zaragoza, pp.65-82.
- **ROTH C.H, HELMING K., 1992**: Dynamics of surface sealing, runoff formation and interrill erosion loss as related to rainfall intensity, microrelief, and slope. Zeitschrift f¨ur Pflanzenern¨ahrung und Bodenkunde 155: 209–216. Salles, C., Poesen J., Sempere-Torres, D.,

2002: Kinetic energy of rainfall and its functional relationship with intensity Hydrol 2002; 257: 256-70.

- **SCHONWIESE, C.D., RAPP, J., 1997**: Climate Trend Atlas of European Based on observations 1891-1990. On the statistical analysis sense of observations. Secretariat of the world Meteorological Organization (192pp)
- Seeger, M., 2007: Uncertainty of factors determining runoff and erosion processes as quantified by rainfall simulations. Catena 71: 56–67.
- **Serrano-Muela. M.P., Nadal-Romero E., Lana-Renault. N., Gonzalez-Hidalgo.J.C., Lopez-Moreno. J.I., Begueria, S., Sanjuan. Y., Garcia-Kuiz. J.M., 2013**: An exceptional rainfall event in central western Pyrenees: Spatial patterns in discharge and impact. Land Degradation & Development DOI: 10.10002/idr.2221.
- **SHELTON, C.H., VON BERNUTH, R. D., AND RAJBHANDARI, S. P., 1985**: A continuous application rainfall simulator. Transactions of the American Society of Agricultural Engineers 28(4):1115–1119.
- **SUTHERLAND, R. A., 1998A**: Rolled erosion control systems for hillslope surface protection: A critical review, synthesis, and analysis of available data. I. Background and formative years. Land Degrad. & Develop. 9:465-486.
- **SUTHERLAND, RA., 1998B**: Rolled erosion control systems for hillslope surface protection: A critical review, synthesis, and analysis of available data. II. The post-1990 period. Land Degrad. & Develop. 9:487-511.
- **Tocic, I., Hmjak, I., Gavrilov, M.B., Unkasevic, Markovic, S.B., Lukic, T., 2014:** Annual and Seasonal Variability of Precipitation in Vojvodina.T heor. Appl. Climatol. 117-341. Htt://dx.doi.org/10.1007/s00704-013-1007-9
- **VAN DIJK, A. J. M., BRUIJNZEEL, L.A. AND C.J. ROSEWELL. 2002**: Rainfall intensity – kinetic energy relationships: A critical literature appraisal. J. Hydrology 261:1-23.
- **WILCOX, B.P., TROMBLE, J. T., WOOD, M K, AND WARD, T J., 1986:** A hand-portable single nozzle rainfall simulator designed for use on steep slopes. J. Range Management 39(4):375-377.
- **WOLLMER, STEPHEN HENNING., 1994**: "Effects of Multiple Use on Rain Splash Erosion and Runoff in Semiarid Rangeland. Master's Thesis, San Francisco State University.

APPENDIX

Appendix(A)

Table I to XII: Shows the nozzle calibration result (data analysis) for each of the three nozzles use at a pressure of 1.6, 1.8, 2.0, and 2.2 bars for each test run.

Appendix(B)

Figure I: Show the remaining results for the spatial distribution map created for each nozzle calibration that was not shown in the result section.

Nozle calibration

Date:	04/08/2016	
Time:	02:16:00 PM	15:00
Jet: Highest	wider opening	
Height of jet:	160	cm
Pressure:	1.6	bar
Duration of measurement:	44	min
Surveyors:		

HIGHEST NOZZLE

Vessel number	Vessel veight [g]			Vessel area	Vessel position [cm]		Rain intensity	Rain intensity
	Tara	Brutto	Netto	[cm^2]	x	y	[$mm.min^{-1}$]	[$mm.h^{-1}$]
1	34.2	226.2	192	79.5	4.8	-4.2	0.548885077	32.93310463
2	34.5	237.8	203.3	79.5	14.7	-4.2	0.581189251	34.87135506
3	34.7	248.9	214.2	79.5	25	-4	0.612349914	36.74099485
4	34.4	253.6	219.2	79.5	35	-4.5	0.626643796	37.59862779
5	34.4	259.3	224.9	79.5	45	-4.5	0.642938822	38.57632933
6	34.6	264	229.4	79.5	54.9	-4.5	0.655803316	39.34819897
7	34.5	261.2	226.7	79.5	64.8	-4.8	0.64808462	38.88507719
8	34.4	247.6	213.2	79.5	75	-4.8	0.609491138	36.56946827
9	34.4	226.7	192.3	79.5	85	-4.7	0.54974271	32.98456261
10	34.5	209.8	175.3	79.5	94.8	-5	0.501143511	30.06861063
11	34.5	253.4	218.9	79.5	4.8	-14.3	0.625786164	37.54716981
12	34.4	271.7	108	79.5	14.7	-14.3	0.308747856	18.52487136
13	34.4	282.7	248.3	79.5	25	-14.4	0.709834191	42.59005146
14	34.5	291.1	256.6	79.5	35	-14.4	0.733562035	44.01372213
15	35.1	299.4	264.3	79.5	45	-14.6	0.755574614	45.33447684
16	34.6	310.1	275.5	79.5	55.2	-14.5	0.78759291	47.25557461
17	34.5	312.8	278.3	79.5	65	-14.6	0.795597484	47.73584906
18	34.4	298.6	264.2	79.5	75.2	-14.5	0.755288736	45.31732419
19	34.5	263.3	228.8	79.5	85	-14.5	0.65408805	39.24528302
20	34.5	229.7	195.2	79.5	95	-14.5	0.558033162	33.48198971
21	34.5	288	253.5	79.5	5	-24.5	0.724699828	43.48198971
22	34.5	316	281.5	79.5	14.8	-24.5	0.804745569	48.28473413
23	34.5	326.5	292	79.5	25	-24	0.834762722	50.08576329
24	34.4	315.5	281.1	79.5	35	-24.2	0.803602058	48.2161235
25	34.6	310.1	275.5	79.5	45	-24.4	0.78759291	47.25557461
26	34.7	319	284.3	79.5	55	-24.4	0.812750143	48.76500858
27	34.5	333.6	299.1	79.5	65	-24.7	0.855060034	51.30360206
28	34.4	314.3	279.9	79.5	75.2	-24.7	0.800171527	48.0102916
29	34.5	315.1	280.6	79.5	85.3	-24.8	0.80217267	48.13036021
30	34.6	262.6	228	79.5	95	-24.5	0.651801029	39.10806175
31	34.5	333.2	298.7	79.5	4.5	-34	0.853916524	51.23499142
32	34.5	362.5	328	79.5	14.5	-34	0.937678674	56.26072041
33	34.5	324.7	290.2	79.5	25	-34.2	0.829616924	49.77701544
34	34.4	317.2	282.8	79.5	75.3	-34.6	0.808461978	48.5077187
35	34.6	348.7	314.1	79.5	85	-34.8	0.897941681	53.87650086
36	34.6	302.9	268.3	79.5	95	-34.6	0.76700972	46.02058319
37	34.6	354.8	320.2	79.5	4.2	-44.5	0.915380217	54.92281304
38	34.7	359.1	324.4	79.5	14.5	-44.5	0.927387078	55.6432247
39	34.4	285.9	251.5	79.5	24.3	-45.2	0.718982276	43.13893654
40	34	281.6	247.6	79.5	74.5	-44.5	0.707833047	42.46998285
41	34.5	334.7	300.2	79.5	84.5	-44.8	0.858204688	51.4922813
42	34.3	320.5	286.2	79.5	94.5	-45.1	0.818181818	49.09090909
43	34.6	346.7	312.1	79.5	4.8	-55.2	0.892224128	53.53344768
44	34.6	339.5	304.9	79.5	15	-55.5	0.871640938	52.29845626
45	34.5	282.3	247.8	79.5	25	-56.2	0.708404803	42.50428816
46	34.3	269.4	235.1	79.5	74	-55	0.672098342	40.32590051
47	34.4	315.8	281.4	79.5	84.4	-55	0.804459691	48.26758148
48	34.6	318.7	284.1	79.5	94.7	-55.1	0.812178388	48.73070326
49	34.6	295.2	260.6	79.5	4.8	-67	0.744997141	44.69982847
50	34.6	311.4	276.8	79.5	15	-67.5	0.79130932	47.47855918
51	34.4	287.3	252.9	79.5	25.3	-67.2	0.722984563	43.37907376
52	34.7	275.3	240.6	79.5	74	-66.5	0.687821612	41.26929674
53	34.5	300.3	265.8	79.5	84.9	-67.8	0.759862779	45.59176672
54	34.6	292.5	257.9	79.5	94.8	-67.2	0.737278445	44.23670669
55	34.5	244.8	210.3	79.5	4.8	-79.5	0.601200686	36.07204117
56	34.6	263.1	228.5	79.5	14.5	-79	0.653230417	39.19382504
57	34.4	266.8	232.4	79.5	24.8	-79.5	0.664379646	39.86277873
58	34.4	267.1	232.7	79.5	73	-80	0.665237278	39.91423671
59	34.5	270.4	235.9	79.5	83.9	-80	0.674385363	40.46312178
60	34.6	255.2	220.6	79.5	94.3	-80.5	0.630646083	37.83876501
61	34.6	204.6	170	79.5	5	-94	0.485991995	29.15951973
62	34.5	216.5	182	79.5	15	-94	0.520297313	31.21783877
63	34.4	222.2	187.8	79.5	24.7	-94	0.536878216	32.21269297
64	34.7	224.9	190.2	79.5	34.5	-94.2	0.54373928	32.62435678
65	34.4	225.8	191.4	79.5	44	-93.5	0.547169811	32.83018868
66	34.5	230	195.5	79.5	53.8	-94	0.558890795	33.53344768
67	34.4	233	198.6	79.5	64	-94	0.567753002	34.0651801
68	34.4	234.7	200.3	79.5	73.8	-94	0.572612922	34.3567753
69	34.5	231	196.5	79.5	84	-94	0.561749571	33.70497427
70	50.9	433.8	382.9	125.5	37.2	-36.3	0.693408185	41.60449113
71	51	422	371	125.5	50	-36.8	0.671858022	40.31148135
72	51.2	434.7	383.5	125.5	62.5	-37	0.694494748	41.6696849
73	51	391.9	340.9	125.5	37	-49.5	0.617348787	37.0409272
74	51.2	381.4	330.2	125.5	50	-50	0.597971749	35.87830496
75	51	389.5	338.5	125.5	62.5	-50	0.613002535	36.78015212
76	50.9	420.8	369.9	125.5	36.5	-63.8	0.669865991	40.19195943
77	51	403.1	352.1	125.5	49.5	-62.5	0.637631293	38.25787758
78	51	407.8	356.8	125.5	62.5	-64	0.646142702	38.76856212
79	51.2	407.8	356.6	125.5	36.5	-79.5	0.645780514	38.74683086
80	51	400.3	349.3	125.5	49.4	-78.5	0.632560666	37.95363999
81	51	400.8	349.8	125.5	62.5	-78	0.633466135	38.00796813
82	27.5	231.3	203.8	84	94.2	-94.3	0.551406926	33.08441558

mean	0.693569406
min	0.308747856
max	0.937678674

Table I: Highest nozzle at a pressure of 1.6 bar

Nozle calibration

Date:	05/08/2016	
Time:	11:28:00 AM	12:07
Jet:Highest	wider openning	
Height of jet:	160	cm
Pressure:	1.8	bar
Duration of measurement:	39	min
Surveyors:		

HIGHEST NOZZLE

Vessel number	Vessel veight [g]			Vessel area	Vessel position [cm]		Rain intensity	Rain intensity
	Tara	Brutto	Netto	[cm^2]	x	y	[$mm.min^{-1}$]	[$mm.h^{-1}$]
1	34.2	233.2	199	79.5	4.8	-4.2	0.641831963	38.50991776
2	34.5	254.4	219.9	79.5	14.7	-4.2	0.709240445	42.55442671
3	34.7	367.8	333.1	79.5	25	-4	1.074342848	64.46057088
4	34.4	264.2	229.8	79.5	35	-4.5	0.741170779	44.47024673
5	34.4	259.3	224.9	79.5	45	-4.5	0.725366876	43.52201258
6	34.6	251.6	217	79.5	54.9	-4.5	0.699887115	41.9932269
7	34.5	242.6	208.1	79.5	64.8	-4.8	0.671182067	40.27092404
8	34.4	232.2	197.8	79.5	75	-4.8	0.637961619	38.27769715
9	34.4	218.1	183.7	79.5	85	-4.7	0.592485083	35.54910498
10	34.5	199.3	164.8	79.5	94.8	-5	0.531527173	31.89163038
11	34.5	259.5	225	79.5	4.8	-14.3	0.725689405	43.5413643
12	34.4	292.7	108	79.5	14.7	-14.3	0.348330914	20.89985486
13	34.4	305.8	271.4	79.5	25	-14.4	0.875342687	52.5205612
14	34.5	303.9	269.4	79.5	35	-14.4	0.868892114	52.13352685
15	35.1	287.9	252.8	79.5	45	-14.6	0.815352363	48.92114175
16	34.6	277.5	242.9	79.5	55.2	-14.5	0.783422029	47.00532172
17	34.5	268.8	234.3	79.5	65	-14.6	0.755684567	45.34107402
18	34.4	257.5	223.1	79.5	75.2	-14.5	0.719561361	43.17368166
19	34.5	245.5	211	79.5	85	-14.5	0.680535398	40.83212385
20	34.5	218.9	184.4	79.5	95	-14.5	0.594742783	35.68456701
21	34.5	291.4	256.9	79.5	5	-24.5	0.828576036	49.71456217
22	34.5	328.8	294.3	79.5	14.8	-24.5	0.949201742	56.9521045
23	34.5	344.8	310.3	79.5	25	-24	1.000806322	60.04837929
24	34.4	321.5	287.1	79.5	35	-24.2	0.925979681	55.55878084
25	34.6	297.3	262.7	79.5	45	-24.4	0.847282696	50.83696178
26	34.7	286.1	251.4	79.5	55	-24.4	0.810836962	48.65021771
27	34.5	279.2	244.7	79.5	65	-24.7	0.789227544	47.35365264
28	34.4	277.5	243.1	79.5	75.2	-24.7	0.784067086	47.04402516
29	34.5	271.9	237.4	79.5	85.3	-24.8	0.765682954	45.94097726
30	34.6	238.3	203.7	79.5	95	-24.5	0.656990808	39.41944848
31	34.5	306.2	271.7	79.5	4.5	-34	0.876310273	52.57861635
32	34.5	347.7	313.2	79.5	14.5	-34	1.010159652	60.6095791
33	34.5	288.6	254.1	79.5	25	-34.2	0.819545235	49.17271408
34	34.4	291.2	256.8	79.5	75.3	-34.6	0.828253507	49.69521045
35	34.6	294.1	259.5	79.5	85	-34.8	0.83696178	50.21770682
36	34.6	265.4	230.8	79.5	95	-34.6	0.744396065	44.66376391
37	34.6	305.3	270.7	79.5	4.2	-44.5	0.873084986	52.38509918
38	34.7	331	296.3	79.5	14.5	-44.5	0.955652314	57.33913885
39	34.4	301.3	266.9	79.5	24.3	-45.2	0.860828899	51.64973391
40	34	311.1	277.1	79.5	74.5	-44.5	0.893726818	53.6236091
41	34.5	313.3	278.8	79.5	84.5	-44.8	0.899209805	53.95258829
42	34.3	278.4	244.1	79.5	94.5	-45.1	0.787292372	47.23754233
43	34.6	330.3	295.7	79.5	4.8	-55.2	0.953717142	57.22302854
44	34.6	299.4	264.8	79.5	15	-55.5	0.854055797	51.24334785
45	34.5	275.3	240.8	79.5	25	-56.2	0.776648928	46.59893566
46	34.3	317.9	283.6	79.5	74	-55	0.914691179	54.88147073
47	34.4	335.3	300.9	79.5	84.4	-55	0.970488631	58.22931785
48	34.6	293.4	258.8	79.5	94.7	-55.1	0.83470408	50.0822448
49	34.6	257.4	222.8	79.5	4.8	-67	0.718593775	43.11562651
50	34.6	279.8	245.2	79.5	15	-67.5	0.790840187	47.45041122
51	34.4	271.4	237	79.5	25.3	-67.2	0.76439284	45.86357039
52	34.7	311	276.3	79.5	74	-66.5	0.891146589	53.46879536
53	34.5	345.1	310.6	79.5	84.9	-67.8	1.001773907	60.10643445
54	34.6	290.2	255.6	79.5	94.8	-67.2	0.824383164	49.46298984
55	34.5	229.5	195	79.5	4.8	-79.5	0.628930818	37.73584906
56	34.6	249.3	214.7	79.5	14.5	-79	0.692468957	41.5481374
57	34.4	264	229.6	79.5	24.8	-79.5	0.740525722	44.4315433
58	34.4	319.5	285.1	79.5	73	-80	0.919529108	55.17174649
59	34.5	314.4	279.9	79.5	83.9	-80	0.90275762	54.16545718
60	34.6	257.3	222.7	79.5	94.3	-80.5	0.718271247	43.09627479
61	34.6	191.8	157.2	79.5	5	-94	0.507014998	30.42089985
62	34.5	205.9	171.4	79.5	15	-94	0.552814062	33.16884373
63	34.4	221.4	187	79.5	24.7	-94	0.603128528	36.18771166
64	34.7	233.4	198.7	79.5	34.5	-94.2	0.640864377	38.4518626
65	34.4	247.5	213.1	79.5	44	-93.5	0.687308499	41.23850992
66	34.5	257.2	222.7	79.5	53.8	-94	0.718271247	43.09627479
67	34.4	263.9	229.5	79.5	64	-94	0.740203193	44.41219158
68	34.4	262.5	228.1	79.5	73.8	-94	0.735687792	44.14126754
69	34.5	243.4	208.9	79.5	84	-94	0.673762296	40.42573778
70	50.9	463.8	412.9	125.5	37.2	-36.3	0.843599959	50.61599755
71	51	451.4	400.4	125.5	50	-36.8	0.818061089	49.08366534
72	51.2	453.5	402.3	125.5	62.5	-37	0.821942997	49.31657983
73	51	407	356	125.5	37	-49.5	0.727347022	43.64082133
74	51.2	412.5	361.3	125.5	50	-50	0.738175503	44.29053019
75	51	440.3	389.3	125.5	62.5	-50	0.795382572	47.72295434
76	50.9	410.4	359.5	125.5	36.5	-63.8	0.734497906	44.06987435
77	51	408.4	357.4	125.5	49.5	-62.5	0.730207376	43.81244254
78	51	428.7	377.7	125.5	62.5	-64	0.771682501	46.30095005
79	51.2	410.7	359.5	125.5	36.5	-79.5	0.734497906	44.06987435
80	51	414.2	363.2	125.5	49.4	-78.5	0.742057411	44.52344468
81	51	444.2	393.2	125.5	62.5	-78	0.8033507	48.20104199
82	27.5	237.2	209.7	84	94.2	-94.3	0.64010989	38.40659341

mean	0.775542813
min	0.348330914
max	1.074342848

Table II: Highest nozzle at a pressure of 1.8 bar

Nozle calibration

Date:	17/08/2016	
Time:	01:43:00 PM	02:19
Jet: Highest Nozzle	wider openning	
Height of jet:	160	cm
Pressure:	2	bar
Duration of measurement:	37	min
Surveyors:		

HIGHEST NOZZLE

Vessel number	Vessel veight [g]			Vessel area [cm^2]	Vessel position [cm]		Rain intensity [$mm.min^{-1}$]	Rain intensity [$mm.h^{-1}$]
	Tara	Brutto	Netto		x	y		
1	34.2	232.1	197.9	79.5	4.8	-4.2	0.672785994	40.36715961
2	34.5	248.5	214	79.5	14.7	-4.2	0.727519973	43.65119837
3	34.7	260	225.3	79.5	25	-4	0.765935747	45.95614482
4	34.4	265.5	231.1	79.5	35	-4.5	0.785653578	47.13921469
5	34.4	266.2	231.8	79.5	45	-4.5	0.788033316	47.28199898
6	34.6	258.9	224.3	79.5	54.9	-4.5	0.762536121	45.75216726
7	34.5	245.4	210.9	79.5	64.8	-4.8	0.716981132	43.01886792
8	34.4	234.6	200.2	79.5	75	-4.8	0.680605133	40.83630801
9	34.4	214.5	180.1	79.5	85	-4.7	0.61227265	36.736359
10	34.5	195.1	160.6	79.5	94.8	-5	0.545979942	32.75879653
11	34.5	258.8	224.3	79.5	4.8	-14.3	0.762536121	45.75216726
12	34.4	286.4	108	79.5	14.7	-14.3	0.367159612	22.02957675
13	34.4	304.8	270.4	79.5	25	-14.4	0.919258882	55.15553289
14	34.5	299	264.5	79.5	35	-14.4	0.899201088	53.95206527
15	35.1	286.3	251.2	79.5	45	-14.6	0.853986062	51.23916369
16	34.6	281.3	246.7	79.5	55.2	-14.5	0.838687744	50.32126466
17	34.5	273.5	239	79.5	65	-14.6	0.812510624	48.75063743
18	34.4	262.5	228.1	79.5	75.2	-14.5	0.7754547	46.527282
19	34.5	243.2	208.7	79.5	85	-14.5	0.709501955	42.57011729
20	34.5	216.8	182.3	79.5	95	-14.5	0.619751827	37.18510964
21	34.5	287.5	253	79.5	5	-24.5	0.860105388	51.6063233
22	34.5	324.3	289.8	79.5	14.8	-24.5	0.985211627	59.1126976
23	34.5	329.2	294.7	79.5	25	-24	1.001869794	60.11218766
24	34.4	309.8	275.4	79.5	35	-24.2	0.936257012	56.1754207
25	34.6	289.9	255.3	79.5	45	-24.4	0.867924528	52.0754717
26	34.7	282.5	247.8	79.5	55	-24.4	0.842427333	50.54563998
27	34.5	283.7	249.2	79.5	65	-24.7	0.847186809	50.83120857
28	34.4	286.5	252.1	79.5	75.2	-24.7	0.857045725	51.4227435
29	34.5	271.1	236.6	79.5	85.3	-24.8	0.804351521	48.26109128
30	34.6	236.3	201.7	79.5	95	-24.5	0.685704572	41.14227435
31	34.5	310.6	276.1	79.5	4.5	-34	0.93863675	56.318205
32	34.5	345.8	311.3	79.5	14.5	-34	1.058303587	63.4982152
33	34.5	315.1	280.6	79.5	25	-34.2	0.953935067	57.23610403
34	34.4	299.8	265.4	79.5	75.3	-34.6	0.902260751	54.13564508
35	34.6	305.9	271.3	79.5	85	-34.8	0.922318545	55.3391127
36	34.6	258.7	224.1	79.5	95	-34.6	0.761856196	45.71137175
37	34.6	317.7	283.1	79.5	4.2	-44.5	0.962434132	57.74604793
38	34.7	339.3	304.6	79.5	14.5	-44.5	1.035526092	62.13156553
39	34.4	285.8	251.4	79.5	24.3	-45.2	0.854665987	51.2799592
40	34	295.9	261.9	79.5	74.5	-44.5	0.89036206	53.42172361
41	34.5	329.2	294.7	79.5	84.5	-44.8	1.001869794	60.11218766
42	34.3	278.7	244.4	79.5	94.5	-45.1	0.830868604	49.85211627
43	34.6	294.2	259.6	79.5	4.8	-55.2	0.88254292	52.95257522
44	34.6	324.4	289.8	79.5	15	-55.5	0.985211627	59.1126976
45	34.5	279	244.5	79.5	25	-56.2	0.831208567	49.87251402
46	34.3	287.7	253.4	79.5	74	-55	0.861465239	51.68791433
47	34.4	338.9	304.5	79.5	84.4	-55	1.03518613	62.11116777
48	34.6	288.4	253.8	79.5	94.7	-55.1	0.862825089	51.76950535
49	34.6	256.7	222.1	79.5	4.8	-67	0.755056944	45.30341662
50	34.6	287.1	252.5	79.5	15	-67.5	0.858405575	51.50433452
51	34.4	283.4	249	79.5	25.3	-67.2	0.846506884	50.79041305
52	34.7	300.6	265.9	79.5	74	-66.5	0.903960564	54.23763386
53	34.5	332	297.5	79.5	84.9	-67.8	1.011388747	60.68332483
54	34.6	266.7	232.1	79.5	94.8	-67.2	0.789053204	47.34319225
55	34.5	221.4	186.9	79.5	4.8	-79.5	0.635390107	38.12340643
56	34.6	242.1	207.5	79.5	14.5	-79	0.705422404	42.32534421
57	34.4	259.6	225.2	79.5	24.8	-79.5	0.765595784	45.93574707
58	34.4	301.3	266.9	79.5	73	-80	0.90736019	54.44161142
59	34.5	278.4	243.9	79.5	83.9	-80	0.829168791	49.75012749
60	34.6	232.6	198	79.5	94.3	-80.5	0.673125956	40.38755737
61	34.6	183.1	148.5	79.5	5	-94	0.504844467	30.29066803
62	34.5	196.5	162	79.5	15	-94	0.550739419	33.04436512
63	34.4	213.3	178.9	79.5	24.7	-94	0.608193099	36.49158593
64	34.7	230.3	195.6	79.5	34.5	-94.2	0.664966854	39.89801122
65	34.4	242.3	207.9	79.5	44	-93.5	0.706782254	42.40693524
66	34.5	249.1	214.6	79.5	53.8	-94	0.729559748	43.77358491
67	34.4	249.7	215.3	79.5	64	-94	0.731939487	43.9163692
68	34.4	242.3	207.9	79.5	73.8	-94	0.706782254	42.40693524
69	34.5	226	191.5	79.5	84	-94	0.651028387	39.06170321
70	50.9	429.5	378.6	125.5	37.2	-36.3	0.815333262	48.91999569
71	51	426.6	375.6	125.5	50	-36.8	0.808872618	48.53235706
72	51.2	438	386.8	125.5	62.5	-37	0.832992355	49.97954129
73	51	366.1	315.1	125.5	37	-49.5	0.678582965	40.71497793
74	51.2	390.9	339.7	125.5	50	-50	0.731560246	43.89361473
75	51	399.4	348.4	125.5	62.5	-50	0.750296113	45.01776677
76	50.9	403.5	352.6	125.5	36.5	-63.8	0.759341014	45.56046086
77	51	391.8	340.8	125.5	49.5	-62.5	0.733929148	44.0357489
78	51	405.7	354.7	125.5	62.5	-64	0.763863465	45.8318079
79	51.2	409.2	358	125.5	36.5	-79.5	0.770970173	46.2582104
80	51	411	360	125.5	49.4	-78.5	0.775277269	46.51663616
81	51	435.8	384.8	125.5	62.5	-78	0.828685259	49.72111554
82	27.5	219.3	191.8	84	94.2	-94.3	0.617117117	37.02702703
						mean	0.796073241	
						min	0.367159612	
						max	1.058303587	

Table III: Highest nozzle at a pressure of 2.0 bar

Nozle calibration

Date:	19/08/2016	
Time:	12:03:00 PM	12:37
Jet: Highest	wider openning	
Height of jet:	160	cm
Pressure:	2.2	bar
Duration of measurement:	34	min
Surveyors:		

HIGHEST NOZZLE

Vessel number	Vessel veight [g]			Vessel area	Vessel position [cm]		Rain intensity	Rain intensity
	Tara	Brutto	Netto	[cm^2]	x	y	[$mm.min^{-1}$]	[$mm.h^{-1}$]
1	34.2	226	191.8	79.5	4.8	-4.2	0.709581946	42.57491676
2	34.5	247.9	213.4	79.5	14.7	-4.2	0.789493156	47.36958935
3	34.7	272.5	237.8	79.5	25	-4	0.879763226	52.78579356
4	34.4	284.9	250.5	79.5	35	-4.5	0.926748058	55.60488346
5	34.4	289.6	255.2	79.5	45	-4.5	0.944136145	56.6481687
6	34.6	292.7	258.1	79.5	54.9	-4.5	0.954864965	57.29189789
7	34.5	287.6	253.1	79.5	64.8	-4.8	0.936367	56.18201998
8	34.4	271	236.6	79.5	75	-4.8	0.875323714	52.51942286
9	34.4	244.4	210	79.5	85	-4.7	0.776914539	46.61487236
10	34.5	217.9	183.4	79.5	94.8	-5	0.678505364	40.71032186
11	34.5	262.2	227.7	79.5	4.8	-14.3	0.842397336	50.54384018
12	34.4	286	108	79.5	14.7	-14.3	0.399556049	23.97336293
13	34.4	292.2	257.8	79.5	25	-14.4	0.953755087	57.22530522
14	34.5	296	261.5	79.5	35	-14.4	0.967443581	58.04661487
15	35.1	293.4	258.3	79.5	45	-14.6	0.955604883	57.33629301
16	34.6	306.2	271.6	79.5	55.2	-14.5	1.004809471	60.28856826
17	34.5	318.5	284	79.5	65	-14.6	1.050684425	63.04106548
18	34.4	317.5	283.1	79.5	75.2	-14.5	1.047354791	62.84128746
19	34.5	292.2	257.7	79.5	85	-14.5	0.953385128	57.20310766
20	34.5	250.2	215.7	79.5	95	-14.5	0.79800222	47.88013319
21	34.5	300.9	266.4	79.5	5	-24.5	0.985571587	59.13429523
22	34.5	317.2	282.7	79.5	14.8	-24.5	1.045874954	62.75249723
23	34.5	325.4	290.9	79.5	25	-24	1.076211617	64.572697
24	34.4	314.9	280.5	79.5	35	-24.2	1.037735849	62.26415094
25	34.6	299.9	265.3	79.5	45	-24.4	0.981502035	58.89012209
26	34.7	301.9	267.2	79.5	55	-24.4	0.988531262	59.31187569
27	34.5	318.3	283.8	79.5	65	-24.7	1.049944506	62.99667037
28	34.4	330.8	296.4	79.5	75.2	-24.7	1.096559378	65.79356271
29	34.5	340	305.5	79.5	85.3	-24.8	1.130225675	67.81354051
30	34.6	296.5	261.9	79.5	95	-24.5	0.968923418	58.13540511
31	34.5	336.3	301.8	79.5	4.5	-34	1.116537181	66.99223085
32	34.5	356.1	321.6	79.5	14.5	-34	1.189789123	71.38734739
33	34.5	343.2	308.7	79.5	25	-34.2	1.142064373	68.52386238
34	34.4	300.8	266.4	79.5	75.3	-34.6	0.985571587	59.13429523
35	34.6	338.4	303.8	79.5	85	-34.8	1.123936367	67.43618202
36	34.6	339.7	305.1	79.5	95	-34.6	1.128745838	67.72475028
37	34.6	356.6	322	79.5	4.2	-44.5	1.19126896	71.47613762
38	34.7	330.1	295.4	79.5	14.5	-44.5	1.092859785	65.57158713
39	34.4	283	248.6	79.5	24.3	-45.2	0.919718831	55.18312986
40	34	271.6	237.6	79.5	74.5	-44.5	0.879023307	52.74139845
41	34.5	310.2	275.7	79.5	84.5	-44.8	1.019977802	61.19866815
42	34.3	346	311.7	79.5	94.5	-45.1	1.153163152	69.18978912
43	34.6	358.8	324.2	79.5	4.8	-55.2	1.199408065	71.96448391
44	34.6	305.6	271	79.5	15	-55.5	1.002589715	60.15538291
45	34.5	252	217.5	79.5	25	-56.2	0.804661487	48.27968923
46	34.3	253.7	219.4	79.5	74	-55	0.811690714	48.70144284
47	34.4	297.6	263.2	79.5	84.4	-55	0.973732889	58.42397336
48	34.6	338.7	304.1	79.5	94.7	-55.1	1.125046245	67.50277469
49	34.6	337.4	302.8	79.5	4.8	-67	1.120236774	67.21420644
50	34.6	306.3	271.7	79.5	15	-67.5	1.00517943	60.31076582
51	34.4	268	233.6	79.5	25.3	-67.2	0.864224935	51.85349612
52	34.7	260.6	225.9	79.5	74	-66.5	0.835738069	50.14428413
53	34.5	299.9	265.4	79.5	84.9	-67.8	0.981871994	58.91231964
54	34.6	307.4	272.8	79.5	94.8	-67.2	1.009248983	60.55493896
55	34.5	280.6	246.1	79.5	4.8	-79.5	0.910469848	54.6281909
56	34.6	281.6	247	79.5	14.5	-79	0.913799482	54.82796892
57	34.4	275.7	241.3	79.5	24.8	-79.5	0.892711802	53.5627081
58	34.4	270.8	236.4	79.5	73	-80	0.874583796	52.47502775
59	34.5	282	247.5	79.5	83.9	-80	0.915649279	54.93895671
60	34.6	259.9	225.3	79.5	94.3	-80.5	0.833518313	50.01109878
61	34.6	214.3	179.7	79.5	5	-94	0.66481687	39.88901221
62	34.5	226.7	192.2	79.5	15	-94	0.711061783	42.66370699
63	34.4	231.5	197.1	79.5	24.7	-94	0.729189789	43.75138735
64	34.7	235.4	200.7	79.5	34.5	-94.2	0.742508324	44.55049945
65	34.4	233.8	199.4	79.5	44	-93.5	0.737698853	44.26193119
66	34.5	242.5	208	79.5	53.8	-94	0.769515353	46.1709212
67	34.4	248	213.6	79.5	64	-94	0.790233074	47.41398446
68	34.4	248.9	214.5	79.5	73.8	-94	0.793562708	47.61376249
69	34.5	233.2	198.7	79.5	84	-94	0.735109138	44.10654828
70	50.9	480.7	429.8	125.5	37.2	-36.3	1.007265057	60.43590345
71	51	455.1	404.1	125.5	50	-36.8	0.947035388	56.82212327
72	51.2	454.7	403.5	125.5	62.5	-37	0.945629248	56.73775486
73	51	394.8	343.8	125.5	37	-49.5	0.805718303	48.3430982
74	51.2	402	350.8	125.5	50	-50	0.822123272	49.3273963
75	51	401.8	350.8	125.5	62.5	-50	0.822123272	49.3273963
76	50.9	388.9	338	125.5	36.5	-63.8	0.792125615	47.52753691
77	51	387.8	336.8	125.5	49.5	-62.5	0.789313335	47.35880009
78	51	392	341	125.5	62.5	-64	0.799156316	47.94937895
79	51.2	413.5	362.3	125.5	36.5	-79.5	0.849074291	50.94445746
80	51	401.1	350.1	125.5	49.4	-78.5	0.820482775	49.22896649
81	51	402.1	351.1	125.5	62.5	-78	0.822826342	49.3695805
82	27.5	228.5	201	84	94.2	-94.3	0.703781513	42.22689076

mean	0.919794392
min	0.399556049
max	1.199408065

Table IV: Highest nozzle at a pressure of 2.2 bar

Nozle calibration

Date:	08/07/2016	
Time:	01:58:00 PM	14:58
Jet: Low (A)	lechler (120)	
Height of jet:	160	cm
Pressure:	1.6	bar
Duration of measurement:	60	min
Surveyors:		

LOW(A) NOZZLE

Vessel number	Vessel veight [g]			Vessel area	Vessel position [cm]		Rain intensity	Rain intensity
	Tara	Brutto	Netto	[cm^2]	x	y	[$mm.min^{-1}$]	[$mm.h^{-1}$]
1	34.2	87.9	53.7	79.5	4.8	-4.2	0.112578616	6.754716981
2	34.5	97.7	63.2	79.5	14.7	-4.2	0.132494759	7.949685535
3	34.7	108.3	73.6	79.5	25	-4	0.154297694	9.257861635
4	34.4	118.1	83.7	79.5	35	-4.5	0.175471698	10.52830189
5	34.4	131.1	96.7	79.5	45	-4.5	0.202725367	12.16352201
6	34.6	150.2	115.6	79.5	54.9	-4.5	0.242348008	14.5408805
7	34.5	169.2	134.7	79.5	64.8	-4.8	0.282389937	16.94339623
8	34.4	171.6	137.2	79.5	75	-4.8	0.287631027	17.25786164
9	34.4	151.4	117	79.5	85	-4.7	0.245283019	14.71698113
10	34.5	129.8	95.3	79.5	94.8	-5	0.199790356	11.98742138
11	34.5	98.4	63.9	79.5	4.8	-14.3	0.133962264	8.037735849
12	34.4	108.5	108	79.5	14.7	-14.3	0.226415094	13.58490566
13	34.4	121.9	87.5	79.5	25	-14.4	0.183438155	11.00628931
14	34.5	137.5	103	79.5	35	-14.4	0.215932914	12.95597484
15	35.1	158.8	123.7	79.5	45	-14.6	0.25932914	15.55974843
16	34.6	189.1	154.5	79.5	55.2	-14.5	0.323899371	19.43396226
17	34.5	221.3	186.8	79.5	65	-14.6	0.391614256	23.49685535
18	34.4	227.6	193.2	79.5	75.2	-14.5	0.405031447	24.30188679
19	34.5	188.3	153.8	79.5	85	-14.5	0.322431866	19.34591195
20	34.5	144.4	109.9	79.5	95	-14.5	0.230398323	13.82389937
21	34.5	108.7	74.2	79.5	5	-24.5	0.155555556	9.333333333
22	34.5	123.3	88.8	79.5	14.8	-24.5	0.186163522	11.16981132
23	34.5	141.3	106.8	79.5	25	-24	0.223899371	13.43396226
24	34.4	163.7	129.3	79.5	35	-24.2	0.271069182	16.26415094
25	34.6	194.2	159.6	79.5	45	-24.4	0.334591195	20.0754717
26	34.7	222.3	187.6	79.5	55	-24.4	0.393291405	23.59748428
27	34.5	252.8	218.3	79.5	65	-24.7	0.457651992	27.4591195
28	34.4	267.1	232.7	79.5	75.2	-24.7	0.487840671	29.27044025
29	34.5	214.6	180.1	79.5	85.3	-24.8	0.377568134	22.65408805
30	34.6	148.4	113.8	79.5	95	-24.5	0.238574423	14.31446541
31	34.5	117.5	83	79.5	4.5	-34	0.174004193	10.44025157
32	34.5	139.7	105.2	79.5	14.5	-34	0.220545073	13.2327044
33	34.5	161.9	127.4	79.5	25	-34.2	0.267085954	16.02515723
34	34.4	242.6	208.2	79.5	75.3	-34.6	0.436477987	26.18867925
35	34.6	210.2	175.6	79.5	85	-34.8	0.368134172	22.08805031
36	34.6	146.7	112.1	79.5	95	-34.6	0.235010482	14.10062893
37	34.6	123.7	89.1	79.5	4.2	-44.5	0.186792453	11.20754717
38	34.7	149.9	115.2	79.5	14.5	-44.5	0.241509434	14.49056604
39	34.4	186.7	152.3	79.5	24.3	-45.2	0.319287212	19.1572327
40	34	213.8	179.8	79.5	74.5	-44.5	0.376939203	22.6163522
41	34.5	182.7	148.2	79.5	84.5	-44.8	0.310691824	18.64150943
42	34.3	135.6	101.3	79.5	94.5	-45.1	0.212368973	12.74213836
43	34.6	129.4	94.8	79.5	4.8	-55.2	0.198742138	11.9245283
44	34.6	160.6	126	79.5	15	-55.5	0.264150943	15.8490566
45	34.5	203	168.5	79.5	25	-56.2	0.353249476	21.19496855
46	34.3	189.3	155	79.5	74	-55	0.324947589	19.49685535
47	34.4	157.2	122.8	79.5	84.4	-55	0.257442348	15.44654088
48	34.6	127.1	92.5	79.5	94.7	-55.1	0.193920335	11.63522013
49	34.6	125.2	90.6	79.5	4.8	-67	0.189937107	11.39622642
50	34.6	160.6	126	79.5	15	-67.5	0.264150943	15.8490566
51	34.4	212	177.6	79.5	25.3	-67.2	0.372327044	22.33962264
52	34.7	164.7	130	79.5	74	-66.5	0.272536688	16.35220126
53	34.5	137.3	102.8	79.5	84.9	-67.8	0.215513627	12.93081761
54	34.6	113.3	78.7	79.5	94.8	-67.2	0.164989518	9.899371069
55	34.5	118.1	83.6	79.5	4.8	-79.5	0.175262055	10.51572327
56	34.6	144.5	109.9	79.5	14.5	-79	0.230398323	13.82389937
57	34.4	187.5	153.1	79.5	24.8	-79.5	0.320964361	19.25786164
58	34.4	145.5	111.1	79.5	73	-80	0.232914046	13.97484277
59	34.5	117.3	82.8	79.5	83.9	-80	0.173584906	10.41509434
60	34.6	99.2	64.6	79.5	94.3	-80.5	0.135429769	8.125786164
61	34.6	104.6	70	79.5	5	-94	0.146750524	8.805031447
62	34.5	118.7	84.2	79.5	15	-94	0.176519916	10.59119497
63	34.4	136.1	101.7	79.5	24.7	-94	0.213207547	12.79245283
64	34.7	156.5	121.8	79.5	34.5	-94.2	0.255345912	15.32075472
65	34.4	171	136.6	79.5	44	-93.5	0.286373166	17.18238994
66	34.5	164.2	129.7	79.5	53.8	-94	0.271907757	16.31446541
67	34.4	145.8	111.4	79.5	64	-94	0.233542977	14.01257862
68	34.4	122.3	87.9	79.5	73.8	-94	0.18427673	11.05660377
69	34.5	102.7	68.2	79.5	84	-94	0.142976939	8.578616352
70	50.9	309	258.1	125.5	37.2	-36.3	0.342762284	20.56573705
71	51	322.9	271.9	125.5	50	-36.8	0.361088977	21.66533865
72	51.2	313.2	262	125.5	62.5	-37	0.347941567	20.87649402
73	51	314.3	263.3	125.5	37	-49.5	0.349667995	20.98007968
74	51.2	286.6	235.4	125.5	50	-50	0.312616202	18.75697211
75	51	305.4	254.4	125.5	62.5	-50	0.337848606	20.27091633
76	50.9	345.8	294.9	125.5	36.5	-63.8	0.391633466	23.49800797
77	51	327	276	125.5	49.5	-62.5	0.366533865	21.99203187
78	51	319.4	268.4	125.5	62.5	-64	0.356440903	21.38645418
79	51.2	373.9	322.7	125.5	36.5	-79.5	0.428552457	25.71314741
80	51	364.7	313.7	125.5	49.4	-78.5	0.416600266	24.99601594
81	51	289.9	238.9	125.5	62.5	-78	0.317264276	19.03585657
82	27.5	85.9	58.4	84	94.2	-94.3	0.115873016	6.952380952

mean	0.267057345
min	0.112578616
max	0.487840671

Table V: Low(A) nozzle at a pressure of 1.6 bar

Nozle calibration

Date:	09/07/2016	
Time:	12:12:00 PM	13:24
Jet: Low (A)	lechler (120)	
Height of jet:	160	cm
Pressure:	1.8	bar
Duration of measurement:	72	min
Surveyors:		

LOW(A) NOZZLE

Vessel number	Vessel veight [g]			Vessel area	Vessel position [cm]		Rain intensity	Rain intensity
	Tara	Brutto	Netto	[cm^2]	x	y	[$mm.min^{-1}$]	[$mm.h^{-1}$]
1	34.2	108.5	74.3	79.5	4.8	-4.2	0.129804333	7.788259958
2	34.5	121.3	86.8	79.5	14.7	-4.2	0.151642208	9.098532495
3	34.7	140.1	105.4	79.5	25	-4	0.184136967	11.04821803
4	34.4	158.1	123.7	79.5	35	-4.5	0.216107617	12.96645702
5	34.4	184.2	149.8	79.5	45	-4.5	0.261705101	15.70230608
6	34.6	227.2	192.6	79.5	54.9	-4.5	0.336477987	20.18867925
7	34.5	256	221.5	79.5	64.8	-4.8	0.386967156	23.21802935
8	34.4	233.9	199.5	79.5	75	-4.8	0.348532495	20.91194969
9	34.4	191.4	157	79.5	85	-4.7	0.274283718	16.45702306
10	34.5	153.7	119.2	79.5	94.8	-5	0.208245982	12.49475891
11	34.5	123.1	88.6	79.5	4.8	-14.3	0.154786862	9.28721174
12	34.4	142.3	108	79.5	14.7	-14.3	0.188679245	11.32075472
13	34.4	161.5	127.1	79.5	25	-14.4	0.222047519	13.32285115
14	34.5	191.8	157.3	79.5	35	-14.4	0.274807827	16.4884696
15	35.1	229.2	194.1	79.5	45	-14.6	0.339098532	20.34591195
16	34.6	298.6	264	79.5	55.2	-14.5	0.461215933	27.67295597
17	34.5	348.2	313.7	79.5	65	-14.6	0.548043326	32.88259958
18	34.4	313.8	279.4	79.5	75.2	-14.5	0.488120196	29.28721174
19	34.5	226.6	192.1	79.5	85	-14.5	0.335604472	20.13626834
20	34.5	167.1	132.6	79.5	95	-14.5	0.231656184	13.89937107
21	34.5	141	106.5	79.5	5	-24.5	0.1860587	11.16352201
22	34.5	163.5	129	79.5	14.8	-24.5	0.225366876	13.52201258
23	34.5	194.4	159.9	79.5	25	-24	0.279350105	16.76100629
24	34.4	237.7	203.3	79.5	35	-24.2	0.355171209	21.31027254
25	34.6	297.4	262.8	79.5	45	-24.4	0.459119497	27.54716981
26	34.7	330.5	295.8	79.5	55	-24.4	0.516771488	31.00628931
27	34.5	369.8	335.3	79.5	65	-24.7	0.585779175	35.14675052
28	34.4	366	331.6	79.5	75.2	-24.7	0.579315164	34.75890985
29	34.5	254.6	220.1	79.5	85.3	-24.8	0.384521314	23.07127883
30	34.6	173.8	139.2	79.5	95	-24.5	0.243186583	14.59119497
31	34.5	152.7	118.2	79.5	4.5	-34	0.206498952	12.38993711
32	34.5	187.8	153.3	79.5	14.5	-34	0.267819706	16.06918239
33	34.5	234.5	200	79.5	25	-34.2	0.34940601	20.96436059
34	34.4	329.6	295.2	79.5	75.3	-34.6	0.51572327	30.94339623
35	34.6	251.7	217.1	79.5	85	-34.8	0.379280224	22.75681342
36	34.6	174.8	140.2	79.5	95	-34.6	0.244933613	14.69601677
37	34.6	164.5	129.9	79.5	4.2	-44.5	0.226939203	13.6163522
38	34.7	215	180.3	79.5	14.5	-44.5	0.314989518	18.89937107
39	34.4	275.9	241.5	79.5	24.3	-45.2	0.421907757	25.31446541
40	34	283.9	249.9	79.5	74.5	-44.5	0.436582809	26.19496855
41	34.5	225.4	190.9	79.5	84.5	-44.8	0.333508036	20.01048218
42	34.3	165.6	131.3	79.5	94.5	-45.1	0.229385045	13.76310273
43	34.6	170.7	136.1	79.5	4.8	-55.2	0.23777079	14.26624738
44	34.6	226.8	192.2	79.5	15	-55.5	0.335779175	20.14675052
45	34.5	295.3	260.8	79.5	25	-56.2	0.455625437	27.33752621
46	34.3	250.4	216.1	79.5	74	-55	0.377533194	22.65199161
47	34.4	202.7	168.3	79.5	84.4	-55	0.294025157	17.64150943
48	34.6	158.4	123.8	79.5	94.7	-55.1	0.21628232	12.9769392
49	34.6	160	125.4	79.5	4.8	-67	0.219077568	13.14465409
50	34.6	219.9	185.3	79.5	15	-67.5	0.323724668	19.42348008
51	34.4	295.6	261.2	79.5	25.3	-67.2	0.456324249	27.37945493
52	34.7	219.6	184.9	79.5	74	-66.5	0.323025856	19.38155136
53	34.5	178.6	144.1	79.5	84.9	-67.8	0.25174703	15.1048218
54	34.6	140	105.4	79.5	94.8	-67.2	0.184136967	11.04821803
55	34.5	149.5	115	79.5	4.8	-79.5	0.200908456	12.05450734
56	34.6	185	150.4	79.5	14.5	-79	0.262753319	15.76519916
57	34.4	245	210.6	79.5	24.8	-79.5	0.367924528	22.0754717
58	34.4	190.6	156.2	79.5	73	-80	0.272886094	16.37316562
59	34.5	146.9	112.4	79.5	83.9	-80	0.196366177	11.78197065
60	34.6	117.4	82.8	79.5	94.3	-80.5	0.144654088	8.679245283
61	34.6	124.3	89.7	79.5	5	-94	0.156708595	9.402515723
62	34.5	147	112.5	79.5	15	-94	0.196540881	11.79245283
63	34.4	167.4	133	79.5	24.7	-94	0.232354997	13.94129979
64	34.7	187.7	153	79.5	34.5	-94.2	0.267295597	16.03773585
65	34.4	202.5	168.1	79.5	44	-93.5	0.293675751	17.62054507
66	34.5	196.8	162.3	79.5	53.8	-94	0.283542977	17.01257862
67	34.4	179	144.6	79.5	64	-94	0.252620545	15.1572327
68	34.4	152.1	117.7	79.5	73.8	-94	0.205625437	12.33752621
69	34.5	124.5	90	79.5	84	-94	0.157232704	9.433962264
70	50.9	452.1	401.2	125.5	37.2	-36.3	0.444001771	26.64010624
71	51	425.1	374.1	125.5	50	-36.8	0.414010624	24.84063745
72	51.2	426.5	375.3	125.5	62.5	-37	0.415338645	24.92031873
73	51	436.5	385.5	125.5	37	-49.5	0.426626826	25.59760956
74	51.2	390.6	339.4	125.5	50	-50	0.375608676	22.53652058
75	51	425.4	374.4	125.5	62.5	-50	0.414342629	24.86055777
76	50.9	492.1	441.2	125.5	36.5	-63.8	0.488269146	29.29614874
77	51	456.7	405.7	125.5	49.5	-62.5	0.44898185	26.93891102
78	51	446.2	395.2	125.5	62.5	-64	0.437361664	26.24169987
79	51.2	478.4	427.2	125.5	36.5	-79.5	0.472775564	28.36653386
80	51	491.4	440.4	125.5	49.4	-78.5	0.487383798	29.24302789
81	51	392.6	341.6	125.5	62.5	-78	0.378043382	22.68260292
82	27.5	100.7	73.2	84	94.2	-94.3	0.121031746	7.261904762

mean	0.316749961
min	0.121031746
max	0.585779175

Table VI: Low(A) nozzle at pressure of 1.8 bar

Nozle calibration

Date:	18/07/2016	
Time:	11:15:00 AM	12:25
Jet:Low (A)	lechler (120)	small open
Height of jet:	160	cm
Pressure:	2	bar
Duration of measurement:	70	min
Surveyors:		

LOW(A) NOZZLE

Vessel number	Vessel veight [g]			Vessel area	Vessel position [cm]		Rain intensity	Rain intensity
	Tara	Brutto	Netto	[cm^2]	x	y	[$mm.min^{-1}$]	[$mm.h^{-1}$]
1	34.2	102.8	68.6	79.5	4.8	-4.2	0.12327044	7.396226415
2	34.5	118.7	84.2	79.5	14.7	-4.2	0.151302785	9.078167116
3	34.7	139.6	104.9	79.5	25	-4	0.188499551	11.30997305
4	34.4	159.8	125.4	79.5	35	-4.5	0.225336927	13.52021563
5	34.4	187.6	153.2	79.5	45	-4.5	0.275292004	16.51752022
6	34.6	225.6	191	79.5	54.9	-4.5	0.343216532	20.59299191
7	34.5	247.9	213.4	79.5	64.8	-4.8	0.383468104	23.00808625
8	34.4	220.7	186.3	79.5	75	-4.8	0.334770889	20.08625337
9	34.4	179	144.6	79.5	85	-4.7	0.259838275	15.5902965
10	34.5	152	117.5	79.5	94.8	-5	0.21114106	12.66846361
11	34.5	120.4	85.9	79.5	4.8	-14.3	0.154357592	9.261455526
12	34.4	141.2	108	79.5	14.7	-14.3	0.194070081	11.64420485
13	34.4	166.3	131.9	79.5	25	-14.4	0.237017071	14.22102426
14	34.5	199.9	165.4	79.5	35	-14.4	0.297214735	17.8328841
15	35.1	250.3	215.2	79.5	45	-14.6	0.386702606	23.20215633
16	34.6	322.1	287.5	79.5	55.2	-14.5	0.516621743	30.99730458
17	34.5	350.3	315.8	79.5	65	-14.6	0.567475292	34.04851752
18	34.4	295.2	260.8	79.5	75.2	-14.5	0.468643306	28.11859838
19	34.5	214.1	179.6	79.5	85	-14.5	0.322731357	19.3638814
20	34.5	158.9	124.4	79.5	95	-14.5	0.223539982	13.41239892
21	34.5	139.6	105.1	79.5	5	-24.5	0.18885894	11.33153639
22	34.5	166.2	131.7	79.5	14.8	-24.5	0.236657682	14.19946092
23	34.5	204.8	170.3	79.5	25	-24	0.306019766	18.36118598
24	34.4	261.8	227.4	79.5	35	-24.2	0.408625337	24.51752022
25	34.6	325.3	290.7	79.5	45	-24.4	0.522371968	31.34231806
26	34.7	345.1	310.4	79.5	55	-24.4	0.557771788	33.46630728
27	34.5	366.8	332.3	79.5	65	-24.7	0.597124888	35.82749326
28	34.4	340	305.6	79.5	75.2	-24.7	0.549146451	32.94878706
29	34.5	236.7	202.2	79.5	85.3	-24.8	0.363342318	21.80053908
30	34.6	167.3	132.7	79.5	95	-24.5	0.238454627	14.30727763
31	34.5	152.5	118	79.5	4.5	-34	0.212039533	12.72237197
32	34.5	194	159.5	79.5	14.5	-34	0.286612758	17.1967655
33	34.5	252.8	218.3	79.5	25	-34.2	0.392273136	23.53638814
34	34.4	303	268.6	79.5	75.3	-34.6	0.482659479	28.95956873
35	34.6	239	204.4	79.5	85	-34.8	0.367295597	22.03773585
36	34.6	168.6	134	79.5	95	-34.6	0.240790656	14.44743935
37	34.6	162.8	128.2	79.5	4.2	-44.5	0.230368374	13.82210243
38	34.7	226.1	191.4	79.5	14.5	-44.5	0.34393531	20.6361186
39	34.4	296.8	262.4	79.5	24.3	-45.2	0.471518419	28.29110512
40	34	263.3	229.3	79.5	74.5	-44.5	0.412039533	24.72237197
41	34.5	220.3	185.8	79.5	84.5	-44.8	0.333872417	20.03234501
42	34.3	163.1	128.8	79.5	94.5	-45.1	0.231446541	13.88679245
43	34.6	164.8	130.2	79.5	4.8	-55.2	0.233962264	14.03773585
44	34.6	234.6	200	79.5	15	-55.5	0.359389039	21.56334232
45	34.5	313	278.5	79.5	25	-56.2	0.500449236	30.02695418
46	34.3	236.3	202	79.5	74	-55	0.362982929	21.77897574
47	34.4	198	163.6	79.5	84.4	-55	0.293980234	17.63881402
48	34.6	156.8	122.2	79.5	94.7	-55.1	0.219586703	13.17520216
49	34.6	156.2	121.6	79.5	4.8	-67	0.218508535	13.11051213
50	34.6	220.8	186.2	79.5	15	-67.5	0.334591195	20.0754717
51	34.4	300.2	265.8	79.5	25.3	-67.2	0.477628032	28.65768194
52	34.7	213.25	178.55	79.5	74	-66.5	0.320844564	19.25067385
53	34.5	168.8	134.3	79.5	84.9	-67.8	0.241329739	14.47978437
54	34.6	134.8	100.2	79.5	94.8	-67.2	0.180053908	10.8032345
55	34.5	144.1	109.6	79.5	4.8	-79.5	0.196945193	11.81671159
56	34.6	180.5	145.9	79.5	14.5	-79	0.262174304	15.73045822
57	34.4	237.5	203.1	79.5	24.8	-79.5	0.364959569	21.89757412
58	34.4	187.9	153.5	79.5	73	-80	0.275831087	16.54986523
59	34.5	142.1	107.6	79.5	83.9	-80	0.193351303	11.60107817
60	34.6	110	75.4	79.5	94.3	-80.5	0.135489668	8.129380054
61	34.6	117.3	82.7	79.5	5	-94	0.148607367	8.916442049
62	34.5	138.6	104.1	79.5	15	-94	0.187061995	11.22371968
63	34.4	159.1	124.7	79.5	24.7	-94	0.224079066	13.44474394
64	34.7	178.5	143.8	79.5	34.5	-94.2	0.258400719	15.50404313
65	34.4	189.4	155	79.5	44	-93.5	0.278526505	16.7115903
66	34.5	180.7	146.2	79.5	53.8	-94	0.262713387	15.76280323
67	34.4	166.6	132.2	79.5	64	-94	0.237556155	14.25336927
68	34.4	144.1	109.7	79.5	73.8	-94	0.197124888	11.82749326
69	34.5	116.2	81.7	79.5	84	-94	0.146810422	8.808625337
70	50.9	468.4	417.5	125.5	37.2	-36.3	0.47524189	28.51451338
71	51	404.6	353.6	125.5	50	-36.8	0.402504269	24.15025612
72	51.2	418.4	367.2	125.5	62.5	-37	0.417985202	25.07911212
73	51	432	381	125.5	37	-49.5	0.433693796	26.02162777
74	51.2	386	334.8	125.5	50	-50	0.381104155	22.86624929
75	51	406.2	355.2	125.5	62.5	-50	0.404325555	24.2595333
76	50.9	497	446.1	125.5	36.5	-63.8	0.507797382	30.46784291
77	51	446.6	395.6	125.5	49.5	-62.5	0.450313034	27.01878201
78	51	424.7	373.7	125.5	62.5	-64	0.425384178	25.52305065
79	51.2	458.5	407.3	125.5	36.5	-79.5	0.46363119	27.81787137
80	51	461.3	410.3	125.5	49.4	-78.5	0.467046101	28.02276608
81	51	377.2	326.2	125.5	62.5	-78	0.371314741	22.27888446
82	27.5	93.9	66.4	84	94.2	-94.3	0.11292517	6.775510204

mean	0.320291958
min	0.11292517
max	0.597124888

Table VII: Low(A) nozzle at a pressure of 2.0 bar

Nozle calibration

Date:	18/07/2016	
Time:	02:00:00 PM	14:54
Jet:Low (A)	lechler (120)	small open
Height of jet:	160	cm
Pressure:	2.2	bar
Duration of measurement:	54	min
Surveyors:		

LOW(A) NOZZLE

Vessel number	Vessel veight [g]			Vessel area [cm^2]	Vessel position [cm]		Rain intensity [$mm.min^{-1}$]	Rain intensity [$mm.h^{-1}$]
	Tara	Brutto	Netto		x	y		
1	34.2	92	57.8	79.5	4.8	-4.2	0.134637782	8.078266946
2	34.5	105.8	71.3	79.5	14.7	-4.2	0.166084323	9.965059399
3	34.7	122.7	88	79.5	25	-4	0.204984859	12.29909154
4	34.4	140	105.6	79.5	35	-4.5	0.245981831	14.75890985
5	34.4	155.2	120.8	79.5	45	-4.5	0.281388307	16.88329839
6	34.6	161	126.4	79.5	54.9	-4.5	0.294432798	17.66596785
7	34.5	162.7	128.2	79.5	64.8	-4.8	0.29862567	17.91754018
8	34.4	164.2	129.8	79.5	75	-4.8	0.302352667	18.14116003
9	34.4	153.2	118.8	79.5	85	-4.7	0.27672956	16.60377358
10	34.5	134	99.5	79.5	94.8	-5	0.231772653	13.90635919
11	34.5	108.7	74.2	79.5	4.8	-14.3	0.172839506	10.37037037
12	34.4	129.3	108	79.5	14.7	-14.3	0.251572327	15.09433962
13	34.4	157.9	123.5	79.5	25	-14.4	0.287677615	17.26065688
14	34.5	190.8	156.3	79.5	35	-14.4	0.364081062	21.84486373
15	35.1	216.2	181.1	79.5	45	-14.6	0.421849522	25.31097135
16	34.6	230.6	196	79.5	55.2	-14.5	0.456557186	27.39343117
17	34.5	235.3	200.8	79.5	65	-14.6	0.467738178	28.06429071
18	34.4	225.2	190.8	79.5	75.2	-14.5	0.444444444	26.66666667
19	34.5	194.5	160	79.5	85	-14.5	0.372699744	22.36198463
20	34.5	158.4	123.9	79.5	95	-14.5	0.288609364	17.31656184
21	34.5	126.5	92	79.5	5	-24.5	0.214302353	12.85814116
22	34.5	157.9	123.4	79.5	14.8	-24.5	0.287444677	17.24668064
23	34.5	206.1	171.6	79.5	25	-24	0.399720475	23.98322851
24	34.4	258.3	223.9	79.5	35	-24.2	0.521546704	31.29280224
25	34.6	296.7	262.1	79.5	45	-24.4	0.610528768	36.63172607
26	34.7	336.2	301.5	79.5	55	-24.4	0.70230608	42.13836478
27	34.5	364.3	329.8	79.5	65	-24.7	0.768227347	46.09364081
28	34.4	347.1	312.7	79.5	75.2	-24.7	0.728395062	43.7037037
29	34.5	250.5	216	79.5	85.3	-24.8	0.503144654	30.18867925
30	34.6	175.1	140.5	79.5	95	-24.5	0.327276962	19.63661775
31	34.5	139.6	105.1	79.5	4.5	-34	0.244817144	14.68902865
32	34.5	188.7	154.2	79.5	14.5	-34	0.359189378	21.55136268
33	34.5	251.4	216.9	79.5	25	-34.2	0.50524109	30.31446541
34	34.4	350.8	316.4	79.5	75.3	-34.6	0.737013743	44.2208246
35	34.6	294.3	259.7	79.5	85	-34.8	0.604938272	36.2962963
36	34.6	182.5	147.9	79.5	95	-34.6	0.344514326	20.67085954
37	34.6	147.8	113.2	79.5	4.2	-44.5	0.263685069	15.82110412
38	34.7	205.2	170.5	79.5	14.5	-44.5	0.397158164	23.82948987
39	34.4	282.7	248.3	79.5	24.3	-45.2	0.578383415	34.70300489
40	34	290.6	256.6	79.5	74.5	-44.5	0.597717214	35.86303284
41	34.5	259.3	224.8	79.5	84.5	-44.8	0.52364314	31.4185884
42	34.3	171.5	137.2	79.5	94.5	-45.1	0.31959003	19.17540182
43	34.6	154.8	120.2	79.5	4.8	-55.2	0.279990683	16.79944095
44	34.6	215	180.4	79.5	15	-55.5	0.420218961	25.21313767
45	34.5	293.8	259.3	79.5	25	-56.2	0.604006522	36.24039133
46	34.3	250.7	216.4	79.5	74	-55	0.504076403	30.24458421
47	34.4	211.3	176.9	79.5	84.4	-55	0.412066154	24.72396925
48	34.6	140.8	106.2	79.5	94.7	-55.1	0.247379455	14.8427673
49	34.6	146.5	111.9	79.5	4.8	-67	0.260656883	15.639413
50	34.6	204.8	170.2	79.5	15	-67.5	0.396459352	23.78756115
51	34.4	277.7	243.3	79.5	25.3	-67.2	0.566736548	34.00419287
52	34.7	204.3	169.6	79.5	74	-66.5	0.395061728	23.7037037
53	34.5	168.4	133.9	79.5	84.9	-67.8	0.311903098	18.71418588
54	34.6	125.6	91	79.5	94.8	-67.2	0.211972979	12.71837876
55	34.5	134.5	100	79.5	4.8	-79.5	0.23293734	13.97624039
56	34.6	170.2	135.6	79.5	14.5	-79	0.315863033	18.95178197
57	34.4	221.7	187.3	79.5	24.8	-79.5	0.436291638	26.17749825
58	34.4	156.2	121.8	79.5	73	-80	0.28371768	17.0230608
59	34.5	120.8	86.3	79.5	83.9	-80	0.201024924	12.06149546
60	34.6	98.4	63.8	79.5	94.3	-80.5	0.148614023	8.91684137
61	34.6	111.6	77	79.5	5	-94	0.179361752	10.7617051
62	34.5	129.4	94.9	79.5	15	-94	0.221057536	13.26345213
63	34.4	146.3	111.9	79.5	24.7	-94	0.260656883	15.639413
64	34.7	159.5	124.8	79.5	34.5	-94.2	0.2907058	17.44234801
65	34.4	164.3	129.9	79.5	44	-93.5	0.302585604	18.15513627
66	34.5	157.1	122.6	79.5	53.8	-94	0.285581179	17.13487072
67	34.4	138.9	104.5	79.5	64	-94	0.24341952	14.60517121
68	34.4	116.4	82	79.5	73.8	-94	0.191008619	11.46051712
69	34.5	96	61.5	79.5	84	-94	0.143256464	8.595387841
70	50.9	446.6	395.7	125.5	37.2	-36.3	0.583886676	35.03320053
71	51	400.4	349.4	125.5	50	-36.8	0.51556736	30.93404161
72	51.2	382.8	331.6	125.5	62.5	-37	0.489302051	29.35812306
73	51	409.2	358.2	125.5	37	-49.5	0.528552457	31.71314741
74	51.2	352.5	301.3	125.5	50	-50	0.444592002	26.67552014
75	51	371.3	320.3	125.5	62.5	-50	0.472628006	28.35768039
76	50.9	453	402.1	125.5	36.5	-63.8	0.593330382	35.59982293
77	51	414.3	363.3	125.5	49.5	-62.5	0.536077911	32.16467463
78	51	383.2	332.2	125.5	62.5	-64	0.490187399	29.41124391
79	51.2	402	350.8	125.5	36.5	-79.5	0.517633171	31.05799026
80	51	387.7	336.7	125.5	49.4	-78.5	0.496827505	29.80965029
81	51	315.2	264.2	125.5	62.5	-78	0.389848015	23.39088092
82	27.5	78.3	50.8	84	94.2	-94.3	0.111992945	6.71957672

mean	0.378303416
min	0.111992945
max	0.768227347

Table VIII: Low(A) nozzle at a pressure of 2.2 bar

Nozle calibration

Date:	23/08/2016	
Time:	10:36:00 AM	11:52
Jet: Low(B)	smallest open	
Height of jet:	160	cm
Pressure:	1.6	bar
Duration of measurement:	76	min
Surveyors:		

LOW(B) NOZZLE

Vessel number	Vessel veight [g]			Vessel area [cm^2]	Vessel position [cm]		Rain intensity [$mm.min^{-1}$]	Rain intensity [$mm.h^{-1}$]
	Tara	Brutto	Netto		x	y		
1	34.2	122.4	88.2	79.5	4.8	-4.2	0.145978153	8.758689176
2	34.5	135.4	100.9	79.5	14.7	-4.2	0.166997683	10.01986097
3	34.7	149	114.3	79.5	25	-4	0.18917577	11.35054618
4	34.4	159.5	125.1	79.5	35	-4.5	0.207050645	12.42303873
5	34.4	170.7	136.3	79.5	45	-4.5	0.225587554	13.53525323
6	34.6	179	144.4	79.5	54.9	-4.5	0.238993711	14.33962264
7	34.5	173.2	138.7	79.5	64.8	-4.8	0.229559748	13.77358491
8	34.4	160.1	125.7	79.5	75	-4.8	0.208043694	12.48262165
9	34.4	134.5	100.1	79.5	85	-4.7	0.165673618	9.94041708
10	34.5	115.5	81	79.5	94.8	-5	0.134061569	8.043694141
11	34.5	140.4	105.9	79.5	4.8	-14.3	0.175273088	10.5163853
12	34.4	157.5	108	79.5	14.7	-14.3	0.178748759	10.72492552
13	34.4	178.6	144.2	79.5	25	-14.4	0.238662694	14.31976167
14	34.5	199.6	165.1	79.5	35	-14.4	0.273253889	16.39523337
15	35.1	223.1	188	79.5	45	-14.6	0.311155247	18.6693148
16	34.6	241.8	207.2	79.5	55.2	-14.5	0.342932804	20.57596822
17	34.5	232.1	197.6	79.5	65	-14.6	0.327044025	19.62264151
18	34.4	200.4	166	79.5	75.2	-14.5	0.274743462	16.48460775
19	34.5	157.4	122.9	79.5	85	-14.5	0.203409467	12.20456802
20	34.5	128.9	94.4	79.5	95	-14.5	0.156239656	9.374379345
21	34.5	162.1	127.6	79.5	5	-24.5	0.211188348	12.67130089
22	34.5	187.8	153.3	79.5	14.8	-24.5	0.253723932	15.22343595
23	34.5	221.8	187.3	79.5	25	-24	0.30999669	18.59980139
24	34.4	273.9	239.5	79.5	35	-24.2	0.396391923	23.78351539
25	34.6	295.7	261.1	79.5	45	-24.4	0.432141675	25.9285005
26	34.7	312.4	277.7	79.5	55	-24.4	0.459616021	27.57696127
27	34.5	305.2	270.7	79.5	65	-24.7	0.448030453	26.88182721
28	34.4	245.8	211.4	79.5	75.2	-24.7	0.349884144	20.99304866
29	34.5	182.8	148.3	79.5	85.3	-24.8	0.245448527	14.72691162
30	34.6	141.1	106.5	79.5	95	-24.5	0.176266137	10.57596822
31	34.5	190.4	155.9	79.5	4.5	-34	0.258027143	15.4816286
32	34.5	248.9	214.4	79.5	14.5	-34	0.354849388	21.29096326
33	34.5	307.6	273.1	79.5	25	-34.2	0.452002648	27.12015889
34	34.4	287	252.6	79.5	75.3	-34.6	0.418073486	25.08440914
35	34.6	202.2	167.6	79.5	85	-34.8	0.277391592	16.64349553
36	34.6	152.9	118.3	79.5	95	-34.6	0.195796094	11.74776564
37	34.6	211	176.4	79.5	4.2	-44.5	0.291956306	17.51737835
38	34.7	297.5	262.8	79.5	14.5	-44.5	0.434955313	26.09731877
39	34.4	344.3	309.9	79.5	24.3	-45.2	0.512909633	30.77457795
40	34	280.3	246.3	79.5	74.5	-44.5	0.407646475	24.45878848
41	34.5	212.9	178.4	79.5	84.5	-44.8	0.295266468	17.71598808
42	34.3	158.5	124.2	79.5	94.5	-45.1	0.205561072	12.33366435
43	34.6	221.5	186.9	79.5	4.8	-55.2	0.309334657	18.56007944
44	34.6	312.3	277.7	79.5	15	-55.5	0.459616021	27.57696127
45	34.5	337.3	302.8	79.5	25	-56.2	0.501158557	30.06951341
46	34.3	255.6	221.3	79.5	74	-55	0.366269447	21.97616683
47	34.4	205.4	171	79.5	84.4	-55	0.283018868	16.98113208
48	34.6	157.5	122.9	79.5	94.7	-55.1	0.203409467	12.20456802
49	34.6	192.8	158.2	79.5	4.8	-67	0.26183383	15.71002979
50	34.6	263.8	229.2	79.5	15	-67.5	0.379344588	22.76067527
51	34.4	309.1	274.7	79.5	25.3	-67.2	0.454650778	27.27904667
52	34.7	224.8	190.1	79.5	74	-66.5	0.314630917	18.87785501
53	34.5	183	148.5	79.5	84.9	-67.8	0.245779543	14.74677259
54	34.6	147.4	112.8	79.5	94.8	-67.2	0.186693148	11.20158888
55	34.5	159.9	125.4	79.5	4.8	-79.5	0.20754717	12.45283019
56	34.6	192.1	157.5	79.5	14.5	-79	0.260675273	15.64051639
57	34.4	233.6	199.2	79.5	24.8	-79.5	0.329692155	19.78152929
58	34.4	183.7	149.3	79.5	73	-80	0.247103608	14.82621648
59	34.5	155.7	121.2	79.5	83.9	-80	0.200595829	12.03574975
60	34.6	133.7	99.1	79.5	94.3	-80.5	0.164018537	9.841112214
61	34.6	127.9	93.3	79.5	5	-94	0.154419067	9.265143992
62	34.5	144.4	109.9	79.5	15	-94	0.181893413	10.91360477
63	34.4	159.6	125.2	79.5	24.7	-94	0.207216154	12.43296922
64	34.7	170.7	136	79.5	34.5	-94.2	0.225091029	13.50546177
65	34.4	174.5	140.1	79.5	44	-93.5	0.231876862	13.91261172
66	34.5	169.2	134.7	79.5	53.8	-94	0.222939424	13.37636544
67	34.4	156.5	122.1	79.5	64	-94	0.202085402	12.12512413
68	34.4	139.9	105.5	79.5	73.8	-94	0.174611056	10.47666336
69	34.5	124.6	90.1	79.5	84	-94	0.149122807	8.947368421
70	50.9	464.4	413.5	125.5	37.2	-36.3	0.433529042	26.0117425
71	51	439.9	388.9	125.5	50	-36.8	0.407737471	24.46424827
72	51.2	497	445.8	125.5	62.5	-37	0.467393584	28.04361501
73	51	375.3	324.3	125.5	37	-49.5	0.340008388	20.40050325
74	51.2	367.5	316.3	125.5	50	-50	0.331620885	19.89725309
75	51	402.8	351.8	125.5	62.5	-50	0.368840428	22.13042567
76	50.9	462.1	411.2	125.5	36.5	-63.8	0.431117635	25.86705808
77	51	411.8	360.8	125.5	49.5	-62.5	0.378276368	22.69658209
78	51	390.4	339.4	125.5	62.5	-64	0.355839799	21.35038792
79	51.2	395.7	344.5	125.5	36.5	-79.5	0.361186832	21.6712099
80	51	376.9	325.9	125.5	49.4	-78.5	0.341685888	20.50115328
81	51	336.9	285.9	125.5	62.5	-78	0.299748375	17.9849025
82	27.5	112.9	85.4	84	94.2	-94.3	0.13377193	8.026315789

mean	0.287257231
min	0.13377193
max	0.512909633

Table IX: Low(B) nozzle at a pressure of 1.6 bar

Nozle calibration

Date:	23/08/2016	
Time:	02:43:00 PM	15:39
Jet:Low(B)	smallest open	
Height of jet:	160	cm
Pressure:	1.8	bar
Duration of measurement:	56	min
Surveyors:		

LOW(B) NOZZLE

Vessel number	Vessel veight [g]			Vessel area [cm^2]	Vessel position [cm]		Rain intensity [$mm.min^{-1}$]	Rain intensity [$mm.h^{-1}$]
	Tara	Brutto	Netto		x	y		
1	34.2	89.5	55.3	79.5	4.8	-4.2	0.124213836	7.452830189
2	34.5	100.8	66.3	79.5	14.7	-4.2	0.148921833	8.935309973
3	34.7	118.5	83.8	79.5	25	-4	0.188230009	11.29380054
4	34.4	137.3	102.9	79.5	35	-4.5	0.231132075	13.86792453
5	34.4	156.7	122.3	79.5	45	-4.5	0.274707996	16.48247978
6	34.6	170	135.4	79.5	54.9	-4.5	0.304132974	18.24797844
7	34.5	162.7	128.2	79.5	64.8	-4.8	0.287960467	17.27762803
8	34.4	142	107.6	79.5	75	-4.8	0.241689128	14.50134771
9	34.4	120.2	85.8	79.5	85	-4.7	0.192722372	11.56334232
10	34.5	104.6	70.1	79.5	94.8	-5	0.157457323	9.447439353
11	34.5	102	67.5	79.5	4.8	-14.3	0.151617251	9.09703504
12	34.4	115.2	108	79.5	14.7	-14.3	0.242587601	14.55525606
13	34.4	135.2	100.8	79.5	25	-14.4	0.226415094	13.58490566
14	34.5	161.6	127.1	79.5	35	-14.4	0.285489668	17.12938005
15	35.1	192.8	157.7	79.5	45	-14.6	0.354222821	21.25336927
16	34.6	217.1	182.5	79.5	55.2	-14.5	0.409928122	24.59568733
17	34.5	211.3	176.8	79.5	65	-14.6	0.397124888	23.82749326
18	34.4	175.8	141.4	79.5	75.2	-14.5	0.317610063	19.05660377
19	34.5	139.5	105	79.5	85	-14.5	0.235849057	14.1509434
20	34.5	115	80.5	79.5	95	-14.5	0.18081761	10.8490566
21	34.5	113.1	78.6	79.5	5	-24.5	0.176549865	10.59299191
22	34.5	131.1	96.6	79.5	14.8	-24.5	0.216981132	13.01886792
23	34.5	157.8	123.3	79.5	25	-24	0.276954178	16.61725067
24	34.4	198.1	163.7	79.5	35	-24.2	0.36769991	22.06199461
25	34.6	237.9	203.3	79.5	45	-24.4	0.456648697	27.39892183
26	34.7	257.6	222.9	79.5	55	-24.4	0.500673854	30.04043127
27	34.5	252.5	218	79.5	65	-24.7	0.489667565	29.38005391
28	34.4	210	175.6	79.5	75.2	-24.7	0.39442947	23.66576819
29	34.5	158.6	124.1	79.5	85.3	-24.8	0.278751123	16.72506739
30	34.6	123.6	89	79.5	95	-24.5	0.199910153	11.99460916
31	34.5	126.6	92.1	79.5	4.5	-34	0.206873315	12.41239892
32	34.5	153.4	118.9	79.5	14.5	-34	0.267070979	16.02425876
33	34.5	190	155.5	79.5	25	-34.2	0.349281222	20.95687332
34	34.4	224	189.6	79.5	75.3	-34.6	0.425876011	25.55256065
35	34.6	168.1	133.5	79.5	85	-34.8	0.299865229	17.99191375
36	34.6	131.2	96.6	79.5	95	-34.6	0.216981132	13.01886792
37	34.6	141.9	107.3	79.5	4.2	-44.5	0.241015274	14.46091644
38	34.7	180.5	145.8	79.5	14.5	-44.5	0.327493261	19.64959569
39	34.4	230	195.6	79.5	24.3	-45.2	0.4393531	26.36118598
40	34	217	183	79.5	74.5	-44.5	0.411051213	24.66307278
41	34.5	163.8	129.3	79.5	84.5	-44.8	0.290431267	17.42587601
42	34.3	125.2	90.9	79.5	94.5	-45.1	0.204177898	12.25067385
43	34.6	150	115.4	79.5	4.8	-55.2	0.259209344	15.55256065
44	34.6	209.6	175	79.5	15	-55.5	0.393081761	23.58490566
45	34.5	254.7	220.2	79.5	25	-56.2	0.494609164	29.67654987
46	34.3	190.3	156	79.5	74	-55	0.350404313	21.02425876
47	34.4	152.4	118	79.5	84.4	-55	0.265049416	15.90296496
48	34.6	118.5	83.9	79.5	94.7	-55.1	0.188454627	11.30727763
49	34.6	153.2	118.6	79.5	4.8	-67	0.266397125	15.98382749
50	34.6	216.1	181.5	79.5	15	-67.5	0.407681941	24.46091644
51	34.4	281.8	247.4	79.5	25.3	-67.2	0.555705301	33.34231806
52	34.7	170.8	136.1	79.5	74	-66.5	0.305705301	18.34231806
53	34.5	135.5	101	79.5	84.9	-67.8	0.226864331	13.61185984
54	34.6	110	75.4	79.5	94.8	-67.2	0.169362084	10.16172507
55	34.5	135.8	101.3	79.5	4.8	-79.5	0.227538185	13.65229111
56	34.6	180.5	145.9	79.5	14.5	-79	0.32771788	19.66307278
57	34.4	234.9	200.5	79.5	24.8	-79.5	0.450359389	27.02156334
58	34.4	148.3	113.9	79.5	73	-80	0.255840072	15.35040431
59	34.5	119.1	84.6	79.5	83.9	-80	0.190026954	11.40161725
60	34.6	99.2	64.6	79.5	94.3	-80.5	0.145103324	8.706199461
61	34.6	113.7	79.1	79.5	5	-94	0.177672956	10.66037736
62	34.5	130.5	96	79.5	15	-94	0.215633423	12.93800539
63	34.4	148.7	114.3	79.5	24.7	-94	0.256738544	15.40431267
64	34.7	166	131.3	79.5	34.5	-94.2	0.29492363	17.69541779
65	34.4	166.3	131.9	79.5	44	-93.5	0.296271339	17.77628032
66	34.5	153.8	119.3	79.5	53.8	-94	0.267969452	16.07816712
67	34.4	139.8	105.4	79.5	64	-94	0.236747529	14.20485175
68	34.4	120.1	85.7	79.5	73.8	-94	0.192497754	11.54986523
69	34.5	100.3	65.8	79.5	84	-94	0.147798742	8.867924528
70	50.9	356.9	306	125.5	37.2	-36.3	0.435401252	26.12407513
71	51	321.4	270.4	125.5	50	-36.8	0.384746727	23.08480364
72	51.2	345.9	294.7	125.5	62.5	-37	0.419322709	25.15936255
73	51	321.5	270.5	125.5	37	-49.5	0.384889015	23.09334092
74	51.2	295.6	244.4	125.5	50	-50	0.34775185	20.86511098
75	51	317.5	266.5	125.5	62.5	-50	0.379197496	22.75184974
76	50.9	383.4	332.5	125.5	36.5	-63.8	0.47310757	28.38645418
77	51	347	296	125.5	49.5	-62.5	0.421172453	25.27034718
78	51	320.9	269.9	125.5	62.5	-64	0.384035287	23.04211725
79	51.2	398.1	346.9	125.5	36.5	-79.5	0.49359704	29.61582242
80	51	349.4	298.4	125.5	49.4	-78.5	0.424587365	25.47524189
81	51	284.6	233.6	125.5	62.5	-78	0.332384747	19.9430848
82	27.5	83	55.5	84	94.2	-94.3	0.117984694	7.079081633

mean	0.299440343
min	0.117984694
max	0.555705301

Table X: Low(B) nozzle at a pressure of 1.8 bar

Nozle calibration

Date:	25/08/2016	
Time:	12:44:00 PM	13:48
Jet: Low(B)	smallest open	
Height of jet:	160	cm
Pressure:	2	bar
Duration of measurement:	64	min
Surveyors:		

LOW(B) NOZZLE

Vessel number	Vessel veight [g]			Vessel area [cm^2]	Vessel position [cm]		Rain intensity [$mm.min^{-1}$]	Rain intensity [$mm.h^{-1}$]
	Tara	Brutto	Netto		x	y		
1	34.2	97.2	63	79.5	4.8	-4.2	0.123820755	7.429245283
2	34.5	116.2	81.7	79.5	14.7	-4.2	0.160573899	9.634433962
3	34.7	144.6	109.9	79.5	25	-4	0.215998428	12.95990566
4	34.4	176.2	141.8	79.5	35	-4.5	0.278694969	16.72169811
5	34.4	200.8	166.4	79.5	45	-4.5	0.327044025	19.62264151
6	34.6	202.8	168.2	79.5	54.9	-4.5	0.330581761	19.83490566
7	34.5	178	143.5	79.5	64.8	-4.8	0.282036164	16.92216981
8	34.4	153.4	119	79.5	75	-4.8	0.233883648	14.03301887
9	34.4	130.4	96	79.5	85	-4.7	0.188679245	11.32075472
10	34.5	111.5	77	79.5	94.8	-5	0.151336478	9.080188679
11	34.5	113.4	78.9	79.5	4.8	-14.3	0.155070755	9.304245283
12	34.4	138.8	108	79.5	14.7	-14.3	0.212264151	12.73584906
13	34.4	179.5	145.1	79.5	25	-14.4	0.285180818	17.11084906
14	34.5	230.1	195.6	79.5	35	-14.4	0.384433962	23.06603774
15	35.1	270	234.9	79.5	45	-14.6	0.461674528	27.7004717
16	34.6	265.8	231.2	79.5	55.2	-14.5	0.454402516	27.26415094
17	34.5	226.8	192.3	79.5	65	-14.6	0.377948113	22.67688679
18	34.4	188.3	153.9	79.5	75.2	-14.5	0.302476415	18.14858491
19	34.5	150.8	116.3	79.5	85	-14.5	0.228577044	13.71462264
20	34.5	125.7	91.2	79.5	95	-14.5	0.179245283	10.75471698
21	34.5	130	95.5	79.5	5	-24.5	0.187696541	11.26179245
22	34.5	162.1	127.6	79.5	14.8	-24.5	0.250786164	15.04716981
23	34.5	211.9	177.4	79.5	25	-24	0.348663522	20.91981132
24	34.4	266.6	232.2	79.5	35	-24.2	0.456367925	27.38207547
25	34.6	293.8	259.2	79.5	45	-24.4	0.509433962	30.56603774
26	34.7	303.7	269	79.5	55	-24.4	0.528694969	31.72169811
27	34.5	270.7	236.2	79.5	65	-24.7	0.46422956	27.85377358
28	34.4	213.7	179.3	79.5	75.2	-24.7	0.352397799	21.14386792
29	34.5	170.8	136.3	79.5	85.3	-24.8	0.26788522	16.07311321
30	34.6	137.7	103.1	79.5	95	-24.5	0.202633648	12.15801887
31	34.5	143.8	109.3	79.5	4.5	-34	0.214819182	12.88915094
32	34.5	181.6	147.1	79.5	14.5	-34	0.289111635	17.34669811
33	34.5	234	199.5	79.5	25	-34.2	0.392099057	23.5259434
34	34.4	230.4	196	79.5	75.3	-34.6	0.385220126	23.11320755
35	34.6	180.4	145.8	79.5	85	-34.8	0.286556604	17.19339623
36	34.6	143.3	108.7	79.5	95	-34.6	0.213639937	12.81839623
37	34.6	160.3	125.7	79.5	4.2	-44.5	0.247051887	14.82311321
38	34.7	204.3	169.6	79.5	14.5	-44.5	0.333333333	20
39	34.4	267.1	232.7	79.5	24.3	-45.2	0.457350629	27.44103774
40	34	236	202	79.5	74.5	-44.5	0.397012579	23.82075472
41	34.5	181.3	146.8	79.5	84.5	-44.8	0.288522013	17.31132075
42	34.3	146.6	112.3	79.5	94.5	-45.1	0.220715409	13.24292453
43	34.6	170.2	135.6	79.5	4.8	-55.2	0.266509434	15.99056604
44	34.6	240.1	205.5	79.5	15	-55.5	0.403891509	24.23349057
45	34.5	303.9	269.4	79.5	25	-56.2	0.529481132	31.76886792
46	34.3	227.6	193.3	79.5	74	-55	0.379913522	22.79481132
47	34.4	181.1	146.7	79.5	84.4	-55	0.288325472	17.2995283
48	34.6	142.8	108.2	79.5	94.7	-55.1	0.212657233	12.75943396
49	34.6	172.6	138	79.5	4.8	-67	0.271226415	16.27358491
50	34.6	262.4	227.8	79.5	15	-67.5	0.447720126	26.86320755
51	34.4	344.4	310	79.5	25.3	-67.2	0.60927673	36.55660377
52	34.7	215.7	181	79.5	74	-66.5	0.355738994	21.34433962
53	34.5	169.3	134.8	79.5	84.9	-67.8	0.264937107	15.89622642
54	34.6	134.9	100.3	79.5	94.8	-67.2	0.197130503	11.82783019
55	34.5	156.8	122.3	79.5	4.8	-79.5	0.240369497	14.42216981
56	34.6	216.1	181.5	79.5	14.5	-79	0.356721698	21.40330189
57	34.4	325.7	291.3	79.5	24.8	-79.5	0.572523585	34.35141509
58	34.4	194.8	160.4	79.5	73	-80	0.315251572	18.91509434
59	34.5	150	115.5	79.5	83.9	-80	0.227004717	13.62028302
60	34.6	119.3	84.7	79.5	94.3	-80.5	0.166470126	9.988207547
61	34.6	123.3	88.7	79.5	5	-94	0.174331761	10.45990566
62	34.5	148.9	114.4	79.5	15	-94	0.224842767	13.49056604
63	34.4	192.5	158.1	79.5	24.7	-94	0.310731132	18.64386792
64	34.7	232.5	197.8	79.5	34.5	-94.2	0.388757862	23.3254717
65	34.4	224.4	190	79.5	44	-93.5	0.373427673	22.40566038
66	34.5	200.3	165.8	79.5	53.8	-94	0.32586478	19.55188679
67	34.4	173.9	139.5	79.5	64	-94	0.274174528	16.4504717
68	34.4	147.3	112.9	79.5	73.8	-94	0.221894654	13.31367925
69	34.5	120.4	85.9	79.5	84	-94	0.168828616	10.12971698
70	50.9	438.8	387.9	125.5	37.2	-36.3	0.482943227	28.97659363
71	51	406.2	355.2	125.5	50	-36.8	0.442231076	26.53386454
72	51.2	431.1	379.9	125.5	62.5	-37	0.472983068	28.37898406
73	51	404.5	353.5	125.5	37	-49.5	0.440114542	26.40687251
74	51.2	369.9	318.7	125.5	50	-50	0.396787849	23.80727092
75	51	403.6	352.6	125.5	62.5	-50	0.438994024	26.33964143
76	50.9	444	393.1	125.5	36.5	-63.8	0.489417331	29.36503984
77	51	414.7	363.7	125.5	49.5	-62.5	0.452813745	27.1688247
78	51	412.1	361.1	125.5	62.5	-64	0.449576693	26.97460159
79	51.2	551.5	500.3	125.5	36.5	-79.5	0.622883466	37.37300797
80	51	484.7	433.7	125.5	49.4	-78.5	0.539965139	32.39790837
81	51	391	340	125.5	62.5	-78	0.423306773	25.39840637
82	27.5	96.6	69.1	84	94.2	-94.3	0.128534226	7.712053571

mean	0.328984134
min	0.123820755
max	0.622883466

Table XI: Low(B) nozzle at a pressure of 2.0 bar

Nozle calibration

Date:	26/08/2016	
Time:	10:19:00 AM	11:17
Jet: Low(B)	smallest open	
Height of jet:	160	cm
Pressure:	2.2	bar
Duration of measurement:	58	min
Surveyors:		

LOW(B) NOZZLE

Vessel number	Vessel veight [g]			Vessel area	Vessel position [cm]		Rain intensity	Rain intensity
	Tara	Brutto	Netto	[cm^2]	x	y	[$mm.min^{-1}$]	[$mm.h^{-1}$]
1	34.2	101.8	67.6	79.5	4.8	-4.2	0.146605942	8.796356539
2	34.5	114.3	79.8	79.5	14.7	-4.2	0.173064411	10.38386467
3	34.7	127.7	93	79.5	25	-4	0.201691607	12.10149642
4	34.4	140.2	105.8	79.5	35	-4.5	0.229451312	13.76707872
5	34.4	154.7	120.3	79.5	45	-4.5	0.260897853	15.65387118
6	34.6	167.7	133.1	79.5	54.9	-4.5	0.288657558	17.31945348
7	34.5	172.5	138	79.5	64.8	-4.8	0.29928432	17.95705921
8	34.4	151.7	117.3	79.5	75	-4.8	0.254391672	15.26350033
9	34.4	125.1	90.7	79.5	85	-4.7	0.196703535	11.8022121
10	34.5	103.1	68.6	79.5	94.8	-5	0.148774669	8.926480156
11	34.5	121.5	87	79.5	4.8	-14.3	0.188679245	11.32075472
12	34.4	139.4	108	79.5	14.7	-14.3	0.234222511	14.05335068
13	34.4	159.5	125.1	79.5	25	-14.4	0.271307742	16.27846454
14	34.5	182.6	148.1	79.5	35	-14.4	0.321188462	19.27130774
15	35.1	208.9	173.8	79.5	45	-14.6	0.376924745	22.61548471
16	34.6	235.9	201.3	79.5	55.2	-14.5	0.436564736	26.19388419
17	34.5	243.1	208.6	79.5	65	-14.6	0.452396443	27.1437866
18	34.4	196.9	162.5	79.5	75.2	-14.5	0.352418131	21.14508783
19	34.5	152.4	117.9	79.5	85	-14.5	0.255692908	15.3415745
20	34.5	118.5	84	79.5	95	-14.5	0.182173064	10.93038386
21	34.5	146.7	112.2	79.5	5	-24.5	0.243331165	14.59986988
22	34.5	171.9	137.4	79.5	14.8	-24.5	0.297983084	17.87898504
23	34.5	201	166.5	79.5	25	-24	0.361093038	21.6655823
24	34.4	239.7	205.3	79.5	35	-24.2	0.445239644	26.71437866
25	34.6	285.9	251.3	79.5	45	-24.4	0.545001084	32.70006506
26	34.7	310.6	275.9	79.5	55	-24.4	0.598351768	35.90110605
27	34.5	296	261.5	79.5	65	-24.7	0.567122099	34.02732596
28	34.4	246.1	211.7	79.5	75.2	-24.7	0.459119497	27.54716981
29	34.5	184.7	150.2	79.5	85.3	-24.8	0.325742789	19.54456734
30	34.6	139.2	104.6	79.5	95	-24.5	0.22684884	13.61093038
31	34.5	171.1	136.6	79.5	4.5	-34	0.296248102	17.77488614
32	34.5	216.1	181.6	79.5	14.5	-34	0.393840815	23.63044893
33	34.5	259.9	225.4	79.5	25	-34.2	0.488831056	29.32986337
34	34.4	273.4	239	79.5	75.3	-34.6	0.518325743	31.09954457
35	34.6	206.2	171.6	79.5	85	-34.8	0.372153546	22.32921275
36	34.6	152.9	118.3	79.5	95	-34.6	0.256560399	15.39362394
37	34.6	193.5	158.9	79.5	4.2	-44.5	0.344610714	20.67664281
38	34.7	274.8	240.1	79.5	14.5	-44.5	0.520711342	31.24268055
39	34.4	321.1	286.7	79.5	24.3	-45.2	0.621774019	37.30644112
40	34	272.5	238.5	79.5	74.5	-44.5	0.517241379	31.03448276
41	34.5	214.1	179.6	79.5	84.5	-44.8	0.389503362	23.37020169
42	34.3	159	124.7	79.5	94.5	-45.1	0.270440252	16.22641509
43	34.6	215.1	180.5	79.5	4.8	-55.2	0.391455216	23.48731295
44	34.6	332.8	298.2	79.5	15	-55.5	0.646714379	38.80286272
45	34.5	349.5	315	79.5	25	-56.2	0.683148992	40.98893949
46	34.3	255.2	220.9	79.5	74	-55	0.479071785	28.74430709
47	34.4	203.3	168.9	79.5	84.4	-55	0.366297983	21.97787899
48	34.6	154.9	120.3	79.5	94.7	-55.1	0.260897853	15.65387118
49	34.6	195.1	160.5	79.5	4.8	-67	0.348080677	20.8848406
50	34.6	312.7	278.1	79.5	15	-67.5	0.603122967	36.18737801
51	34.4	358.1	323.7	79.5	25.3	-67.2	0.702016916	42.12101496
52	34.7	224.8	190.1	79.5	74	-66.5	0.412274995	24.73649967
53	34.5	177.1	142.6	79.5	84.9	-67.8	0.309260464	18.55562785
54	34.6	140.2	105.6	79.5	94.8	-67.2	0.229017567	13.741054
55	34.5	153.4	118.9	79.5	4.8	-79.5	0.257861635	15.47169811
56	34.6	201.6	167	79.5	14.5	-79	0.362177402	21.73064411
57	34.4	255.5	221.1	79.5	24.8	-79.5	0.47950553	28.77033182
58	34.4	182.9	148.5	79.5	73	-80	0.322055953	19.32335719
59	34.5	146.4	111.9	79.5	83.9	-80	0.242680547	14.56083279
60	34.6	117.8	83.2	79.5	94.3	-80.5	0.180438083	10.82628497
61	34.6	115	80.4	79.5	5	-94	0.174365647	10.46193884
62	34.5	131.4	96.9	79.5	15	-94	0.210149642	12.60897853
63	34.4	144.5	110.1	79.5	24.7	-94	0.238776838	14.32661028
64	34.7	157.3	122.6	79.5	34.5	-94.2	0.265885925	15.9531555
65	34.4	165	130.6	79.5	44	-93.5	0.283235741	16.99414444
66	34.5	161.2	126.7	79.5	53.8	-94	0.274777705	16.48666233
67	34.4	144.4	110	79.5	64	-94	0.238559965	14.31359792
68	34.4	126.7	92.3	79.5	73.8	-94	0.200173498	12.01040989
69	34.5	109.2	74.7	79.5	84	-94	0.162003904	9.720234223
70	50.9	463.4	412.5	125.5	37.2	-36.3	0.566698722	34.00192334
71	51	440.8	389.8	125.5	50	-36.8	0.53551312	32.1307872
72	51.2	457.4	406.2	125.5	62.5	-37	0.558043687	33.48262124
73	51	381.7	330.7	125.5	37	-49.5	0.454320648	27.25923891
74	51.2	365.4	314.2	125.5	50	-50	0.4316527	25.89916197
75	51	404.7	353.7	125.5	62.5	-50	0.485918395	29.15510372
76	50.9	481.6	430.7	125.5	36.5	-63.8	0.591702157	35.50212941
77	51	426.2	375.2	125.5	49.5	-62.5	0.51545542	30.92732518
78	51	409.4	358.4	125.5	62.5	-64	0.492375326	29.54251958
79	51.2	422.8	371.6	125.5	36.5	-79.5	0.510509685	30.63058112
80	51	396.5	345.5	125.5	49.4	-78.5	0.474653112	28.4791867
81	51	344.6	293.6	125.5	62.5	-78	0.403352109	24.20112653
82	27.5	92.6	65.1	84	94.2	-94.3	0.13362069	8.017241379

mean	0.363524246
min	0.13362069
max	0.702016916

Table XII: Low(B) nozzle at a pressure of 2.2 bar

Highest Nozzle (1.6 bar)

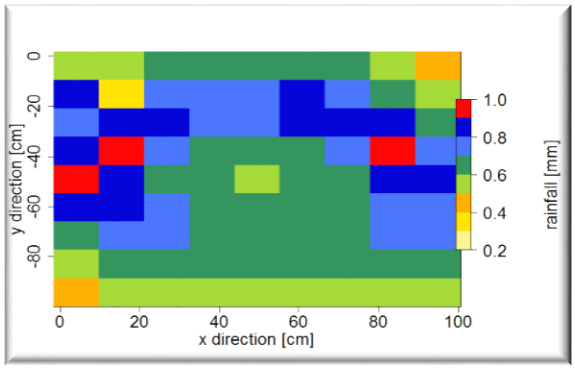

Highest Nozzle (2.0 bar)

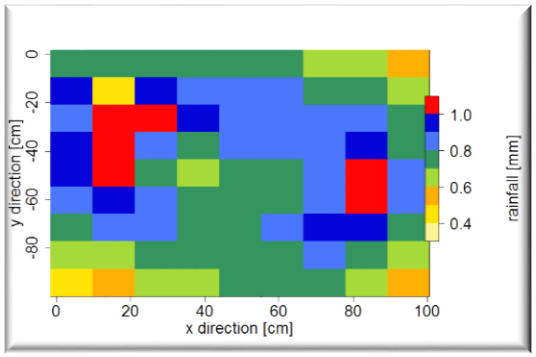

Low(A) Nozzle (1.8 bar)

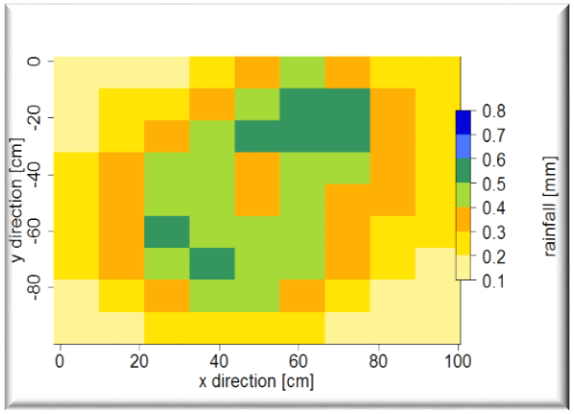

Low(A) Nozzle (2.0 bar)

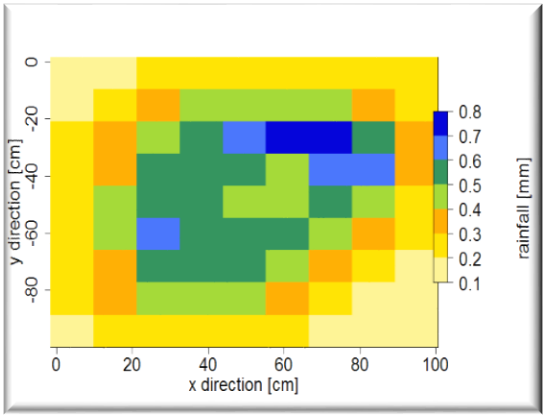

Low(B) Nozzle (2.0 bar)

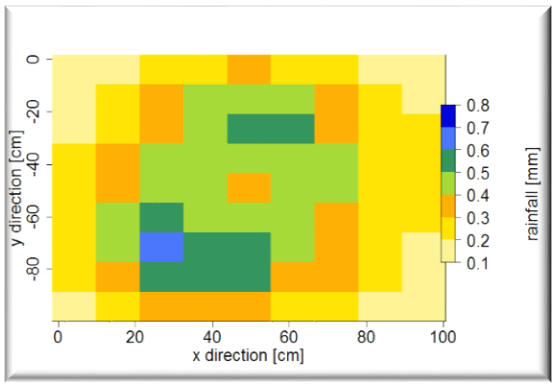

Low(B) Nozzle (2.2 bar)

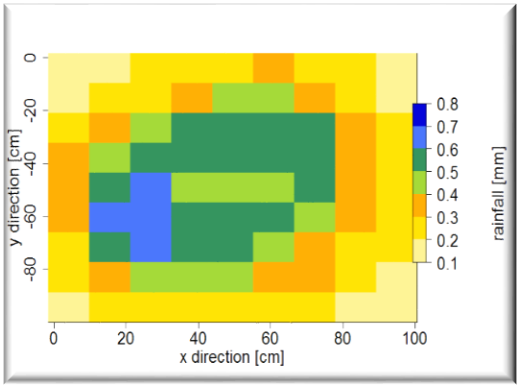

Figure 1: Spatial rainfall intensity distribution in rainfall simulator (measure with containers) with two flow rate each for Highest nozzle, Low(A) nozzle, and Low(B) nozzle. This is the remaining results which were not shown in the result section of this work.